

# UNIVERSITY OF NAPLES “FEDERICO II”



## DOCTORATE SCHOOL IN BIOLOGY

Cycle XXXIV

*“Enhanced drug delivery of neuroprotective peptides  
in the Central Nervous System”*

### **Supervisor**

Prof. Salvatore Valiante

### **PhD. Student**

Teresa Barra

### **Coordinator**

Prof. Sergio Esposito

Academic Year 2020-2021

## **Index**

<i>Sinossi</i> .....	4
<i>Synopsis</i> .....	5
<i>Chapter 1: General Introduction</i> .....	6
<i>Chapter 2: “gH625-liposomes deliver PACAP through a dynamic <i>in vitro</i> model of blood-brain barrier”</i> .....	12
<i>Chapter 3: “Neuroprotective effects of gH625-lipoPACAP in an <i>in vitro</i> fluid-dynamic model of Parkinson’s disease”</i> .....	47
<i>Chapter 4: “Comparison between a dynamic millifluidic system and a static system to study 3D brain tumor co-culture”</i> .....	76
<i>Chapter 5: “gH625-lipoPACAP in a 3D dynamic <i>in vitro</i> model of blood-brain barrier”</i> .....	105
<i>Chapter 6: “Delivery test of gH625-liposome in minibrains”</i> .....	117
<i>Chapter 7: Conclusion</i> .....	124
<i>Publications</i> .....	126

## **Sinossi**

La barriera ematoencefalica (BEE) è in grado di proteggere il sistema nervoso centrale (SNC) da insulti esterni escludendo l'ingresso di molte molecole, tra cui agenti terapeutici. Nasce ad oggi l'esigenza di sviluppare un modello di BEE affidabile per studiare le malattie neurodegenerative ed i loro possibili farmaci. Per studiare meglio il potenziamento del rilascio del farmaco nel SNC, abbiamo utilizzato un bioreattore millifluidico costituito da una doppia camera separata da una membrana porosa che imita sia il compartimento basolaterale che quello apicale della barriera fisiologica. Partendo dal componente principale della BEE, le cellule endoteliali cerebrali, abbiamo ottimizzato in tre anni un modello fluidodinamico in vitro aggiungendo anche linee cellulari neurali e gliali. Utilizzando strutture cellulari 3D, siamo in grado, ad oggi, di imitare una barriera fisiologica estremamente importante, al fine di studiare il rilascio di nanoparticelle caricate con un agente neuroprotettivo potenzialmente utilizzabile per il trattamento di malattie neurodegenerative come il morbo di Parkinson.

## **Synopsis**

The blood brain barrier (BBB) is able to protect central nervous system (CNS) from external injuries avoiding the entrance of many molecules, harming substances as well therapeutic agents. It is mandatory to develop a reliable BBB model in order to study neurodegenerative disease and their possible therapeutic drugs. To better study the enhance of drug delivery in the CNS, we have used a millifluidic bioreactor consisting in a double chamber separated by a porous membrane that mimic both basolateral and apical compartment of the physiological barrier. Starting from the main component of BBB, brain endothelial cells, we have optimized for three years an in vitro fluid dynamic model adding also neural and glial cell line. Using 3D cell biostructure, we are able, to date, to mimic the physiological barrier to study the delivery of nanoparticles loaded with neuroprotective agent potentially useful for the treatment of neurodegenerative diseases such as Parkinson's disease.

# **Chapter 1:**

## **General Introduction**

## General Introduction

In the last decades, several therapeutic strategies have been developed to improve Central Nervous System (CNS) drug delivery to treat neurological disease to ameliorate life quality of patients. One of the main objectives of the pharmaceutical industries, is to produce drugs able to access the CNS. The absorption in the CNS is strictly dependent on the presence of the blood-brain barrier (BBB). BBB is an anatomical-functional structure that protects the brain tissue from fluctuations in the plasma components. BBB constitutes also a physical barrier given by the presence of tight junctions (TJ) and adherent junctions (AJ) between adjacent endothelial cells (Alyautdin et al., 2014). limiting the passage of endogenous compounds potentially neurotoxic (Alavijeh et al., 2005). Brain endothelial cells are associated with numerous neuronal, vascular and immune cells. These include: pericytes, astrocytes, and microglia cells. The rigid regulation of brain homeostasis results in the inability of some therapeutic compounds to cross the BBB leading ineffective treatment of neurological disorders (Gabathuler, 2010). Recently, enormous results have been obtained for specific drug therapies deriving from nanotechnology. In addition to the mandatory requirements such as biocompatibility, biodegradability, biodistribution, pharmacokinetics and pharmacodynamics, maximal therapeutic effects and minimal side effects, nanoparticles, provides an attractive and modern alternative to develop innovative delivery system for the state of the CNS treatment. Due to their inherent characteristics mainly driven by size and surface properties, nanoparticles are ideal and versatile candidates for engineering high-performance *nanopharmaceuticals*. They have become an essential topic of drug delivery research because they can load and deliver more drugs for almost any organ/area of the body, providing targeted, controlled and sustained therapeutic effects (Hans et al., 2002). During my PhD, I studied the drug delivery of neuroprotective peptides in the CNS through an *in vitro* dynamic model of BBB. The *in vitro* dynamic model is represented by a bioreactor, "Livebox2" (LB2, IVtech; Italy) used to mimic physiological barriers (Giusti et al., 2014), consisting of two different chambers, upper and lower, each with an independent flow, separated by a porous membrane. During the first year of my PhD, in the upper chamber, murine endothelial brain cells (bEnd.3), commonly used for BBB *in vitro*, (Rodrigues, 2019) were seeded on the porous membrane in aseptic conditions. Subsequently liposomes with 20 $\mu$ M of rhodamine-labelled pituitary adenylate cyclase activating peptide (PACAP) (gH625-lipoPACAP-Rho) were injected in the upper tube of the upper chamber. PACAP can act as a neurotransmitter, neuromodulator and neuroprotective

factor (Vaudry et al., 2009) but has a short half-life in the bloodstream. For this reason, Valiante and colleagues have developed a nanodelivery system based on cell-penetrating peptide to transport PACAP, involving the use of the gH625 peptide. gH625 peptide is a membranotropic peptide, deriving from the H glycoprotein of *Herpes simplex* virus type 1 (Falanga et al., 2011). We also improved this 3D fluid dynamic *in vitro* system by adding a neuronal culture in the lower chamber of LB2, performing again the passage of gH625-lipoPACAP-Rho in this device. Results will show in the **Chapter 2** of this thesis, adapted from the article in preparation: “gH625-liposomes deliver PACAP through a dynamic *in vitro* model of blood-brain barrier” Invitation from *Frontiers in Physiology* (2021), Research Topic: 3Rs Approach (Replace, Reduce and Refine Animal Models) to Improve Preclinical Research. In 2018, Zhu and colleagues showed that PACAP can be considered an anti-inflammatory molecule in SH-SY5Y cells and in animals treated with MPTP (1-methyl 4-phenyl 1,2,3,6-tetrahydro-pyridine), a neurodegenerative agent, thus preventing neurodegeneration. In the second step of my PhD, I worked on studying the neuroprotective effects of PACAP. Neuronal spheroids were placed in Livebox1 (LB1, IVTech, Italy) bioreactor. Livebox1 is a single flow bioreactor with an only chamber that can also be easily connected to the Liveflow (IVTech, Italy) peristaltic pump. I treated spheroids with a neurodegenerative toxin, 1-methyl-4-phenylpyridinium (MPP<sup>+</sup>). This toxin causes neuronal death showing a similar Parkinsonians. Once established suitable dynamic flow conditions, neuronal spheroids were transferred in the lower chamber of LB2 bioreactor containing brain endothelial cells monolayer in the upper chamber. Results will show in the **Chapter 3** of this thesis, adapted from the article in preparation: “Neuroprotective effects of gH625-lipoPACAP in an *in vitro* fluid-dynamic model of Parkinson’s disease”, Invitation from MDPI, *biomedicines*, Research Topic: "Drug Delivery across the Blood-Brain Barrier for the Treatment of Brain Diseases". In the third step of my PhD, I worked on implementing 3D BBB *in vitro* dynamic system, adding a glial cell line in co-culture with neuronal spheroids. Primary experiments conducted with LB1, helped us to set the suitable flow conditions. Further I carried out a comparison with a 24-Ultra low attachment static system which helped to better discriminate the differences with our improved fluid dynamic system. Results about differences between 3D static culture and 3D dynamic culture will show in the **Chapter 4** of this thesis: Adapted from the article in preparation: “Comparison between a dynamic millifluidic system and a static system to study 3D brain tumor co-culture”. Then, we evaluated the passage of functionalized liposomes, placing the spheroids in co-culture in the lower chamber of LB2 in

which endothelial brain cells were seeded in the upper chamber of the porous membrane. Results will show in the **Chapter 5** of this thesis: “gH625- lipoPACAP in a 3D dynamic *in vitro* model of blood brain barrier”. Finally, during this last year, we have established a scientific collaboration with Professor Adrien Roux from Tissue Engineering Laboratory, Haute école du paysage, d’ingénierie et d’architecture de Geneva, Switzerland, allowing the study of the internalization of functionalized liposomes within minibrains. Minibrains are neuronal organoids generated by the non-direct differentiation of neural stem cells derived from human iPSCs which express neuron, oligodendrocyte, astrocyte marker genes of cortical regions such as striatum, subpallium, layer 6 of the motor cortex, piriformis, anterior cingulate and occipital cortex (Govindal et al., 2021). Functionalized liposomes (gH625-liposomeRHO-PE) or liposomes (liposome-RHO-PE) labeled in the phospholipid bilayer with Rhodamine, were internalized by placing minibrains in the incubator for 24 hours under orbital shaking. Results will show in the **Chapter 6** of this thesis: “Delivery test of gH625-liposome in minibrains”.

## References

- Alavijeh, M.S., Chishty, M., Qaiser, M.Z., Palmer, A.M. (2005). Drug metabolism and pharmacokinetics, the blood-brain barrier, and central nervous system drug discovery. *NeuroRx*. 2005 Oct;2(4):554-71. doi: 10.1602/neurorx.2.4.554.
- Alyautdin, R., Khalin, I., Nafeeza, M.I., Haron, M.H., Kuznetsov, D. (2016). Nanoscale drug delivery systems and the blood-brain barrier. *Int J Nanomedicine*. 2014 Feb 7;9:795-811. doi: 10.2147/IJN.S52236. PMID: 24550672; PMCID: PMC3926460.
- Falanga, A., Vitiello, M.T., Cantisani, M., Tarallo, R., Guarnieri, D., Mignogna, E., Netti, P., Pedone, C., Galdiero, M., Galdiero, S. (2011). A peptide derived from herpes simplex virus type 1 glycoprotein H: membrane translocation and applications to the delivery of quantum dots *Nanomedicine*. 2011; 7:925– 934.
- Gabathuler, R. (2010) Approaches to transport therapeutic drugs across the blood-brain barrier to treat brain diseases. *Neurobiol Dis*. 2010 Jan;37(1):48-57. doi: 10.1016/j.nbd.2009.07.028. Epub 2009 Aug 5.
- Garbuzova-Davis, S., Thomson, A., Kurien, C., Shytle, RD., Sanberg, PR. (2016). Potential new complication in drug therapy development for amyotrophic lateral sclerosis. *Expert Rev. Neurother*. 16, 1397–1405 (2016).
- Govindan, S., Batti, L., Osterop, S.F., Stoppini, L., Roux, A. (2021). Mass Generation, Neuron Labeling, and 3D Imaging of Minibrains. *Front Bioeng Biotechnol*. 2021 Jan 7;8:582650. doi: 10.3389/fbioe.2020.582650. PMID: 33598450; PMCID: PMC7883898.
- Giusti, S., Sbrana, T., La Marca, M., Di Patria, V., Martinucci, V., Tirella, A., Domenici, C., Ahluwalia, A. (2014). A novel dual-flow bioreactor simulates increased fluorescein permeability in epithelial tissue barriers. *Biotechnol J*. 2014 Sep;9(9):1175-84. doi: 10.1002/biot.201400004. Epub 2014 Jun 3.
- Hans, M.L. and Lowman, A.M. (2002) Biodegradable Nanoparticles for Drug Delivery and Targeting. *Current Opinion in Solid State and Materials Science*, 6, 319-327. [https://doi.org/10.1016/S1359-0286\(02\)00117-1](https://doi.org/10.1016/S1359-0286(02)00117-1).

Nzou, G., Wicks, R.T., Wicks, E.E. et al. Human Cortex Spheroid with a Functional Blood Brain Barrier for High-Throughput Neurotoxicity Screening and Disease Modeling. *Sci Rep*8, 7413 (2018). <https://doi.org/10.1038/s41598-018-25603-5>.

Rodrigues B, Lakkadwala S, Kanekiyo T, Singh J. Development and screening of braintargeted lipid-based nanoparticles with enhanced cell penetration and gene delivery properties (2019). *Int J Nanomedicine*. 2019 Aug 14;14:6497-6517. doi: 10.2147/IJN.S215941. eCollection 2019.

Valiante S, Falanga A, Cigliano L, Iachetta G, Busiello RA, La Marca V, Galdiero M, Lombardi A, Galdiero S (2015). Peptide gH625 enters into neuron and astrocyte cell lines and crosses the blood-brain barrier in rats. *Int J Nanomedicine*. 2015 Mar 10;10:1885-98. doi: 10.2147/IJN.S77734. eCollection 2015. 13.

Vaudry D, Falluel-Morel A, Bourgault S, Basille M, Burel D, Wurtz O, Fournier A, Chow BK, Hashimoto H, Galas L, Vaudry H. Pituitary adenylate cyclase-activating polypeptide and its receptors: 20 years after the discovery. *Pharmacol Rev*. 2009 Sep;61(3):283-357. doi: 10.1124/pr.109.001370. Review.

## Chapter 2:

### **gH625-liposomes deliver PACAP through a dynamic *in vitro* model of blood-brain barrier**

Adapted from the article in preparation:

#### **gH625-liposomes deliver PACAP through a dynamic *in vitro* model of blood brain barrier**

Teresa Barra<sup>1</sup>, Annarita Falanga<sup>2</sup>, Rosa Bellavita<sup>2</sup>, Stefania Galdiero<sup>2</sup>, Salvatore Valiante<sup>1</sup>

<sup>1</sup>Department of Biology, University of Naples, Federico II, Naples, Italy.

<sup>2</sup>Department of Pharmacy, School of Medicine, University of Naples 'Federico II', Naples, Italy.

*Invitation from Frontiers in Physiology (2021), Research Topic:*

*3Rs Approach (Replace, Reduce and Refine Animal Models) to Improve Preclinical Research*

## **Abstract**

The blood brain barrier (BBB) selectively protects the central nervous system (CNS) from external insults, but its function can represent a limit for the passage of therapeutic molecules. Numerous *in vitro* models of the BBB have been realized in order to study the passage of drugs for neurodegenerative diseases, but these *in vitro* static models are not very representative of the physiological conditions because of a limited supply of oxygen and nutrients. To reduce this phenomenon, we used a millifluidic bioreactor model that ensures a circulation of the medium and therefore of the nutrients thanks to the continuous laminar flow. This dynamic model consists of a double culture chamber separated by a membrane on which brain endothelial cells are cultured in order to evaluate the passage of the drug. Furthermore, in the lower chamber SH-SY5Y were seeded as 3D spheroids to evaluate the passage through these cells. In this study we used as nanodelivery system, liposomes functionalized with viral fusion peptide and loaded with a neuroprotective agent, pituitary adenylate cyclase-activating polypeptide (PACAP).

## 1. Introduction

The blood-brain barrier (BBB) is an anatomical structure that separates blood from extracellular fluid in the central nervous system (CNS). BBB can protect brain from substances that can damage it and allows to maintain a constant brain environment. In fact, the passage of drugs through the BBB is very limited due to the presence of tight junctions (TJs) between basement membranes (Sandoval and Witt, 2008). Therefore, the delivery and release of drugs in the brain is a challenging topic and attracts a lot of attention considering the growing number of neurodegenerative diseases such as Alzheimer's disease (Cummings et al., 2002), Parkinson's disease (Alavijeh et al., 2005), Huntington's chorea (Wohlfart et al., 2012) and HIV encephalitis (Spindler and Hsu, 2012). The functions of the blood-brain barrier rely on the cellular components, mainly the specialized endothelial cells forming brain capillaries. These cells act as a continuous and selective physical barrier for hydrophilic substances and are involved in the control of molecular trafficking in the CNS (Abbott et al., 2006). They are held together by TJs, astrocytes, pericytes and basal membranes (Abbott et al., 2006; Reese and Karnovsky, 1967). Moreover, they express a number of transporters responsible for the regulated exchange of nutrients and toxic products (Abbott et al., 2006), including ATP-binding cassette (ABC) transporters, which are present in a higher percentage than other proteins, providing protection for BBB and also limiting the transport of drugs to the brain (Alyautdin et al., 2014). The ability to recreate a BBB model *in vitro* and to reproduce as closely as possible the physiological conditions associated with it, represents a crucial point for managing neurodegenerative diseases and for formulating a valid pharmacological approach. However, *in vitro* static models are not very representative of physiological reality and are based on the use of cells in highly controlled and repeatable conditions which simplify the complex phenomena that occur *in vivo* (Rouwkema et al., 2011). For this reason, different approaches have been proposed to develop *in vitro* dynamic models of BBB able to get as close as possible to the situation *in vivo* considering and simulating the main stimuli that act on cells in the human body. In this regard, dynamic millifluidic models mimic the anatomic-physiological complexity of the BBB *in vivo*, based on ideal criteria, such as reproducibility, easiness of culture, fidelity of physiological architecture, expression of the transporters and response to chemical-physical stimuli external. In recent years, the need to develop advanced *in vitro* models has grown to reproduce 3D multicellular architecture and to modulate the cell culture environment, finely controlling parameters such as temperature, pH and pressure hydrostatic (Giusti et al., 2017). In fact, the

cells inside the body, live in a dynamic environment, whose behavior is influenced by crosstalk between the different cell types (Bilodeau and Mantovani, 2006). A valid tool that responds to these needs is the bioreactor, capable of recreating the physiological flow to which the cells are subjected *in vivo*. Flow is an essential physical stimulus, which increases the exchange of nutrients, and to which the cells respond through stretching, orientation in space, cytoskeletal reorganization and increase in membrane permeability. In the light of the above reasons, this study aims to evaluate the efficiency of a nanodelivery system to delivery pituitary adenylate cyclase-activating polypeptide (PACAP) through a dynamic millifluidic bioreactor model of BBB (Livebox2, LB2). PACAP is the most conserved peptide of the secretin/ glucagon superfamily, to which it belongs, by length and aminoacid nucleotide sequence (Vaudry et al., 2000). In the CNS, PACAP is present at high concentrations in the hypothalamus (Arimura et al., 1991) and in other brain regions, such as the cerebral cortex (Ghatei et al., 1993; Fukuhara et al., 1997). Indeed, PACAP exerts neurotrophic actions (Yuhara et al., 2001; Erhardt and Sherwood, 2004; Reglodi et al., 2004; Shioda et al., 2006) and, in the cells of the cerebellar granules, inhibits programmed cell death (Campbell and Scanes, 1992; Canonico et al., 1996; Cavallaro et al., 1996; Chang et al., 1996; Gonzalez et al., 1997), stimulating elongation of neuritis (Gonzalez et al., 1997). PACAP has also anti-inflammatory properties in dopaminergic SH-SY5Y cells (Brown et al., 2013); it protects neurons from 1-methyl-4-phenyl-1,2,3,6-tetrahydropyridine (MPTP) neurotoxic effects in animal models of Parkinson's disease (Deguil et al., 2010) leading to recovery of dopaminergic function (Reglodi et al., 2004; Somogyvari-Vighet and Reglodi, 2004; Takei et al., 1998; Wang et al., 2008). A synthetic PACAP analog was used to restore tyrosine hydroxylase expression into the substantia nigra and to modulate the inflammatory response in mice (Lamine et al., 2016). PACAP has several beneficial effects in some pathological processes due to its neuroprotective and neurotrophic action (Harmar et al., 2012; Vaudry et al., 2009). The action on the signaling pathways and therefore the physiological effects depend on the receptors expressed in the different tissues (Vaudry et al., 2009). These receptors (PAC<sub>1</sub>-R, VPAC<sub>1</sub>, VPAC<sub>2</sub>) are associated with adenylate cyclase via cyclic adenosine monophosphate (cAMP) and activate protein kinase A (PKA), which in turn can activate the mitogen-activated protein kinase (MAPK) pathway. PAC<sub>1</sub>-R is also coupled to phospholipase C, the activation of which stimulates the mobilization of Ca<sup>2+</sup> and the activation of protein kinase C (Shioda et al., 2016). Detailed analyzes showed that PACAP levels were reduced in the human entorhinal cortex, mid-temporal, superior frontal, and primary visual

cortex at both the mRNA and protein levels associated with pathological signs of Alzheimer's disease: PACAP levels were reduced more in the amyloid plaque but not in the primary visual cortex, a region spared in most cases of the disease (Wu et al., 2006). PACAP is also reduced in several dementias representing a link between its reduction and age related (Han et al., 2014). Another demonstration of its lesser presence in advanced states, was an upregulation of PAC1-R in the superior frontal gyrus (Han et al., 2015). In pond snail ganglia was also observed a marked decline in PACAP, useful in memory formation (Pirger et al., 2014). In the basal ganglia of Parkinsonian macaque monkey was observed an important and specific decline of the PACAP receptor, in the pathway PACAP/PAC<sub>1</sub>-R (Feher et al., 2018). Lowering of the age influence also the capability of PACAP to cross the BBB (Nonaka et al., 2002). However, PACAP, as an intravenous therapeutic agent, presents some difficulties, such as rapid degradation in the blood and low bioavailability. A useful approach for the targeted administration of PACAP to the CNS involves the use of liposomes as cargo, modified with amphipathic peptides capable of crossing biological membranes and transporting small molecules and proteins. The gH625 peptide (Galdiero et al., 2005), which is a disturbing domain of the membrane derived from the *Herpes simplex* type 1 virus has suitable features in this regard. The hydrophobic domain is fundamental for the insertion of the peptide into the membrane, promoting vesicular fusion (Falanga et al., 2011). gH625 enters in SH-SY5Y cells and U-87MG glioblastoma cells *in vitro* and can efficiently cross the rat BBB *in vivo* labelling cell neurites, showing no toxic effects (Valiante et al., 2015). It has also been demonstrated that the intravenous administration of gH625-liposomes loaded with rhodaminated PACAP permits its releasing across rat BBB (Iachetta et al., 2019). Based on this background, the aim of this study is to evaluate the ability of gH625-liposomes to delivery PACAP through a dynamic *in vitro* model of BBB consisting in a millifluidic bioreactor (LB2) in which endothelial brain cells (bEnd.3) were seeded in an upper chamber and the human 3D cell lines SH-SY5Y (neuroblastoma cells) were cultured in the lower chamber.

## **2. Materials and Methods**

### **2.1 Peptide synthesis**

The gH625 with the cysteine at C-terminal (Ac-HGLASTLTRWAHYNALIRAF-Cys)-and PACAP27 (HSDGIFTDSYSRYRKQMAVKKYLA AVL-CONH<sub>2</sub>) peptides were synthesized

using a standard Fmoc solid-phase (GL Bio chem Ltd, Shanghai, China) as previously reported (Iachetta et al., 2019) and were obtained with good yields about 40%. PACAP27 was labeled on resin with Rhodamine (5(6)-Carboxytetramethylrhodamine N-succinimidyl ester) for fluorescence measurements, as reported (Rapaport and Shai, 1991). Peptides were fully deprotected and cleaved from the resin with an acid solution of trifluoroacetic acid and scavengers. The crude peptides were precipitated with ice cold ethyl ether, and purified by preparative reverse-phase HPLC with a solvent mixture of H<sub>2</sub>O and 0.1% trifluoroacetic acid (solvent A) and CH<sub>3</sub>CN and 0.1% trifluoroacetic acid (solvent B), with a linear gradient B over 20 min at a flow rate of 15 ml/min. Peptide identity was confirmed using a LTQ-XL Thermo Scientific linear ion trap mass spectrometer. For the synthesis of DSPE-PEG2000-gH625, 1 eq of DSPE-PEG2000-Mal was reacted with 1 eq. of pure gH625-Cys in DMF in presence of 5 eq of triethylamine (5 eq) for 24 h. The reaction was monitored by RP-HPLC, when completed the solvent was evaporated and the product analyzed using an LTQ-XL. 1,2-Dipalmitoyl-sn-glycero-3-phosphocholine (DPPE), cholesterol, 1,2-distearoyl-sn-glycero-3-phosphoethanolamine-N- [maleimide (polyethylene glycol)-2000] (DSPE-PEG2000-Mal) were purchased from Avanti Polar Lipids (Birmingham, AL, USA). Coupling reagents, N,N-diisopropylethylamine (DIEA), piperidine, trifluoroacetic acid (TFA), Rhodamine (5(6)-Carboxytetramethylrhodamine N-succinimidyl ester and Rink amide resin (0.62 mmol/g of loading substitution), were purchased from Iris-Biotech GMBH.

## 2.2 Liposome preparations

Large unilamellar vesicles (LUV) consisting of DPPC/Chol (70/30 mol/mol) were prepared as previously reported (Galdiero et al., 2005). Briefly, lipids, DSPE-PEG2000-gH625 and PACAP-Rho were dissolved in chloroform, the solvent was removed with a nitrogen gas stream and the sample was lyophilized overnight to obtain a lipid film. The obtained film was suspended in buffer to produce LUVs, freeze-thawed eight times and then extruded 10 times through polycarbonate membranes with 0.1  $\mu$ m diameter pores (Northern Lipids). The hydrodynamic diameters ( $D_H$ ) and polydispersity index (PDI) of PACAP-Rho loaded liposomes (Lipo) and PACAP-Rho loaded gH625-liposomes (gH625-Lipo) were measured using dynamic light scattering (DLS) (Malvern Zetasizer Nano ZS, Malvern, UK). The analysis was performed with He-Ne laser 4 mW operating at 633 nm at scattering angle fixed at 173° and at 25°.

### 2.3 bEnd.3 cell culture

Murine endothelial brain cells (bEnd.3) were grown in Dulbecco's Modified Eagle's Medium High glucose, supplemented with fetal bovine serum (10%, Sigma-Aldrich-Saint Louis, USA), penicillin/streptomycin (100 U/ml, Sigma-Aldrich-Saint Louis, USA), L-glutamine (2mM, Sigma-Aldrich-Saint Louis, USA), gentamycin (40µg/ml, Sigma-Aldrich-Saint Louis, MO, USA) at 37°C, 5%CO<sub>2</sub> in a humidified incubator. Cells grow adherent in 25 cm<sup>2</sup> flasks. Medium was changed twice a week. When 70% confluent, cells were enzymatically detached with trypsin-EDTA (Sigma-Aldrich-Saint Louis, USA).

### 2.4 Lucifer yellow assay

Lucifer yellow (LY) is a hydrophilic dye and its fluorescence can be used to determine the permeability coefficient (P<sub>c</sub>) of cerebral endothelial monolayer, thus the barrier integrity (Zhao et al., 2019). In *in vitro* BBB models, P<sub>c</sub> values are considered in the order of 10<sup>-4</sup> cm/min for different solutes (Wolff et al., 2015; Cecchelli et al., 2007; Reichel et al., 2003; Deli et al., 2005). Moreover LY has a Stokes shift about 108 nm, compared to other small Stokes shift (Ren et al., 2018), this allows to determine a spectral separation such as to provide enough fluorescence data to determine cell permeability. Our experiments are carried out using a dynamic microfluidic tool called LB2, IVTech, Italy made of polydimethylsiloxane (PDMS), commonly used to mimic physiological barriers (Giusti et al., 2014). This bioreactor is composed of two parts: lower chamber and upper chamber each with an independent flow, divided by a porous membrane (ipPORE, Belgium). These membranes, thanks to their porosity, (0,45 µm) allow the passage of nutrients but prevent the passage of cells, causing easy adhesion and reducing the binding of non-specific molecules. The chambers are also connected to a peristaltic pump circuit (Liveflow, IVTech, Italy) which allows a continuous recycling of nutrients and allows to evaluate the diffusion of drugs between the two chambers. The cells seeded on the porous membrane are bEnd.3 (murine endothelioma) commonly used for BBB *in vitro* (Dos Santos Rodrigues et al., 2019). This membrane was first adapted in 80% ethanol for 15 min. Then, the wet membrane is laid on the lower part of the holder. Once assembled, the holder is placed in 6-well plates covered with complete DMEM culture medium for 24h. After 24h, the LB2 culture chamber is assembled with the holder containing the membrane, in the central portion

between the upper and lower chamber (**Fig.1**). Later, 1 ml of DMEM complete medium was injected into the lower chamber and 150,000 bEnd.3 cells in 100  $\mu$ l of DMEM complete medium were seeded onto the membrane from the inlet tube of the upper chamber, adding 500  $\mu$ l of complete DMEM to make the cells in the inlet tube flow. The LB2 was then placed in an incubator for a week at 37 ° and 5% of CO<sub>2</sub>. To adapt the cells to the flow, the LB2 chamber was connected to the Liveflow. The circuit was first connected to the mixing chambers containing 8 mL of DMEM complete medium and then, LB2 was connected at the LiveFlow at a nominal flow of 250  $\mu$ l/min. In the mixing chambers, medium was changed twice a week. Permeability measurements were carried out in different days: 1, 3, 6 and 8. In these different days, the growth medium was removed and it was added 1 ml of pre-warmed (37 °C) transport buffer (25 mM HEPES, 145 mM NaCl, 3 mM KCl, 1 mM CaCl<sub>2</sub>, 0.5 mM MgCl<sub>2</sub>, 1 mM NaH<sub>2</sub>PO<sub>4</sub>, 5 mM glucose, pH 7.4) to the basolateral side (Zhao et al., 2019). In the apical side of the porous membrane, 20  $\mu$ M of LY (Sigma-Aldrich-Saint Louis, USA) was added and were incubate at 37°C for 60 min. Then, 30  $\mu$ l of the LY sample was removed from each apical compartment and transferred in tubes diluting the sample 10-fold using transport buffer. After removing 500  $\mu$ l from basolateral compartment, a series of LY standards have been prepared. Each standard was performed in duplicate in a black 96-well plate. Fluorescence has been measured using Synergy HTX Multi mode microplate reader (Ex: 428 nm, Em: 536 nm). Permeation coefficient (Pc) was calculated from this equation:

$$Pc \left( \frac{cm}{sec} \right) = \frac{Vb \times Cb}{Ca \times A \times T}$$

Vb is the volume of lower chamber (1mL), Cb is the concentration of LY ( $\mu$ M) in the lower chamber, Ca is the concentration of LY ( $\mu$ M) in the upper chamber, A is the membrane area (1,12 cm<sup>2</sup>) (Giusti et al., 2014), and T is the time of transport (3600 sec). This test was useful to determine when bEnd3 cells forms the tightest monolayer as maximum barrier integrity.

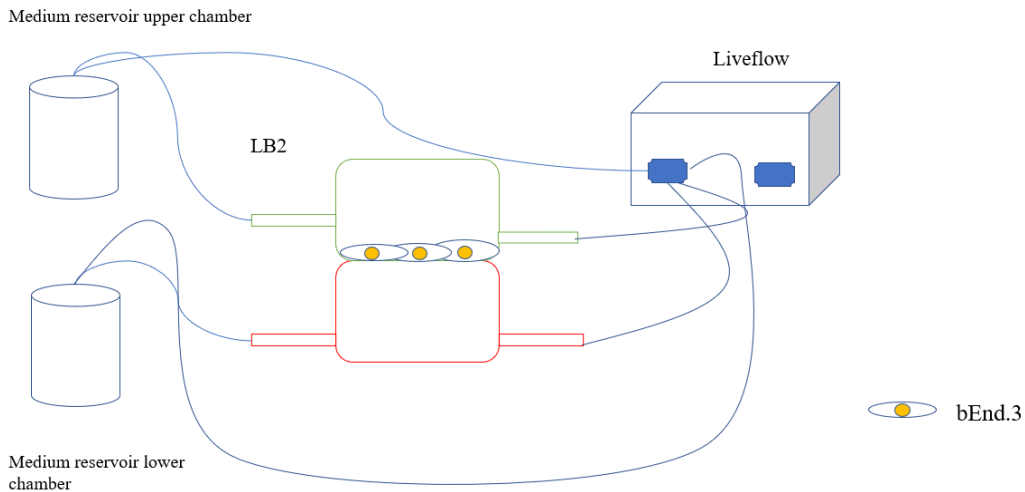


**Fig.1:**

Schematic view of a dynamic bioreactor: Live Box 2 (LB2) is composed by an upper chamber connected to a medium reservoir and to a Liveflow pump (250  $\mu\text{L}/\text{min}$ ) and a lower chamber connected to a medium reservoir and to a Liveflow pump (250  $\mu\text{L}/\text{min}$ ). In the upper chamber, bEnd.3 cells are seeded on the porous membrane in the holder.

## 2.5 Immunofluorescence assay

Lucifer yellow assay indicate us the formation of a stable and integral barrier to the day 6 to 8. After a week, different indirect immunofluorescence assays were performed to evaluate protein junction formation on bEnd.3 cells cultured on the porous membrane of LB2 connected to LiveFlow at a nominal flow of 250  $\mu\text{L}/\text{min}$ . After 7 days, cells were washed with phosphate-buffered saline (PBS) and fixed with a 4% paraformaldehyde solution (PFA) for 15min. PFA was subsequently saturated by incubation with 0,1M Glycine. Cells were then permeabilized with PBS 0.4% Triton X 100 followed by another permeabilization with PBS 0,1% Triton X100. Blocking was performed using 4% BSA for 30min followed by incubation with the antibodies: Anti-ZO1 tight junctions' protein (3 $\mu\text{g}/\text{ml}$  in 1%BSA/PBS, Abcam, Cambridge, UK), Anti- N-cadherin adherens junctions' protein, (1:100 in 1% BSA/PBS, Santacruz biotechnology, California, USA), Anti- $\beta$  catenin adherens junctions' protein (1:100 in

1%BSA/PBS, Abcam, Cambridge, UK) overnight at 4°C. After 24h, cells were washed three times with PBS and then incubated with AlexaFluor 488 (1:200, Cambridge, UK) secondary antibody for 1h. Nuclei were stained with Hoechst 33258 (1:1000, Invitrogen, Carlsbad, USA) for 15 min at room temperature. Cells were acquired with an Axioskop epifluorescence microscope (Carl Zeiss) with 40x objective, using the filter for the Hoechst 33258 (ex: 360 nm, em: 452 nm) and that for Alexa Fluor 488 (ex: 488 nm, em: 530 nm), an Axiocam MRc5 camera (Carl Zeiss) and Axiovision 4.7 software (Carl Zeiss). Similar cellular fields were chosen for the different experimental groups. For each experimental condition were repeated three immunofluorescences and were randomly chosen different fields for data analysis. For each experimental condition three immunofluorescences were repeated and were randomly chosen different fields for data analysis. The acquired images were corrected for brightness and contrast through Fiji software.

## **2.6 LDH assay**

Lactate dehydrogenase (LDH) assay (ThermoFisher Scientific, Massachusetts, USA) was used to test the cytotoxicity of the bEnd.3 cells on the porous membrane of LB2. It is a colorimetric method used to quantify cellular cytotoxicity. Damaged plasma membrane releases lactate dehydrogenase (LDH), a cytosolic enzyme found in several types of cells. LDH catalyzes the conversion of lactate to pyruvate via reduced NAD<sup>+</sup> to NADH. Diaphorase then uses NADH to reduce the tetrazolium to formazan salt which can be measured at 490 nm. The amount of formazan is proportional to the amount of LDH released into the medium, indicative of cytotoxicity. To perform the LDH assay, after 7 days, bEnd.3 cells are lysed with a 1mM PBS/EDTA solution and then transferred to a 96-well plate. Subsequently, the spontaneous and maximum LDH activity is measured: 50µl of all the samples are transferred to a new 96-well plate to which 50µl of reaction mixture will be added. After incubating for 30 min in the dark, 50µl of stop solution will be added to each well. Non-viable cells convert the tetrazolium salts into formazan red. To measure the absorbance, expressed in optical density (O.D), a spectrophotometric reading was carried out at 490 nm and using a plate reader (Synergy HTX Multi mode microplate reader). The absorbance of this compound is directly proportional to the amount of LDH released by the cells. Three assays were performed and for each experimental class the test was performed in triplicate.

## **2.7 Spectrofluorimetry assay**

Spectrofluorimetry assay was performed to evaluate the ability of gH-625 liposome compared to only liposome to delivery PACAP through bEnd.3 monolayer in a millifluidic bioreactor (LB2). After 7 days of bEnd.3 culture in LB2, liposomes were injected into the upper chamber, in correspondence of the membrane, with PACAP-Rho 20  $\mu$ M (gH625-lipoPACAP-Rho). To evaluate the passage of the gH625-lipoPACAP-Rho in the lower chamber, a spectrofluorimetric experiment was performed on samples of medium taken at regular intervals (30, 60, 90, 120 min). Briefly, after 30 minutes to the injection of the gH625-lipoPACAP-Rho in the upper chamber, the supernatant (100  $\mu$ l) was taken from the outlet tube of the upper chamber and from the outlet tube of the lower chamber and placed in a 96-well plate. The control group was obtained with liposome-PACAP-Rho. This solution was read at 540 nm-580 nm fluorescence with an Infinite 200M spectrophotometer (TECAN). Each spectrofluorimetric assay was performed in triplicate.

## **2.8 SH-SY5Y cell culture**

Neuroblastoma cell line enriched to neural portion (SH-SY5Y-N) were grown in Dulbecco's Modified Eagle's Medium High glucose, supplemented with fetal bovine serum (10%, Sigma-Aldrich-Saint Louis, USA), penicillin/streptomycin (100 U/ml, Sigma-Aldrich-Saint Louis, USA), L-glutamine (2mM, Sigma-Aldrich-Saint Louis, USA), gentamycin (40 $\mu$ g/ml, Sigma-Aldrich-Saint Louis, MO, USA) at 37°C, 5%CO<sub>2</sub> in an humidified incubator. Cells grow adherent in 25 cm<sup>2</sup> flasks. Medium was changed twice a week. When 70% confluent, cells were enzymatically detached with trypsin-EDTA (Sigma-Aldrich-Saint Louis, USA).

## **2.9 PACAP ELISA assay**

ELISA assay (Mybiosource, San Diego, USA) was performed to evaluate the amount of PACAP released by gH625-liposome. bEnd.3 cells were cultured in LB2 connected to a Livebox1 (LB1, IVTech, Italy) containing SH-SY5Y differentiated in dopaminergic neuron by retinoic acid 10  $\mu$ M. LB1 is a bioreactor with an only one chamber connected to a single mixing chamber. This bioreactor is useful for the preliminary experiments to set the suitable flow that

does not cause *shear-stress* to the cells. The mixing chambers of both Liveboxes contained 8 ml of DMEM culture medium. Once the cells were adapted to the Liveflow (250  $\mu$ l/min), in the upper mixing chamber of LB2, liposomes were injected with PACAP (gH625-lipoPACAP) at a concentration of PACAP of 20 $\mu$ M. Samples of medium were taken at regular intervals (30, 60, 90, 120 min). Specifically, after 30 min, the supernatant (100  $\mu$ l) was taken from the outlet tube of the upper chamber, from the outlet tube of the lower chamber of the LB2 and from the outlet tube of the LB1. Finally, 1 ml of samples were collected from the upper and lower mixing chambers of LB2 and from the mixing chamber of the LB1. Indirect ELISA protocol was performed using standards from 0 to 1000 pg/ml. To measure the absorbance, expressed in optical density (O.D.), a spectrophotometric reading was performed at 450 nm using an ELISA plate reader (Thermo electron company-Multiskan Ascent).

## **2.10 3D SH-SY5Y cells cultured in LB1**

Hanging drop method was used for the three-dimensional structures of SH-SY5Y cells. This technique has proved useful in hepatocytes and in engineering cardiac spheroids (Shri et al., 2017; Chitnis and Weiner, 2017; Polonchuk et al., 2017) and to study toxicity and in the study of BBB for the employment of neurotoxicity (Nzou et al., 2018). This method exploits the ability of cell-cell and cell-extracellular matrix cohesion (Foty, 2011) within a hydration chamber which, thanks to the force of gravity, the cells, in direct contact with each other, form aggregates. SH-SY5 cells enriched to the neural portion, are deposited in "drops" inside a lid of a 60mm dish. The drops must be spaced apart to allow for the formation of the individual spheroids. 10ml of PBS was placed on the bottom of the dish to create a hydration chamber to favor the formation of aggregates. Once the drops had been sown, the lid of the dish was turned upside down on the bottom containing PBS and placed in an incubator at 37° C, with 5% CO<sub>2</sub> and humidity controlled for 48h. After 48h the formation of the aggregates was checked with the help of a stereomicroscope and these cells were transferred to a LB1 connected to a Liveflow and to his respective mixing chamber with DMEM cell medium to set the nominal flow suitable to not create *shear-stress* conditions for the spheroids. The flow chosen was 150 $\mu$ l/min for 24h.

### 2.11 3D SH-SY5Y Immunofluorescence assay

Different indirect immunofluorescence assays were performed in 3D SH-SY5Y cells in dynamic culture to assess the presence of PACAP receptors (PAC<sub>1</sub>-R, VPAC<sub>1</sub>, VPAC<sub>2</sub>), Ki67 proliferation protein, ZO-1 tight junctions' protein and  $\beta$ 3-Tubulin neural marker. After 24h of flow connection, spheroids were fixed with cold methanol for 15 min and then washed with PBS to eliminate all fixative residues. Non-specific site blocking was performed with 3% BSA (bovine serum albumin) in 0.1% Triton-PBS for 30 min. Incubation with primary antibodies in 1% BSA / PBS were performed for 1:45 min. The antibodies used (1% BSA/PBS) were: Anti-PAC<sub>1</sub>-R, Anti-VPAC<sub>1</sub>, Anti-VPAC<sub>2</sub> (Santacruz biotechnology, California, USA), Anti-Ki67, Anti ZO-1, Anti- $\beta$ 3 Tubulin (Abcam, Cambridge, UK). Subsequently, after three washes in 0.1% Triton-PBS, cells were incubated for 1h with the secondary antibody AlexaFluor 488 (1:500 in 1%BSA/PBS, Invitrogen, Carlsbad, USA). Cell nuclei were labeled with DAPI (1:1000 in PBS, Invitrogen, Carlsbad, USA) for 5 min. Images were acquired with the JuLi™ Stage\_RealTime Cell History Recorder microscope with 10x objective, using two different channels: DAPI and GFP. For each experimental condition, three immunofluorescence assays were repeated, and different fields were randomly selected for data analysis. The captured images were corrected for brightness and contrast using Fiji software.

### 2.12 gH625-lipoPACAP-Rho through a 3D dynamic *in vitro* BBB millifluidic model

Once the 3D SH-SY5Y cells adapted to the flow, after 24h, they were transferred from the LB1 to the lower chamber of the LB2 containing bEnd.3 cells seeded in the upper chamber for 7 days to perform the passage of gH625 functionalized liposomes loaded with rhodaminated PACAP (gH625-lipoPACAP-Rho) in a 3D dynamic *in vitro* BBB millifluidic model (**Fig.11**). LB2 was connected to the respective mixing chamber and to a peristaltic pump, the flow was then set at 150 $\mu$ l /min for 24h. After 24h, gH625-lipoPACAP-Rho were injected into the upper chamber, loaded with 20 $\mu$ M PACAP-Rho.

### 3. Results

#### 3.1 Liposome characterization

Liposomes loaded with PACAP-Rho and functionalized on their surface with gH625 were characterized using dynamic light scattering (DLS). The hydrodynamic diameters ( $D_H$ ) and polydispersity index (PDI) of all liposomes were measured, three independent experiments were performed for each sample and each measurement was performed at least in triplicate. Lipo-PACAP and gH625-lipoPACAP present a polydispersity index (PDI)  $<0.3$  indicating a good size distribution (**Table 1**).

Sample	Mean diameter (nm)	Mean PDI
lipo-PACAP	151.2 $\pm$ 1.274	0.080 $\pm$ 0.010
gH625-lipoPACAP	193.9 $\pm$ 8.050	0.265 $\pm$ 0.025

**Table1:**

Liposome characterization

#### 3.2 Lucifer yellow assay

The LY added in the apical side is expected to traverse the intercellular tight junctions and accumulate in the basolateral side. Greater concentrations of LY in the basolateral side indicate an immature, not-fully functional barrier while lower concentrations reflect restricted transport due to the presence of functional TJs resulting in a mature barrier. LY permeation decreases until day 4 where it remains constant until day 6 to decrease until day 8 also luciferase yellow concentration ( $\mu\text{M}$ ) decreased in 8 days (**Fig.2-3**).

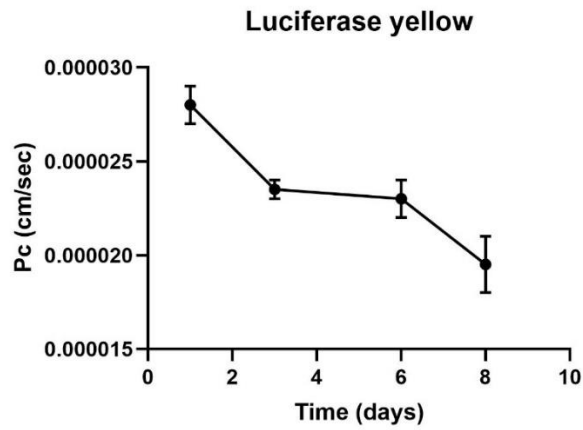


**Fig.2**

Luciferase yellow permeation through bEnd.3 monolayer cells. LY permeation decrease until day 4 where it remains constant until day 6 to decrease until day 8. Lower LY permeation values suggest formation of mature tight junction. Data are expressed  $\pm$  SEM.

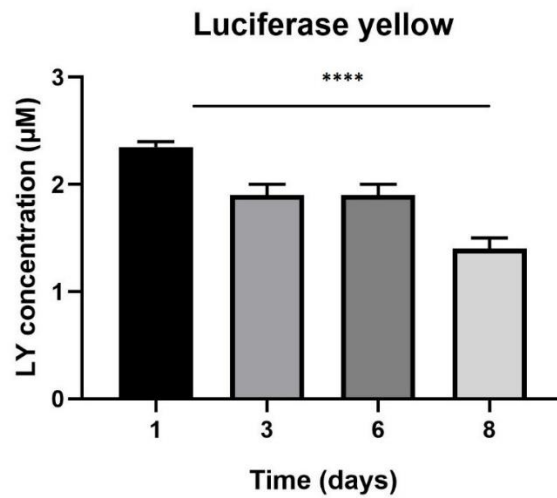


**Fig.3**

Luciferase yellow concentration ( $\mu$ M) in 8 days. The graph shows the means  $\pm$  SEM of three experiments. Statistical analysis was performed through the analysis of variance (ANOVA) and the Dunnet's posttest. The differences were considered significant compared to day one (1).

\*\*\* P < 0.001.

### **3.3 Immunofluorescence assay**

To evaluate the formation of the barrier and its integrity, anti ZO-1, anti N-cadherin and anti- $\beta$  catenin immunofluorescence for bEnd.3 cells was performed. bEnd.3 cells were seeded on the porous membrane of a LB2 and after one week of culture, to encourage the formation of junctions, different indirect immunofluorescence assays were performed. After 24h of the antibodies' incubation, bEnd.3 cells showed an evident fluorescence signal for all three junctions' protein (**Fig.4**). Nuclei were stained with H $\ddot{o}$ chst 33258.

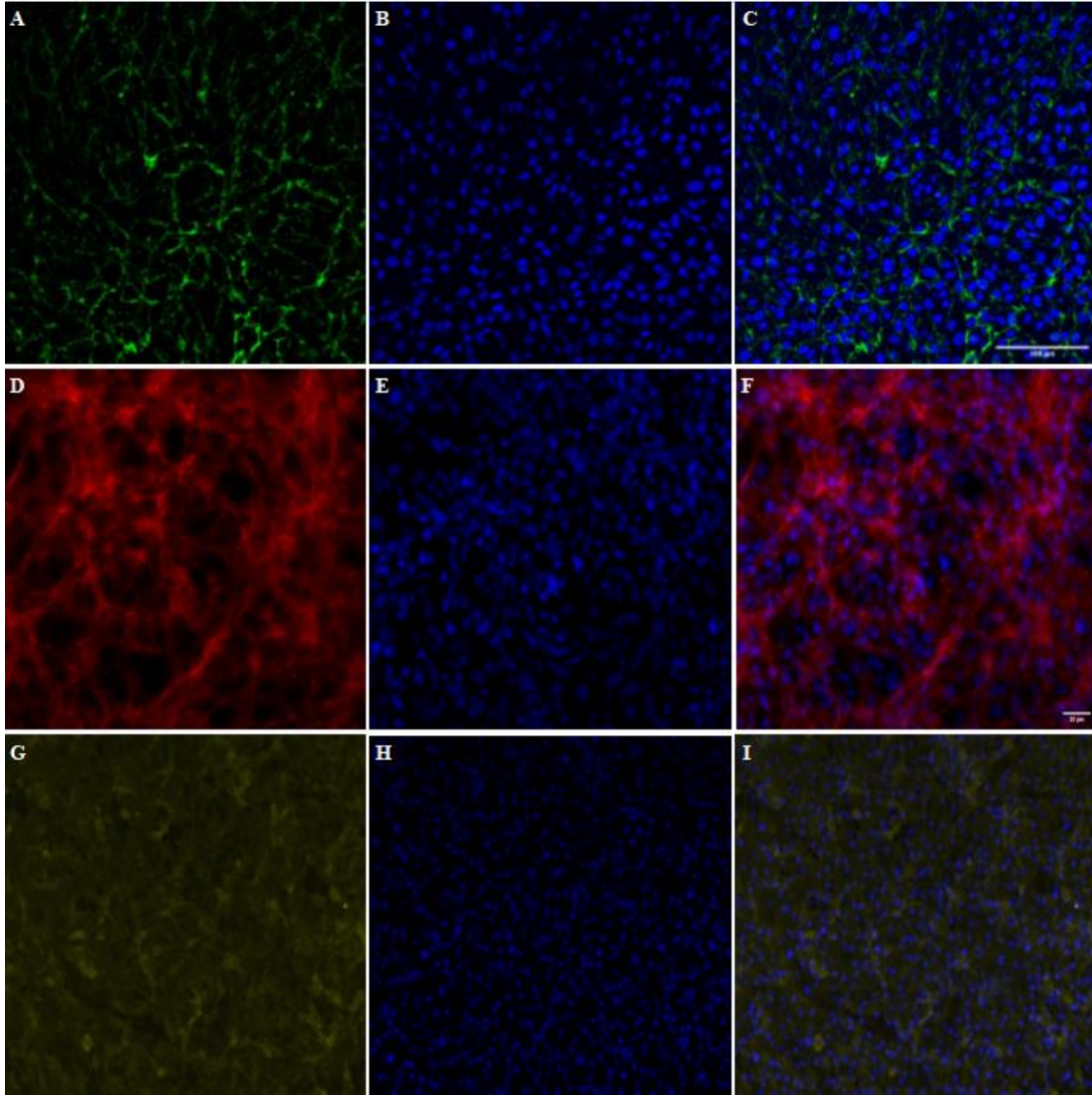


**Fig.4**

Immunofluorescence for ZO1, GFP (A-C),  $\beta$ -catenin, RED (D-F), N-cadherin, Yellow (G-I) on bEnd.3 cultured in LiveBox2 fluid dynamic bio incubator. Secondary antibody, GFP emission. Nuclei were labelled with Hoechst 33258. Scale bar: 20  $\mu$ M.

### 3.4 LDH assay

LDH assay test was used to evaluate the cytotoxicity of the bEnd.3 cells seeded on the porous membrane of a LB2 bioreactor after 7 days. The graph shows an increase in cytotoxicity in bEnd.3 maximum activity rather than bEnd.3 spontaneous activity compared to positive control (Fig.5).

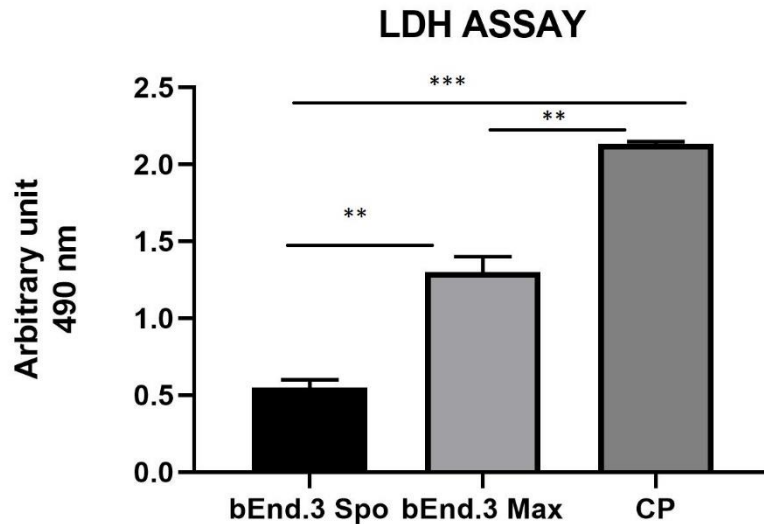


Fig.5

LDH assay for bEnd.3 cells after seeding 8 days. Cytotoxicity is less in bEnd.3 spontaneous activity (bEnd.3 Spo), than in bEnd.3 maximum activity (bEnd.3 Max) compared to Positive Control (CP) at 490 nm. The graph shows the means  $\pm$  SEM of three experiments. Statistical analysis was performed through the analysis of variance (ANOVA) and the Dunnet's posttest. The differences were considered significant compared to Positive Control (CP). \*\*\* $P < 0.0001$ ; \*\* $P < 0.0005$

### 3.5 Spectrofluorimetry assay

To evaluate the passage of PACAP-Rho mediated by gH625-liposome through the porous membrane in LB2 bioreactor containing bEnd.3 cells, spectrofluorimetry was performed. After 30 min of the injection of gH625-lipoPACAP-Rho in the inlet of the upper chamber, samples of medium were taken at regular intervals (30, 60, 90, 120 min) in the outlet of both camera (up and low). There was an increase of PACAP-Rho fluorescence in the lower chamber compared to the upper camera after 30 min of injection (Fig.6) and the fluorescence of the PACAP-Rho bound to gH625-liposome remains high for 2h of the experiment (Fig.7). This increase is more

consistent than the non-functionalized liposome loaded with PACAP-Rho. The LB2 containing the bEnd.3 cells were then placed in the JuLi™ Stage Real-Time Cell History Recorder microscope to continuously acquire images of the cells seeded on the porous membrane before and after the passage of the gh625-liposomePACAP-Rho. The images show an absence of signal for PACAP-Rho on bEnd.3 cells, demonstrating the passage of this latter in the lower chamber. Moreover, cells do not appear to be morphologically damaged by the passage of the gH625-liposomePACAP-Rho (Fig.8).

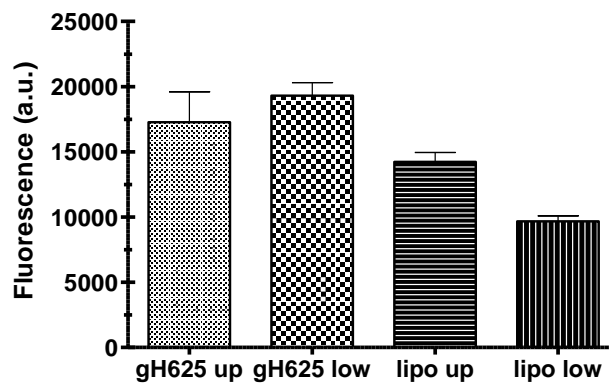
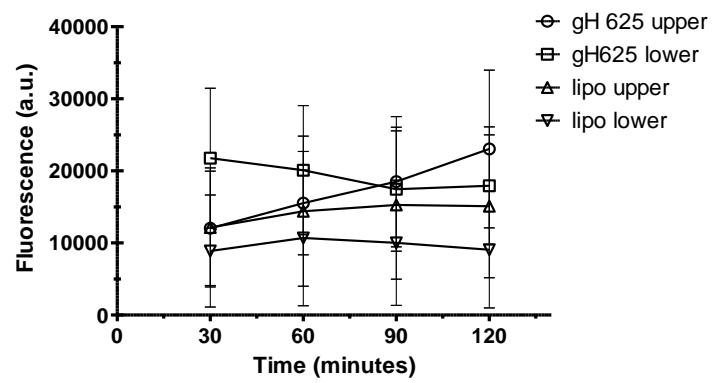


Fig.6

Spectrofluorometric analysis of rhodaminated PACAP (PACAP-Rho) delivery across BBB dynamic in vitro model. Functionalized liposome and non-functionalized liposome were loaded with PACAP-Rho and injected in the upper flow. The passage beyond the endothelial cell layer were then evaluated by sampling downstream the upper flow and the lower flow, respectively.

Dati  $\pm$  SEM.



**Fig.7**

Spectrofluorometric analysis of rhodaminated PACAP (PACAP-Rho) delivery across BBB dynamic in vitro model. Functionalized liposome and non-functionalized liposome were loaded with PACAP-Rho and injected in the upper flow. The passage beyond the endothelial cell layer were then evaluated by sampling downstream the upper flow and the lower flow, respectively.

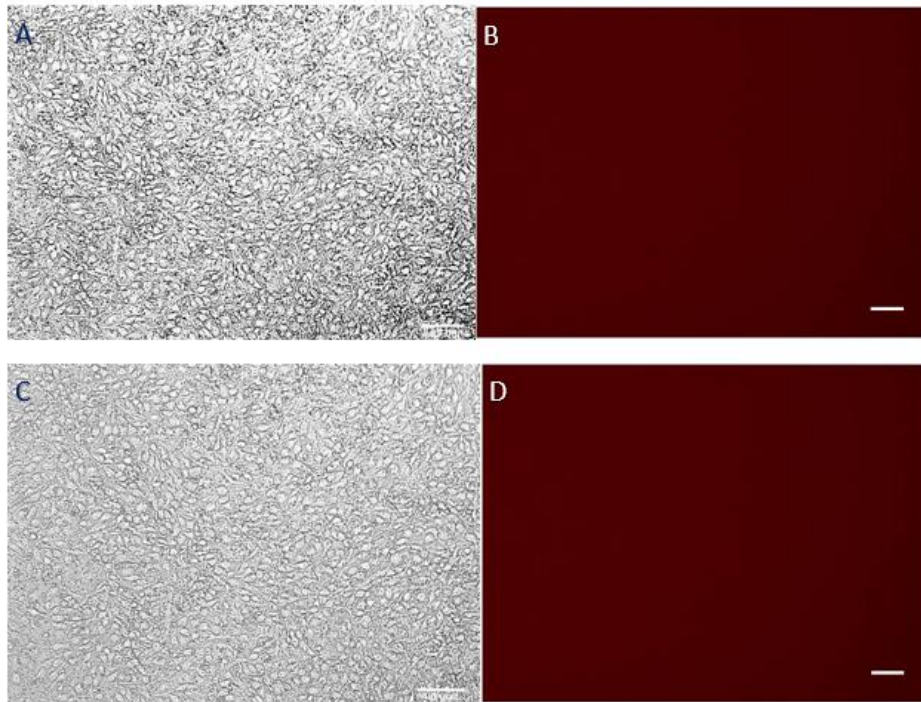


**Fig.8**

bEnd.3 before (A-B) and after (C-D) PACAP loaded functionalized liposome passage. bEnd.3 seeded in LiveBox2 bio incubator do not retain red fluorescence (no PACAP-Rho) indicating that PACAP-Rho loaded functionalized liposomes pass the bEnd3 endothelial layer and become available in the LiveBox2 bottom chamber. Scale bar: 20  $\mu\text{m}$ .

### 3.6 PACAP ELISA assay

Finally, once determined the different passage between gH625-lipoPACAP-Rho and lipo-PACAP-Rho, we performed the time course of PACAP Elisa assay, only for gH625 liposomes. After injection of gH625-lipoPACAP in the endothelial cells compartment, we demonstrated an increase of PACAP concentration endothelial cells chamber during time. SH-SY5Y dopaminergic neurons are exposed to the full concentration (i.e about  $10^{-8}$ M) of PACAP within 60 min (**Fig.9**).

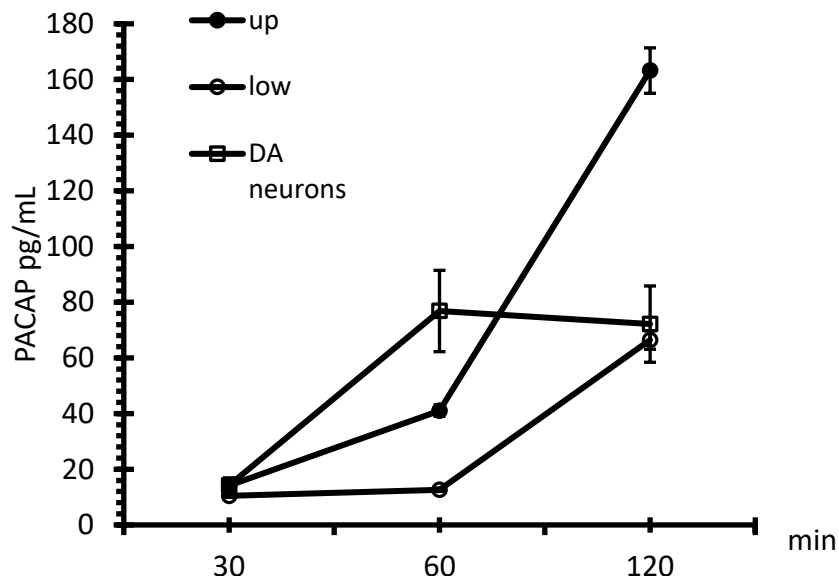


**Fig.9**

Time course of PACAP in the microfluidic millifluidic system, assessed by PACAP Elisa assay. Up= upper chamber, low=lower chamber, DA neurons= dopaminergic neurons. Data are expressed  $\pm$  SEM.

### 3.7 Spheroid immunofluorescence

3D SH-SY5Y were cultured in hanging drop culture and then transferred in LB1 to set the suitable flow condition. Once determined it, different indirect immunofluorescence assays were performed to evaluate the presence of PACAP receptors, (PAC<sub>1</sub>-R, VPAC<sub>1</sub>, VPAC<sub>2</sub>), Ki67, ZO-1 and  $\beta$ 3 Tubulin proteins. After 1:45 min of incubation of these antibodies, 3D SH-SY5Y cells showed an evident fluorescence signal for and PAC<sub>1</sub>-R (**Fig.10A-B**), while the signal for VPAC<sub>1</sub> (**Fig.10 C-D**) and VPAC<sub>2</sub> (**Fig.10 E-F**) was less evident, suggesting, as shown in literature, a major presence of PAC1 in this cell line (Joo et al., 2004). Spheroids also shown the presence of Ki67 (**Fig. 10 G**) proliferation protein, demonstrating the high proliferation of 3D SH-SY5Y cells in dynamic condition. The presence of the tight junction protein ZO-1 shows the tight adhesion of cells under the flow (**Fig. 10 H**), while  $\beta$ 3 Tubulin show neural marker portion of 3D SH-SY5Y enriched (**Fig. 10 I**). Nuclei were stained with DAPI.

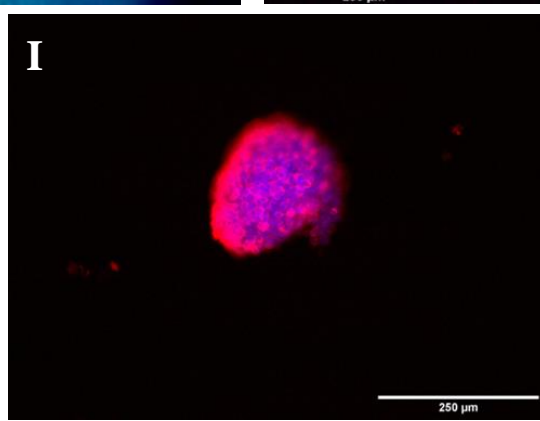
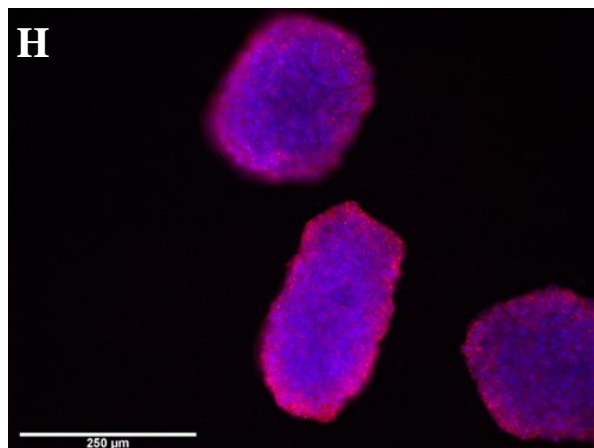
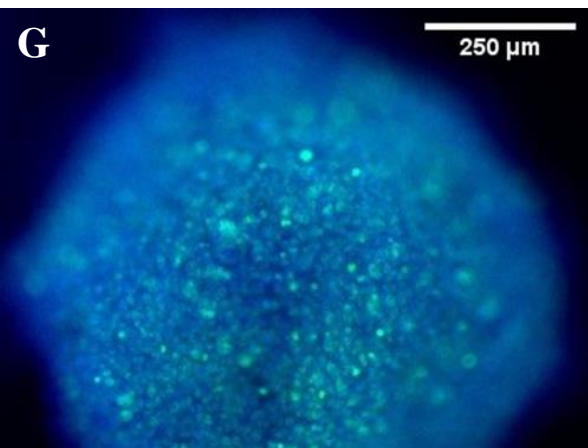
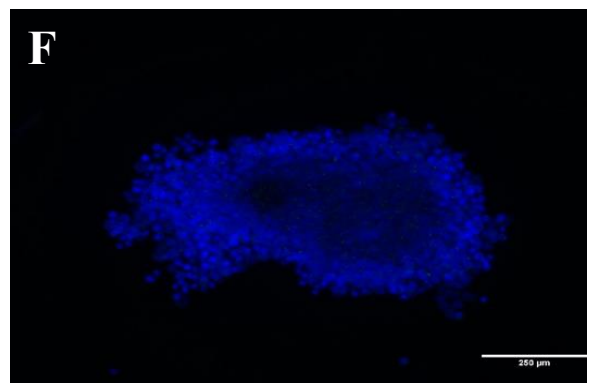
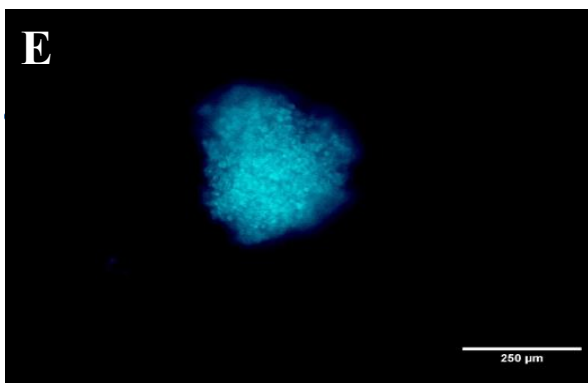
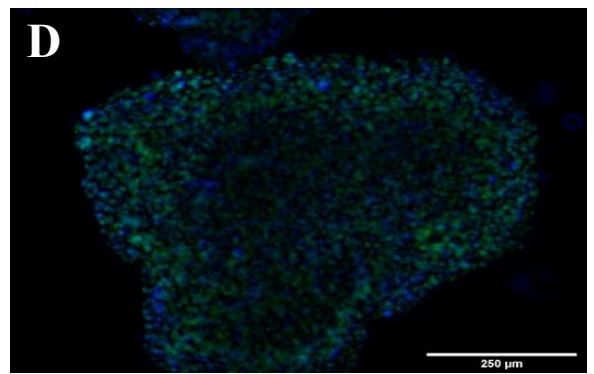
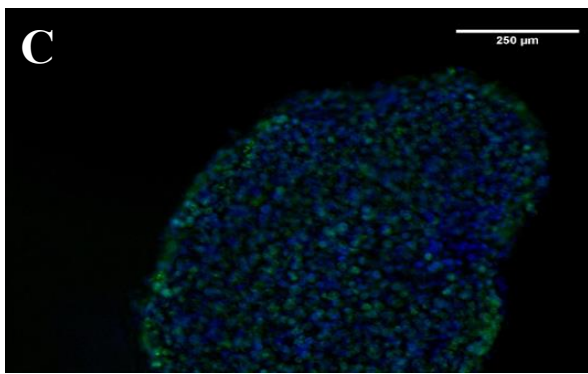
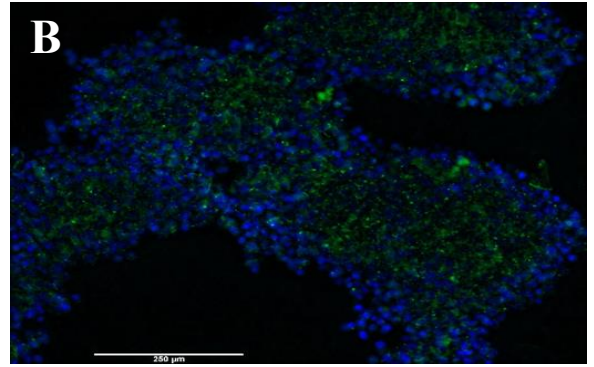
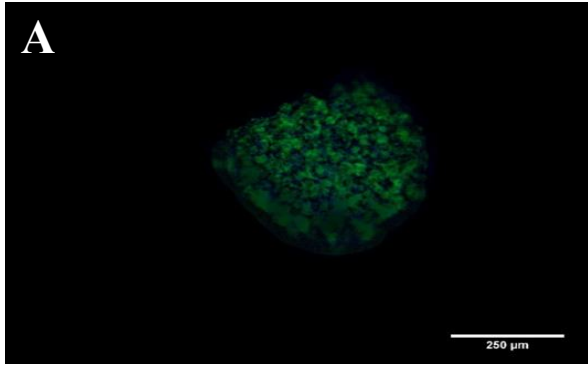


**Fig.10**

Representative image of spheroids obtained by culturing human neuroblastoma SH-SY5Y SH-SY5Y cells in the lower chamber of LB2/bEnd.3 cells. Spheroids were immunoreacted with PACAP RECEPTOR primary antibody (GFP, A-B), VPAC<sub>1</sub> primary antibody (GFP, C-D), VPAC<sub>2</sub> (GFP, E-F). Cells were also immunoreacted to Ki67 antibody, (GFP, G), ZO1 (RFP, H) and  $\beta$ -tubulin III (RFP, I). Nuclei, DAPI. Image were acquired as Z stack with the JuLI Stage fluorescence recorder and maximum intensity projection was showed.

### 3.8 gH625-lipoPACAP-Rho through a 3D dynamic *in vitro* BBB millifluidic model

Once 3D SH-SY5Y cells were adapted to the flow in LB1, after 24h, they were transferred in the lower chamber of LB2 containing bEnd.3 cells seeded in the upper chamber for 7 days. This 3D BBB set is useful to perform the passage of gH625-lipoPACAP-Rho in LB2 (**Fig.11**). After 2h to the injection of the gH625-lipoPACAP-Rho in the inlet tube of the LB2 we can show Rho signal in 3D SH-SY5Y, demonstrating the passage of PACAP-Rho through the endothelial cells' monolayer and the internalization of this latter in 3D SH-SY5Y cells (**Fig.12**).

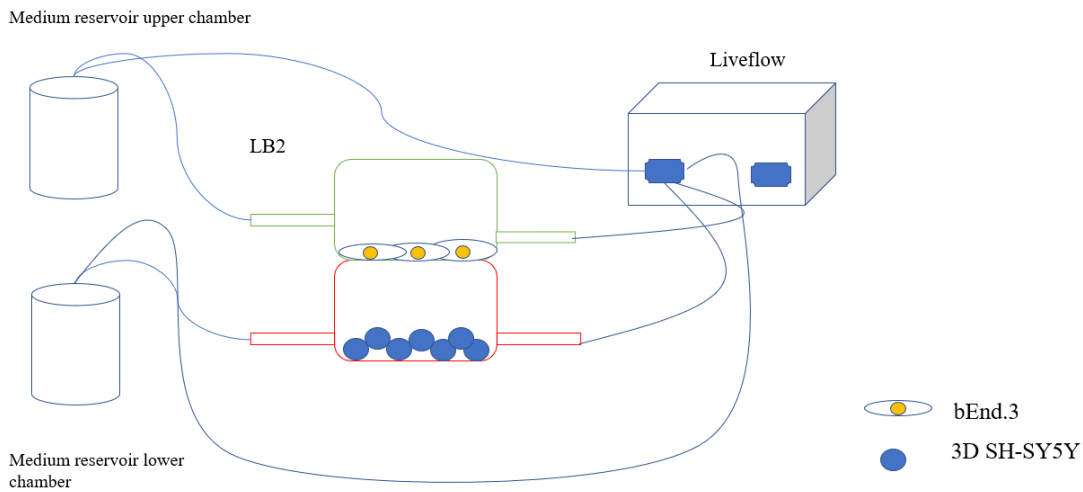


**Fig.11**

Schematic view of a dynamic bioreactor: Live Box 2 (LB2) is composed by an upper chamber connected to a medium reservoir and to a Liveflow pump (250  $\mu$ L/min) and a lower chamber connected to a medium reservoir and to a Liveflow pump (250  $\mu$ L/min). In the upper chamber, bEnd.3 cells are seeded on the porous membrane, in the lower chamber there are neuroblastoma cells (3D SH-SY5Y).

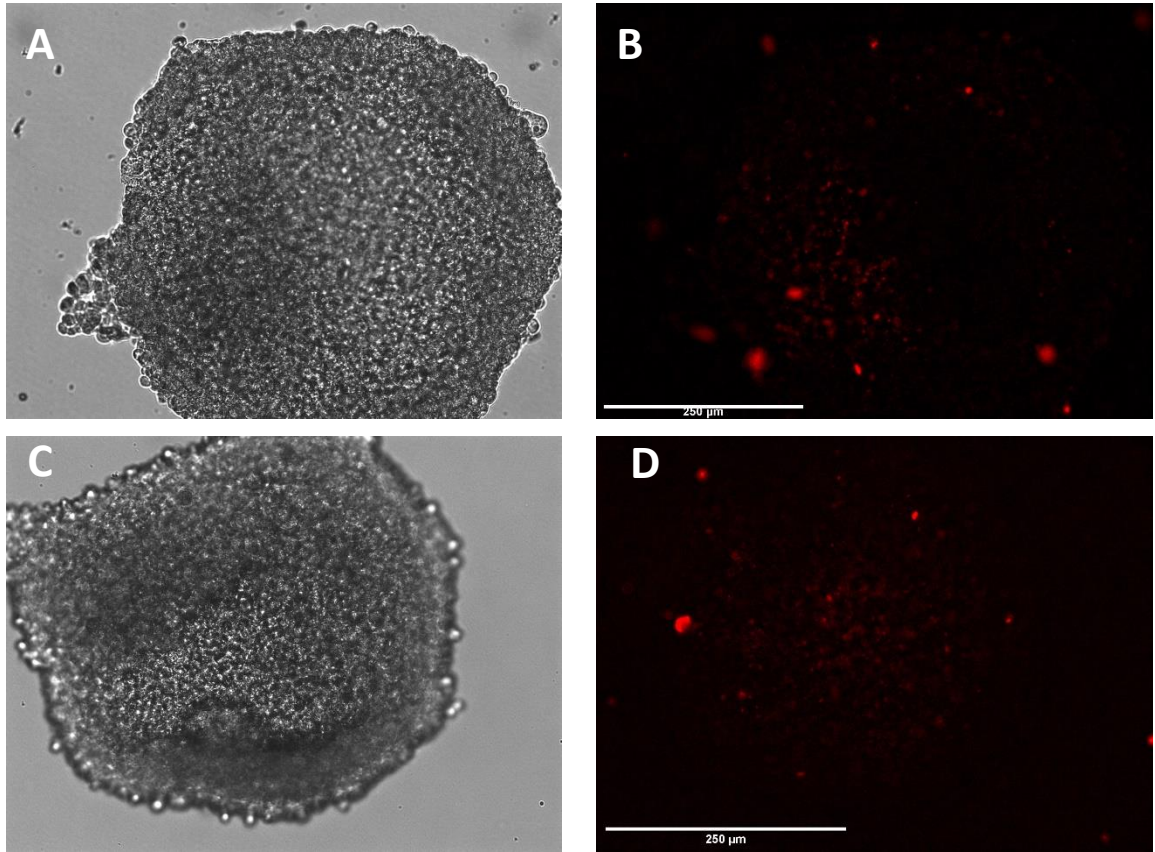


**Fig.12**

Representative image of spheroids obtained by culturing human neuroblastoma SH-SY5Y cells in the lower chamber of LB2/bEnd.3 cells. After the passage of gH625-liposome PACAP-Rho, spheroids retain labeling for PACAP-Rho (B-D). Image were acquired as Z stack with the JuLI Stage fluorescence recorder and maximum intensity projection was showed. Scale bar: 250  $\mu\text{m}$ .

#### 4. Discussion

The BBB is a highly selective anatomical-functional structure. These functions are due to its complex anatomy, which does not allow the diffusion of many solutes from the interstitial fluid to the cerebral parenchyma. This allows the barrier to perform its main neuroprotective function against toxins and metabolites, but at the same time, many drugs are unable to cross the BBB and are pumped externally by an active transporter (Alyautdin et al., 2016). These pumps, while performing a protective action represent, at least in some cases, an obstacle in the treatment of neurodegenerative diseases (Alavijeh et al., 2005). There are numerous *in vitro* approaches that allow to study BBB in order to find a valid pharmacological approach. However, many *in vitro* systems are far from physiological reality, so recently *in vitro* dynamic models have been developed to recreate biological barriers and to modulate cell culture environment to simulate the situation *in vivo* as much as possible (Rouwkema et al., 2011). Among these, there are millifluidic bioreactors that guarantee a continuous circulation of nutrients and a relevant cell density (Giusti et al., 2017). They are characterized by the presence of a membrane that divides an upper and a lower chamber, each with an independent flow. These models allow to test the systemic effects of drugs and have a deeper understanding of the transport mechanisms through the BBB. In fact, the ability to recreate a BBB model *in vitro* and reproduce as closely as possible the physiological conditions associated with it, represents a crucial point for managing neurodegenerative diseases and for formulating a possible cure for them. In this regard, this study aimed to analyze the efficiency of gH625-liposome to deliver PACAP through a dynamic millifluidic bioreactor model of BBB (Livebox2, LB2). To allow a continuous circulation of nutrients, this bioreactor is connected to a peristaltic pump (Liveflow). bEnd.3, commonly used for BBB *in vitro* (Rodrigues, 2019) form an intact monolayer after one week, as Lucifer yellow assay demonstrated. The expression of junction's proteins showed by immunofluorescence analyses confirmed the formation of a stable barrier. Furthermore, cells seem not to be damaged, as showed by morphological analysis, confirmed also by the LDH cytotoxicity test. Results confirming the main ability of bEnd.3 cells to form an integer barrier as demonstrated by Rodrigues in 2019. Moreover, these cells can be easily adapted on the porous membrane of LB2 bioreactor transforming it in a BBB bioreactor without toxic damage. We are currently conducting quantitative analyses of adherent and tight cell junctions to evaluate, the amount of these junctions in the endothelial monolayer, in order to provide more information on the formation of a stable barrier. Furthermore, our system allowed to perform the evaluation of the

PACAP amounts able to cross the layer of bEnd.3, seeded on the porous membrane. After the gH625-lipoPACAP-Rho injection into the inlet of the superior chamber of the bioreactor, we monitored by spectrofluorimetric analyses the distribution of PACAP-Rho between chambers and endothelial layer, respectively. Our results showed an increase in the amount of PACAP in the lower chamber after only 30 min compared to the lipo-PACAP-Rho. In addition, for the whole duration of the experiment the fluorescence of PACAP-Rho bound to the gH625lipo remained high compared to the lipoPACAP-Rho. Hence, the time course indicates a fast passage of PACAP-Rho through the cells if delivered by functionalized nanodelivery system. Morphological analyses on cell layer showed the lack of fluorescent signal before and after the passage of gH625-lipoPACAP-Rho, suggesting that PACAP-Rho was conveyed to the lower chamber through the layer of cells, without any retaining within bEnd3 cells. Furthermore, gH625 peptide results an effective functionalization to realize a useful cargo to transport PACAP across bEnd.3 monolayer without causing cell damage as demonstrated by our morphological analyses. Even if more specific viability assays on this cell line after nanodelivery passage are required to confirm the main ability of gH625 to cross a membrane without disrupt them, our results are in good agreement with literature reporting very low cell toxicity (Valiante et al, 2015). Once determined the greater ability of the functionalized liposome to carry PACAP into the millifluidic LB2, the bioreactor containing bEnd3 cells was connected to a single chamber bioreactor with independent flow, containing dopaminergic neurons. Our results demonstrated that PACAP reaches the dopaminergic compartment at physiological concentration ( $10^{-8}\text{M}$ ). This result is very interesting since PACAP usually acts as neuroprotective agent at this physiological concentration *in vivo* (Vaudry et al., 2009). This finding provided important proof that PACAP can be effectively released by functionalized nanodelivery system through the endothelial layer inside the fluid-dynamic system. To ameliorate our 3D dynamic *in vitro* BBB millifluidic model, we used an LB2 with bEnd.3 cells seeded in the upper chamber and implemented the neuronal compartment with 3D SH-SY5Y-N in the lower chamber, to verify if the delivery of PACAP was affected by 3D spheroid architecture. A neuronal compartment is mandatory to realize a complex 3D dynamic *in vitro* BBB millifluidic model with endothelial cell line (the main component of BBB) and neuronal cell line. 3D neuronal spheroids in LB2 were kept in flow 48h in a single flow bioreactor (LB1) to set the suitable flow condition. PACAP delivery was performed in LB2 in 24h. Our results showed that PACAP-Rho can cross endothelial brain cells from the blood compartment and can

be internalized in complex cell spheroids 3D structures in the neuronal compartment within 24h. Although it is useful to extend experimental conditions such different flow time and spheroid architecture resistance in flow conditions, our results suggest that our nanodelivery system is suitable for enhanced *in vitro* pharmacodynamic and pharmacokinetics studies.

## **5. Conclusion**

The study demonstrated the ability of our nanodelivery system, made by functionalized liposomes and loaded with specific molecule to cross a fluid-dynamic model BBB *in vitro*. We first demonstrated the passage of our functionalized nanodelivery system in a stable, integer and viable brain endothelial cell monolayer. Then, we implemented our BBB *in vitro* model using a neural cell line in a single bioreactor. PACAP efficiently flows through endothelial cells, accumulates in the neuronal compartment at physiological amounts and can be internalized in neural spheroids. This study allows us to state that: a) our fluid dynamic BBB model is suitable for enhanced drug delivery studies; b) gH625 increases the release efficiency of PACAP in our *in vitro* fluid dynamic model of BBB. These findings represent an important step to further experimental investigations on PACAP administration as a therapeutic agent by enhanced drug delivery system.

## References

- Abbott, N.J., Rönnbäck, L., Hansson, E. (2006) Astrocyte-endothelial interactions at the blood-brain barrier. *Nat Rev Neurosci.* Jan;7(1):41-53. doi: 10.1038/nrn1824. PMID: 16371949
- Alavijeh, M.S., Chishty, M., Qaiser, M.Z., Palmer, A.M. (2005). Drug metabolism and pharmacokinetics, the blood-brain barrier, and central nervous system drug discovery. *NeuroRx.* 554-71. doi: 10.1602/neurorx.2.4.554.
- Alyautdin, R., Khalin, I., Nafeeza, M.I., Haron, M.H., Kuznetsov, D. (2014) Nanoscale drug delivery systems and the blood-brain barrier. *Int J Nanomedicine.* Feb 7;9:795-811. doi: 10.2147/IJN.S52236. PMID: 24550672; PMCID: PMC3926460.
- Arimura, A., Somogyvári-Vigh, A., Miyata, A., Mizuno, K., Coy, D.H., Kitada, C. (1991). Tissue distribution of PACAP as determined by RIA: highly abundant in the rat brain and testes. *Endocrinology.* 2787-9. doi: 10.1210/endo-129-5-2787.
- Bilodeau, K., and Mantovani, D. (2006). Bioreactors for tissue engineering: focus on mechanical constraints. A comparative review. *Tissue Eng.* 2367-83. doi: 10.1089/ten.2006.12.2367.
- Brown, D., Tamas, A., Reglödi, D., Tizabi, Y. (2013). PACAP protects against salsolinol-induced toxicity in dopaminergic SH-SY5Y cells: implication for Parkinson's disease. *J Mol Neurosci.* 600-7. doi: 10.1007/s12031-013-0015-7.
- Campbell, R.M., and Scanes, C.G. (1992). Evolution of the growth hormone-releasing factor (GRF) family of peptides. *Growth Regul.* 175-91.
- Canonica, P.L., Copani, A., D'Agata, V., Musco, S., Petralia, S., Travali, S., Stivala, F., Cavallaro, S. (1996). Activation of pituitary adenylate cyclase-activating polypeptide receptors prevents apoptotic cell death in cultured cerebellar granule cells. *Acad Sci.* 805:470–472. doi: 10.1111/j.1749-6632.1996.tb17505. x.
- Cavallaro, S., Copani, A., D'Agata, V., Musco, S., Petralia, S., Ventra, C., Stivala, F., Travali, S., Canonica, P.L. (1996). Pituitary adenylate cyclase activating polypeptide prevents apoptosis in cultured cerebellar granule neurons. *Mol Pharmacol.* 50:60– 66.

- Cecchelli, R., Aday, S., Sevin, E., Almeida, C., Culot, M., Dehouck, L., Coisne, C., Engelhardt, B., Dehouck, M.P., Ferreira, L. (2014). A stable and reproducible human blood-brain barrier model derived from hematopoietic stem cells. *PLoS One*. Jun 17;9(6):e99733. doi: 10.1371/journal.pone.0099733. PMID: 24936790; PMCID: PMC4061029.
- Chang, J.Y., Korolev, V.V., Wang, J.Z. (1996). Cyclic AMP and pituitary adenylate cyclase-activating polypeptide (PACAP) prevent programmed cell death of cultured rat cerebellar granule cells. *Neurosci Lett*. 206:181–184. doi: 10.1002/jnr.10530.
- Chitnis, T., and Weiner, H. L. (2017). CNS inflammation and neurodegeneration. *J. Clin. Invest*. 127, 3577–3587. doi: 10.1172/jci90609.
- Cummings, J.L. and Cole, G. (2002). Alzheimer disease. *Med. Assoc.* 2335–2338. doi: 10.1001/jama.287.18.2335
- Deguil, J., Chavant, F., Lafay-Chebassier, C., Pérault-Pochat, M.C., Fauconneau, B., Pain, S., (2010). Neuroprotective effect of PACAP on translational control alteration and cognitive decline in MPTP parkinsonian mice. *Neurotox Res*. 142-55. doi: 10.1007/s12640-009-9091-4.
- Deli, M. A., Ábrahám, C. S., Kataoka, Y., Niwa, M. (2005). Permeability Studies on In vitro Blood–Brain Barrier Models: Physiology, Pathology, and Pharmacology. *Cellular and Molecular Neurobiology*. 25, (1), 59-127.
- Dos Santos Rodrigues, B., Lakkadwala, S., Kanekiyo, T., Singh, J. (2019). Development and screening of brain-targeted lipid-based nanoparticles with enhanced cell penetration and gene delivery properties. *Int J Nanomedicine*. Aug 14;14:6497-6517. doi: 10.2147/IJN.S215941. PMID: 31616141; PMCID: PMC6699367.
- Erhardt, N.M., and Sherwood, N.M. (2004). PACAP maintains cell cycling and inhibits apoptosis in chick neuroblasts. *Mol Cell Endocrinol*. 221:121–134.
- Falanga, A., Vitiello, M.T., Cantisani, M., Tarallo, R., Guarnieri, D., Mignogna, E., Netti, P., Pedone, C., Galdiero, M., Galdiero, S. (2011). A peptide derived from herpes simplex virus type 1 glycoprotein H: membrane translocation and applications to the delivery of quantum dots *Nanomedicine*. 2011; 7:925– 934.

- Feher, M., Gaszner, B., Tamas, A., Gil-Martinez, A. L., Fernandez-Villalba, E., Herrero, M. T., (2018). Alteration of the PAC1 receptor expression in the basal ganglia of MPTP-induced parkinsonian macaque monkeys. *Neurotox. Res.* 33, 702–715. doi: 10.1007/s12640-017-9841-7.
- Foty, R. (2011). A simple hanging drop cell culture protocol for generation of 3D spheroids. *J Vis Exp.* 2011 May 6;(51):2720. doi: 10.3791/2720. PMID: 21587162; PMCID: PMC3197119.
- Fukuhara, C., Suzuki, N., Matsumoto, Y., Nakayama, Y., Aoki, K., Tsujimoto, G., Inouye, S.I., Masuo, Y. (1997). Day–night variation of pituitary adenylate cyclase activating polypeptide (PACAP) level in the rat suprachiasmatic nucleus. *Neurosci. Lett*; 229: 49–52.
- Galdiero, S., Falanga, A., Vitiello, M., Browne, H., Pedone, C., Galdiero, M. (2005). Fusogenic domains in herpes simplex virus type 1 glycoprotein H. *J. Biol. Chem.*; 280 28632–28643.
- Ghatei, M.A., Takahashi, K., Suzuki, Y., Gardiner, J., Jones, P.M., Bloom, S.R. (1993). Distribution, molecular characterization of pituitary adenylate cyclase activating polypeptide and its precursor encoding messenger RNA in human and rat tissues. *J Endocrinol*; 136:159–166.
- Giusti, S., Mazzei, D., Cacopardo, L., Mattei, G., Domenici, C., Ahluwalia, A. (2017) *Environmental Control in Flow Bioreactors*. Academic Editor: B.WayneBequette; DOI: 10.3390/pr5020016.
- Giusti, S., Sbrana, T., La Marca, M., Di Patria, V., Martinucci, V., Tirella, A., Domenici, C., Ahluwalia, A. (2014) A novel dual-flow bioreactor simulates increased fluorescein permeability in epithelial tissue barriers” *Biotechnol. J*; 9, 1175–1184 DOI 10.1002/biot.201400004.
- Gonzalez, B.J., Basille, M., Vaudry, D., Fournier, A., Vaudry, H. (1997). Pituitary adenylate cyclase-activating polypeptide promotes cell survival and neurite outgrowth in rat cerebellar neuroblasts. *Neuroscience*; 78:419–430.
- Han, P., Tang, Z., Yin, J., Maalouf, M., Beach, T.G., Reiman, E.M., Shi, J. (2014). Pituitary adenylate cyclase-activating polypeptide protects against  $\beta$ -amyloid toxicity. *Neurobiol Aging*.

Sep;35(9):2064-71. doi: 10.1016/j.neurobiolaging.2014.03.022. Epub 2014 Mar 22. PMID: 24726470.

Han, P., Caselli R.J., Baxter, L., Serrano, G., Yin, J., Beach, T.G., Reiman, E.M., Shi, J. (2015). Association of pituitary adenylate cyclase-activating polypeptide with cognitive decline in mild cognitive impairment due to Alzheimer disease. *JAMA Neurol.* Mar;72(3):333-9. doi: 10.1001/jamaneurol.2014.3625. PMID: 25599520; PMCID: PMC5924703.

Harmar, A.J., Arimura, A., Gozes, I., Journot, L., Laburthe, M., Pisegna, J.R., Rawlings, S.R., Robberecht, P., Said, S.I., Sreedharan, S.P. (1998). Nomenclature of receptors for vasoactive intestinal peptide and pituitary adenylate cyclase-activating polypeptide. *International Union of Pharmacology.* XVIII 1998; *Pharmacol Rev* 50:265–270.

Iachetta, G., Falanga, A., Molino, Y., Masse, M., Jabès, F., Mechioukhi, Y., Laforgia, V., Khrestchatsky, M., Galdiero, S., Valiante, S. (2019) gH625-liposomes as tool for pituitary adenylate cyclase-activating polypeptide brain delivery. *Sci Rep.* Jun 24;9(1):9183. doi: 10.1038/s41598-019-45137-8.

Joo, K.M., Chung, Y.H., Kim, M.K., Nam, R.H., Lee, B.L., Lee, K.H., Cha, C.I. (2004). Distribution of vasoactive intestinal peptide and pituitary adenylate cyclase-activating polypeptide receptors (VPAC1, VPAC2, and PAC1 receptor) in the rat brain. *J Comp Neurol.* 2004 Aug 30;476(4):388-413. doi: 10.1002/cne.20231. PMID: 15282712.

Lamine, A., Ngoc Duc, D., Maucotel, J., Couvineau, A., Vaudry, H., Chatenet, D., Vaudry, D., Fournier, A. (2015). Characterizations of a synthetic pituitary adenylate cyclase-activating polypeptide analog displaying potent neuroprotective activity and reduced in vivo cardiovascular side effects in a Parkinson's disease model. *Neuropharmacology.* 2016 Sep; 108:440-50. doi: 10.1016/j.neuropharm.05.014. Epub 2015 May 22.

Nonaka, N., Banks, W.A., Mizushima, H., Shioda, S., Morley, J.E. (2002). Regional differences in PACAP transport across the blood-brain barrier in mice: a possible influence of strain, amyloid beta protein, and age. *Peptides.* Dec;23(12):2197-202. doi: 10.1016/s0196-9781(02)00248-6. PMID: 12535699.

Nzou, G., Wicks, R.T., Wicks, E.E., Seale, S.A., Sane, C.H., Chen, A., Murphy, S.V., Jackson, J.D., Atala, A.J. (2018). Human Cortex Spheroid with a Functional Blood Brain Barrier for

High-Throughput Neurotoxicity Screening and Disease Modeling. *Sci Rep.* May 9;8(1):7413. doi: 10.1038/s41598-018-25603-5. PMID: 29743549; PMCID: PMC5943588.

Pirger, Z, Naskar S, László Z, Kemenes G, Reglődi D, Kemenes I. Reversal of age-related learning deficiency by the vertebrate PACAP and IGF-1 in a novel invertebrate model of aging: the pond snail (*Lymnaea stagnalis*). *J Gerontol A Biol Sci Med Sci.* 2014 Nov;69(11):1331-8. doi: 10.1093/gerona/glu068. Epub 2014 May 20. PMID: 24846768; PMCID: PMC4197904.

Polonchuk, L., Chabria, M., Badi, L., Hoflack, J.C., Figtree, G., Davies, M.J., Gentile, C. (2017). Cardiac spheroids as promising in vitro models to study the human heart microenvironment. *Sci Rep.* Aug 1;7(1):7005. doi: 10.1038/s41598-017-06385-8. PMID: 28765558; PMCID: PMC5539326.

Rapaport, D. and Shai, Y. (1991). Interaction of fluorescently labeled pardaxin and its analogues with lipid bilayers. *J Biol Chem.* Dec 15;266(35):23769-75. PMID: 1748653.

Reese TS, Karnovsky MJ. Fine structural localization of a blood-brain barrier to exogenous peroxidase. *J Cell Biol.* 1967 Jul;34(1):207-17. doi: 10.1083/jcb.34.1.207. PMID: 6033532; PMCID: PMC2107213.

Reichel, A., Begley, D. J., Abbott, N. J. (2003) *The Blood-Brain Barrier*. Springer. 307-324.

Reglodi D, Lubics A, Tamás A, Szalontay L, Lengvári I (2004). Pituitary adenylate cyclase activating polypeptide protects dopaminergic neurons and improves behavioral deficits in a rat model of Parkinson's disease. *Behavioural Brain Research* 151: 303–312.

Ren, T.B., Xu, W., Zhang, W., Zhang, X.X., Wang, Z.Y., Xiang, Z., Yuan, L., Zhang, X.B. (2018). A General Method to Increase Stokes Shift by Introducing Alternating Vibronic Structures. *J Am Chem Soc.* Jun 20;140(24):7716-7722. doi: 10.1021/jacs.8b04404. Epub 2018 Jun 8. PMID: 29792690.

Rouwkema, J., Gibbs, S., Lutolf M., Martin, I., Vunjak-Novakovic, G., Malda, J. (2011). In vitro platforms for tissue engineering: implications to basic research and clinical translation. *J Tissue Eng Regen Med.*; 5(8): e164–e167. doi:10.1002/term.414.

Sandoval, K.E. and Witt, K.A. (2008). Blood-brain barrier tight junction permeability and ischemic stroke, *Neurobiol. Dis.* 32. 200–219.

- Shioda, S., Legradi, G., Leung, W.C., Nakajo, S., Nakaya, K., Arimura, A. (1994). Localization of pituitary adenylate cyclase-activating polypeptide and its messenger ribonucleic acid in the rat testis by light and electron microscopic immunocytochemistry and in situ hybridization. *Endocrinology*; 135:818– 825.
- Shri, M., Agrawal, H., Rani, P., Singh, D., Onteru, S.K. (2017). Hanging Drop, A Best Three-Dimensional (3D) Culture Method for Primary Buffalo and Sheep Hepatocytes. *Sci Rep.* Apr 26;7(1):1203. doi: 10.1038/s41598-017-01355-6. PMID: 28446763; PMCID: PMC5430879.
- Somogyvari-Vigh, A. and Reglodi, D., (2004). Pituitary Adenylate Cyclase Activating Polypeptide: A Potential Neuroprotective Peptide”, *Current Pharmaceutical Design.* 10: 2861.
- Spindler, K.R. and Hsu, T.H. (2012). Viral disruption of the blood-brain barrier. *Trends Microbiol.* Jun;20(6):282-90. doi: 10.1016/j.tim.2012.03.009. Epub 2012 May 6. PMID: 22564250; PMCID: PMC3367119.
- Takei, N., Skoglösa, Y., Lindholm, D. (1998). Neurotrophic and neuroprotective effects of pituitary adenylate cyclase-activating polypeptide (PACAP) on mesencephalic dopaminergic neurons. *Neurosci. Res.* 54, 698-706.
- Valiante, S., Falanga, A., Cigliano, L., Iachetta, G., Busiello, R.A., La Marca, V., Galdiero, M., Lombardi, A., Galdiero, S. (2015). Peptide gH625 enters into neuron and astrocyte cell lines and crosses the blood–brain barrier in rats” *International Journal of Nanomedicine*; 10(1) 1885—1898.
- Vaudry D., Gonzales B.J., Basille M., Yon L., Fournier A. and Vaudry H. “Pituitary adenylate cyclase-activating polypeptide and its receptors: from structure to functions” *Pharmacol.* 2000; Rev. 52: 269-324.
- Vaudry D., Falluel-Morel A., Bourgault S., Basille M., Burel D., Wurtz O., Fournier A., Chow B.K., Hashimoto H., Galas L., Vaudry, H. (2009). Pituitary adenylate cyclase-activating polypeptide and its receptors: 20 years after the discovery. *Pharmacol.* 2009; Rev. 61: 283-357.
- Wang G, Pan J, Tan Y-Y, Sun X-K, Zhang Y-F, Zhou H-Y, Ren R-J, Wang X-J and Chen S-D (2008). Neuroprotective effects of PACAP27 in mice model of Parkinson’s disease involved in

the modulation of K(ATP) subunits and D2 receptors in the striatum. *Neuropeptides* 42, 267-276.

Wohlfart, S., Gelperina, S., Kreuter, J. (2012). Transport of drugs across the blood–brain barrier by nanoparticles, *J. Control. Release* 161 264–273.

Wolff, A., Antfolk, M., Brodin, B., Tenje, M (2015). In vitro Blood-Brain Barrier Models-An Overview of Established Models and New Microfluidic Approaches. *Journal of Pharmaceutical Sciences*. 104, (9), 2727-2746.

Wu, S., Adams, B.A., Fradinger, E.A., Sherwood, N.M. (2006). Role of two genes encoding PACAP in early brain development in zebrafish. *Ann N Y Acad Sci*. Jul; 1070:602-21. doi: 10.1196/annals.1317.091. PMID: 16888233.

Yuhara, A., Nishio, C., Abiru, Y., Hatanaka, H., Takei, N. (2001). PACAP has a neurotrophic effect on cultured basal forebrain cholinergic neurons from adult rats. *Brain Res Dev Brain Res* 2001; 131:41–45.

Zhao, W., Han, L., Bae, Y., Manickam, D.S. (2019). Lucifer Yellow - A Robust Paracellular Permeability Marker in a Cell Model of the Human Blood-brain Barrier. *J Vis Exp*. Aug 19;(150). doi: 10.3791/58900. PMID: 31475964.

## **Chapter 3:**

### **Neuroprotective effects of gH625-lipoPACAP in an *in vitro* fluid-dynamic model of Parkinson's disease**

Adapted from the article in preparation:

#### **Neuroprotective effects of gH625-lipoPACAP in an *in vitro* fluid-dynamic model of Parkinson's disease**

Teresa Barra<sup>1</sup>, Annarita Falanga<sup>2</sup>, Valentina Del Genio<sup>2</sup>, Stefania Galdiero<sup>2</sup>, Salvatore Valiante<sup>1</sup>

<sup>1</sup>Department of Biology, University of Naples, Federico II, Naples, Italy.

<sup>2</sup>Department of Pharmacy, School of Medicine, University of Naples 'Federico II', Naples, Italy.

*Invitation from MDPI, biomedicines, Research Topic:*

*"Drug Delivery across the Blood-Brain Barrier for the Treatment of Brain Diseases"*

## **Abstract**

Parkinson's disease (PD) is an aggressive and devastating age-related disorder. Although the causes are still unclear, several factors including genetic and environmental are involved. Except for symptomatic drugs, there aren't to date real cures for PD. For this purpose, it is necessary develop disease model to better study this disturb. Neuroblastoma cell line, SH-SY5Y treated with retinoic acid represent a good in vitro model to explore PD since it maintains growth cells to differentiated neuron cells. In the present study SH-SY5Y cells were treated with 1-methyl-4-phenylpyridinium (MPP<sup>+</sup>), a neurotoxin that induces Parkinsonism, and the neuroprotective effects of pituitary adenylate cyclase-activating polypeptide (PACAP), delivered by functionalized liposomes in two different fluid dynamic models was evaluated.

## 1. Introduction

Parkinson's disease (PD) is the second common neurodegenerative disease, with a prevalence of 7 million people worldwide with a prediction of 9 million by 2030 (Dorsey et al., 2007; Lo Bianco et al., 2004; Wirdefeldt et al., 2011). It is a chronic, slow-progressing disorder, worsening with advancing age due to motor and non-motor symptoms (Chaudhuri and Schapira, 2009; Xia and Mao, 2012). Pathologically manifestations are characterized by bradykinesia, rigidity and tremor (Lesage and Brice, 2009). Loss of autonomic cognition are attributable to both abnormal protein aggregates containing  $\alpha$ -synuclein (Lewy bodies) in regions of the central nervous system (CNS) (Schapira, 2008) and to death of dopaminergic neuron (DAn) in the substantia nigra (Dexter and Jenner, 2013). The molecular mechanism underlying PD are still unknown so already treatments are not available. To overcome this limitation *in vitro* studies can be very useful. It is therefore mandatory to develop a stable and reliable cell model in order to study the pathogenesis of PD to better validate adequate therapeutic agents. Neuroblastoma cell line, SH-SY5Y represent an ideal *in vitro* PD cell mode. They derived from human neuroblastoma SK-N-SH after three subclone, resulting from a biopsy of human bone marrow (Kovalevich and Langford, 2013). This cell line has been used extensively for the expression of neuronal markers (tyrosine and dopamine- $\beta$ -hydroxylase), specific absorption of norepinephrine and expresses one or more neurofilament proteins; these cells express also opioid, muscarinic and nerve growth factor receptors (Joshi et al., 2006). Therefore, they are adrenergic in the phenotype but express also dopaminergic markers and, as such, are used to study PD, neurogenesis and other cell characteristics cerebral (Lopes et al., 2010; Xie et al., 2010; Xicoy et al., 2017). SH-SY5Y cells can interact spontaneously between two *in vitro* phenotypes, neuroblast-like cells and epithelial cells. The dividing cells are locked in an early neuronal differentiation stage because of few neuronal markers (Biedler et al., 1978; Gilany et al., 2008) but some treatments like retinoic acid (RA), brain-derived neurotrophic factor (BDNF) or the 7 ester of phosphorus 12-O-tetradecanoylforbol-13-acetate (TPA) can force cells to differentiate into neuronal cells. Also, induction of RA causes inhibition of cell growth and an increased norepinephrine production by SH-SY5Y cells. *In vitro*, RA also plays a pivotal role in transition from the proliferating cell to post-mitotic differentiated cell (López-Carballo et al., 2002). SH-SY5Y cells express also dopamine transporter (DAT) that regulates DAn homeostasis (Takahashi et al., 1994). DAT is important for 1-methyl-4-phenylpyridinium (MPP<sup>+</sup>) inclusion into neurons. MPP<sup>+</sup> is a neurotoxic substance derived from 1-methyl 4-phenyl

1,2,3,6-tetrahydro-pyridine (MPTP) that affects the mitochondrial complex I and causes depletion of adenosine triphosphate (ATP), indirectly stimulating the production of reactive species of oxygen (ROS) triggering the release of dopamine in the cytosol from synaptic vesicles, resulting in the induction of apoptosis in DAN (Ito et al., 2017). MPP<sup>+</sup> in non-human primates causes the onset of an experimental parkinsonism which, is to date the most like human idiopathic PD. These deficiencies are associated with a relatively selective loss of cells in the *pars compacta* of the substantia nigra and severe reductions in concentrations of dopamine, norepinephrine and serotonin in the striatum (Gerlach et al., 1991). Reduced activity of complex I and increased susceptibility to MPP<sup>+</sup> have also been observed in cytoplasmic hybrids ("cybrids") containing mitochondrial DNA (mtDNA) from patients with PD (Chaturvedi and Flint, 2013). Some differentiating agents also alter the kinetics of absorption of MPP<sup>+</sup> making SH-SY5Y cells more similar to primary mesencephalic neurons. Another study was conducted using SH-SY5Y cells *in vitro* for study the biological function of microRNA-505 (miR-505) in the MPP<sup>+</sup> induced cytotoxicity. In this regard, SH-SY5Y cells have been treated with MPP<sup>+</sup> to induce disease-associated cell death PD and cytotoxicity (Zhu et al., 2018). Neuropeptides are common signaling molecules in the CNS, involved in a wide range of physiological functions and act as neurotransmitters, neuromodulators and hormones. These, like neurotransmitters can modulate many different processes simultaneously. Human studies revealed that the lack of neuropeptide regulation plays an important role in the pathologies induced by aging like PD (Ma et al., 2015;). Pituitary adenylate cyclase activating polypeptide (PACAP) represents a highly effective cytoprotective peptide that provides endogenous control against a variety of tissue damaging stimuli (Reglodi et al., 2018). It is a polypeptide of 27-38 amino acids conserved of the superfamily secretin / PACAP / glucagon, of which it belongs, for length and nucleotide sequence (Ogata et al., 2015; Watanabe et al., 2016) which shows a particularly high homology with the intestinal peptide vasoactive (VIP). The action on the anti-inflammatory pathways and antioxidant molecules assists the neuroprotective effects (Masmoudi-Kouki et al., 2011; Wada et al., 2013). PACAP stimulates the release and transactivation of other trophic factors, such as BDNF (Fukuchi et al. 2015; Moody et al., 2012; Reglodi et al. 2011). The direct effects of PACAP on nerve cells are further supported by the effects on glial cells, astrocytes, oligodendrocytes and microglial cells (Delgado et al., 2003; Douiri et al., 2016; Masmoudi-Kouki et al., 2011; Vincze et al. 2011). *In vivo* and *in vitro* neuronal cultures, PACAP and VIP possess powerful neuroprotective effects against trauma, ischemia or exogenous toxic

substances such as MPTP and rotenone (Offen et al. 2000; Reglödi et al., 2000; Reglodi et al. 2004; Botia et al. 2011; Rat et al. 2011). Based on these backgrounds, PACAP can offer a therapeutic approach in the treatment of many age-related disorders like PD (Vaudry et al. 2009; Reglodi et al. 2011). In fact, PACAP influences the prevention of DAN degeneration, enhancing DA synthesis (Brown et al., 2013). However, as therapeutic agent present low bioavailability, representing an important concern for the treatment of neurodegenerative disturbs. Liposomes are colloidal systems that carry an active therapeutic agent which can be adsorbed, dissolved, encapsulated or covalently linked. The advantage of loading the therapeutic substances into the nanoparticles for administration to the brain is that of obtaining a high concentration of the drug in the brain parenchyma. Furthermore, these particles can be modified on their surface by various other molecules, such as coating agents, facilitating cellular uptake of the nanoparticles themselves (McCarthy et al., 2014). gH-625 peptide is a cell penetrating peptides (CCPs) derived from the glycoprotein H (gH) of the *Herpes simplex virus 1*. The hydrophobic domain is essential for the insertion of the peptide into the membrane by promoting fusion vesicular (Galdiero et al., 2010; Falanga et al., 2011). It can transport many types of molecules across the membrane bilayer *in vitro* and *in vivo* avoiding endosomal entrapment in the membrane and lysosome degradation (Valiante et al., 2015; Iachetta et al., 2019). Based on this background, we evaluated the neuroprotective effects of PACAP carry out by gH625- liposomes in an *in vitro* fluid-dynamic model of PD. The *in vitro* fluid-dynamic model is represented by two different bioreactors (Livebox1, Livebox2, IVTech, Italy) in which 3D SH-SY5Y cells are treated with MPP+. Through molecular investigations, we were able to show how PACAP can acts against MPP+ effects.

## **2. Material and Methods**

### **2.1 Peptide synthesis**

gH625(Ac-HGLASTLTRWAHYNALIRAF-Cys)-and PACAP27 peptides were synthesized using a standard Fmoc solid-phase (GL Bio chem Ltd, Shanghai, China) (Iachetta et al., 2019) with good yields about 40%. PACAP27 was labeled on resin with Rhodamine for fluorescence measurements (Rapaport and Shai, 1991). An acid solution of trifluoroacetic acid and scavengers was used to deprotect and cleave peptides from the resin. Peptides where purified by preparative reverse-phase HPLC with two different solvent mixtures: H<sub>2</sub>O and 0.1%

trifluoroacetic acid (solvent A), CH<sub>3</sub>CN and 0.1% trifluoroacetic acid (solvent B), with a linear gradient B over 20 min at a flow rate of 15 ml/min. Peptide identity was confirmed with a LTQ-XL linear ion trap mass spectrometer (Thermo Scientific). For the synthesis of DSPE-PEG2000-gH625, 1 eq of DSPE-PEG2000-Mal (Avant Polar Lipids, Birmingham, AL, USA) was reacted with 1 eq. of pure gH625-Cys in DMF in presence of 5 eq of triethylamine (5 eq) for 24 h. The reaction was monitored by RP-HPLC, solvent was evaporated, and the product analyzed using an LTQ-XL. Coupling reagents, N, N-diisopropylethylamine (DIEA), piperidine, trifluoroacetic acid (TFA), Rhodamine (5(6)-Carboxytetramethylrhodamine N-succinimidyl ester and Rink amide resin (0.62 mmol/g of loading substitution), were purchased from Iris-Biotech GMBH.

## **2.2 Liposome preparations**

Large unilamellar vesicles (LUV) derived from PPC/Chol (70/30 mol/mol) were obtained in the protocol previously reported (Galdiero et al., 2005). Lipids, DSPE-PEG2000-gH625 and PACAP-Rho were dissolved in chloroform, then the solvent was removed with a nitrogen gas stream and the sample was lyophilized overnight to obtain a lipid film. This film was suspended in buffer to produce LUVs, freeze-thawed eight times and then extruded 10 times through polycarbonate membranes with 0.1 µm diameter pores (Northern Lipids). The hydrodynamic diameters ( $D_H$ ) and polydispersity index (PDI) of PACAP-Rho loaded liposomes (Lipo) and PACAP-Rho loaded gH625-liposomes (gH625-Lipo) were measured using dynamic light scattering (DLS) (Malvern Zetasizer Nano ZS, Malven, UK). The analysis was performed with He-Ne laser 4 mW operating at 633 nm at scattering angle fixed at 173° and at 25°.

## **2.3 Cell culture**

Human neuroblastoma cells (SH-SY5Y) were grown in Dulbecco's modified Eagle's medium (DMEM) with 10% fetal bovine serum. (FBS), 2 mM of L-glutamine and 100 U/ml penicillin/streptomycin in incubator at 37 °C, with 5% CO<sub>2</sub> and controlled humidity. Cells were enzymatically detached with 0.25% trypsin / EDTA at 70% confluence.

## 2.4 Prestoblue assay

To evaluate the neuroprotective effects of PACAP on SH-SY5Y cells, Prestoblue viability assay was used (Invitrogen). Resazurin, reagent of Prestoblue assay can evaluate the integrity of plasma membrane, DNA synthesis and enzymatic activity. Viable cells continuously convert resazurin, blue-no fluorescent to resoruphin, red, fluorescent. In each well of 96-well plates  $5 \times 10^3$  cells were plated in 100  $\mu$ L of complete DMEM culture medium for 24h. Cells were deprived of FBS for 24h to conduct treatment with RA (SH-SY5Y/RA) at a concentration of 10 $\mu$ M every 24h for four days (Piras et al., 2014). Cells were then treated with PACAP (Thermo Scientific) at concentrations from  $10^{-6}$  M to  $10^{-8}$  M. To establish an in vitro model of PD, these cells, after 4h of exposure, come further treated with MPP<sup>+</sup> (Xico et al., 2017) at concentrations of 500  $\mu$ M, 1mM and 1.5 mM to evaluate the preventive protective effects of PACAP in these cell line treated with MPP<sup>+</sup> (Lamine et al., 2016). To the remaining wells is added in simultaneous, MPP<sup>+</sup> (500  $\mu$ M; 1mM and 1.5 Mm) and PACAP ( $10^{-6}$  M to  $10^{-8}$  M) to evaluate the neuroprotective effects of PACAP in cells treated with MPP<sup>+</sup>. After 24h, 1:10 of Prestoblue reagent was added and the cells were kept for 10 min in an incubator at 37 ° C and 5% of CO<sub>2</sub>. At the end of incubation, viable cells convert resazurin into resoruphin, increasing the fluorescence and causing a change of color from blue to red. To measure absorbance, expressed in optical densities (O.D.), a spectrophotometric reading was made at 570 nm using a plate reader (Synergy HTX Multi mode microplate reader). Absorbance of this compound is directly proportional to the metabolic activity and to the cell viability. For each experimental class, test was performed in triplicate. The same experiment was conducted for gH625-lipoPACAP-Rho, to analyze the differences between PACAP action and PACAP action with liposome functionalized with gH peptide. Briefly, after established PD model on SH-SY5Y/RA cells, gH625-lipoPACAP-Rho was added at a range concentration of PACAP-Rho from  $10^{-6}$ M to  $10^{-8}$ M simultaneously and 4h before MPP<sup>+</sup> action. For each experimental class, Prestoblue test was performed in triplicate.

## 2.5 3D SH-SY5Y in dynamic culture

3D SH-SY5Y cells enriched by neural portion were formed by hanging drop culture. After 48h from the aggregate's formation, they were transferred in a bioreactor (Livebox1, LB1, IVTech,

Italy). LB1 is composed by a polydimethylsiloxane (PDMS) chamber with an inlet and outlet tube connected with its mixing chamber to a peristaltic pump fluid circuit (Liveflow, IVTech, Italy) (Giusti, 2015). Fluid allow a continuous recycle of nutrient in which spheroids are in suspension without attaching in the lower part of the chamber. After 24h of 3D SH-SY5Y in fluid dynamic condition (100  $\mu$ l/min), the mixing chamber containing DMEM complete medium, was substituted with DMEM 1% FBS and MPP<sup>+</sup> at a concentration of 1,5 mM for 24h. This concentration was chosen being the highest to create damage according to previously Prestoblue assay. Control was carried out with another LB1 containing SH-SY5Y no treated with MPP<sup>+</sup> in the same fluid condition. After 24h, morphological check in the JuLi™ Stage RealTime Cell History Recorder microscope was conducted.

## **2.6 Annexin V-FITC / Propidium Iodide assay**

Annexin V-FITC / Propidium Iodide (PI) assay was carried out in 3D SH-SY5Y/MPP<sup>+</sup> and in 3D SH-SY5Y present in two different LB1 after 24h in fluid dynamic conditions. This assay was useful to discriminate the necrotic and apoptotic cells. Annexin V (FITC, green fluorescent dye) highlights the apoptotic cells. PI (red fluorescent) highlights necrotic cells. Spheroids are treated for 15 min with both probes (Annexin V-FITC / PI) dissolved in 1X binding buffer (Biotool). Nuclei were labeled with DAPI (Invitrogen) for 5 min. Images were acquired with the JuLi™ Stage RealTime Cell History Recorder microscope with 10x objective, using three different channels: DAPI, GFP and RFP. For each experimental condition, three morphological checks and three different assays were repeated, and different fields were randomly selected for data analysis. The images were corrected for brightness and contrast using Fiji software.

## **2.7 Spectrofluorimetry assay**

3D SH-SY5Y/MPP<sup>+</sup> and 3D SH-SY5Y were adapted to flow condition in two LB1 for 24h. Once adapted, they were transferred in the lower chamber of three Liveboxes2 (LB2, IVTech, Italy). LB2 is a double chamber (upper and lower) bioreactor with double independent inlet and outlet tube used to mimic physiological barrier (Giusti, 2015). The double chambers are separated by a porous membrane in which mouse endothelial brain cells (bEnd.3) were seeded

for 7 days as previously reported in Chapter 2. 7 days are necessary to form a stable and integer monolayer cells barrier. Three LB2 were organized as reported below:

1. bEnd.3 cells in the upper chamber, 3D SH-SY5Y/MPP<sup>+</sup> in the lower chamber
2. bEnd.3 cells in the upper chamber, 3D SH-SY5Y in the lower chamber
3. bEnd.3 cells in the upper chamber, 3D SH-SY5Y/MPP<sup>+</sup> in the lower chamber

In the first two LB2, the passage of gH625-lipoPACAP-Rho was performed in order to observe the passage of PACAP through a monolayer of endothelial cells. gH625-lipoPACAP-Rho was injected in the inlet tube of the upper chamber at a concentration of  $10^{-8}$  M. The third LB2 represent a control check to observe behavior cells MPP<sup>+</sup> treated without gH625-lipoPACAP-Rho. 100  $\mu$ l/min is the flow chosen from previously experiment that no cause shear-stress to spheroids. Experiments were carried out in 24h.

## **2.8 Prestoblue assay**

Prestoblue assay was performed on the spheroids present in the three LB2 described in 2.7. This assay was useful to determine cell viability on spheroids treated or not with MPP<sup>+</sup> after the passage of gH625-liposomePACAP-Rho. Briefly, after 24h, spheroids were transferred in a 96-well plate and Prestoblue cell reagent was added for 4h (Ham et al., 2016; Lemmo et al., 2014). Absorbance was measured at 570 nm using a plate reader (Synergy HTX Multi mode microplate reader). Three assays were performed and for each experimental class the test was performed in triplicate.

## **3. Results**

### **3.1 Prestoblue assay**

The neuroprotective effect of PACAP was evaluated using the Prestoblue assay on SHSY-5Y neuroblastoma cells differentiated into DAN and treated with the neurodegenerative agent MPP<sup>+</sup>. The concentrations of PACAP used, included a range of values from  $10^{-6}$ M to  $10^{-8}$ M. The treatment was carried out both with PACAP 4h before the MPP<sup>+</sup> administration and PACAP and MPP<sup>+</sup> simultaneously administered. Control cells were represented by neurons

untreated dopamine. After 24h, the results obtained show an increase significant cell viability in the presence of  $10^{-6}$  M to  $10^{-8}$  M PACAP with indication of a neuroprotective action of PACAP at the concentration of  $10^{-7}$  M and  $10^{-8}$  M both in the consecutive and simultaneous treatment (**Fig.1**). The same neuroprotective action of PACAP can be observed when DAn/MPP<sup>+</sup> are treated with gH625-lipoPACAP-Rho at a range of PACAP values from  $10^{-6}$ M to  $10^{-8}$ M. Results obtained show an increase in viability at  $10^{-7}$ M and  $10^{-8}$ M. It can be note that PACAP exerts the same neuroprotective action both in the presence and in the absence of the functionalized peptide (gH625-liposome) (**Fig.2**). Rather, gH625-liposome does not represent an obstacle but can only increase its bioavailability.

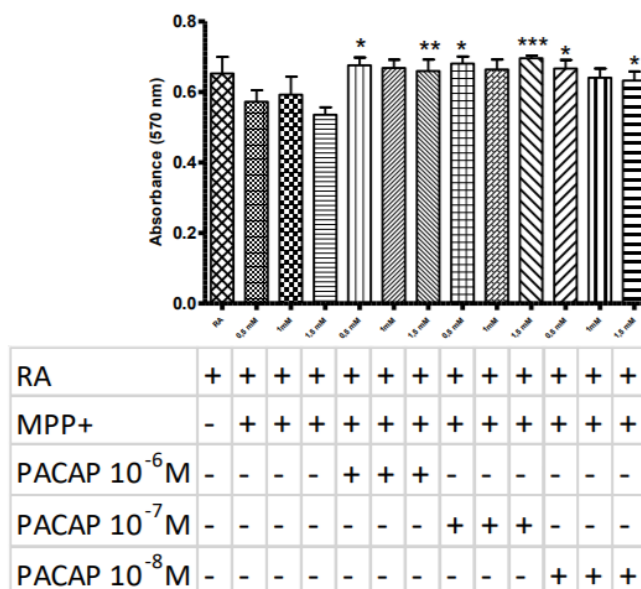


**Fig.1**

Spectrophotometric analysis on the effects of PACAP 4 hours before and MPP<sup>+</sup> after and

PACAP and MPP<sup>+</sup> simultaneously on dopaminergic neurons. The results

show exposure after 24 hours. The graph shows the means  $\pm$  SEM of three

experiments. Statistical analysis was performed through the analysis of variance

(ANOVA) and the Dunnet's posttest. The differences were considered significant

compared to the control MPP<sup>+</sup> concentration. \* P < 0.05, \*\* P < 0.01, \*\*\* P < 0.001.

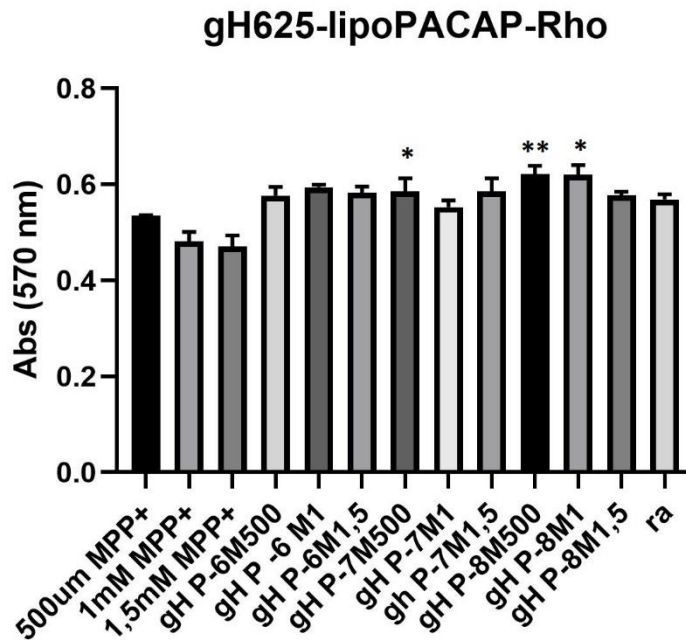


**Fig.2**

Spectrophotometric analysis on the effects of PACAP 4 hours before and MPP<sup>+</sup> after and gH-lipoPACAP-Rho and MPP<sup>+</sup> simultaneously on dopaminergic neurons. The results show exposure after 24 hours. The graph shows the means  $\pm$  SEM of three experiments. Statistical analysis was performed through the analysis of variance (ANOVA) and the Dunnet's posttest. The differences were considered significant compared to the control MPP<sup>+</sup> concentration.

\* P <0.05, \*\* P <0.01.

### **3.2 Annexin V-FITC / Propidium Iodide assay**

3D SH-SY5Y/MPP<sup>+</sup> and 3D SH-SY5Y after 24h in fluid dynamic condition in LB1 were placed in the JuLi™ Stage RealTime Cell History Recorder microscope for morphological control. Figures showed after 24h compared to time 0, a flaking of the 3D SH-SY5Y treated with 1,5 mM of MPP<sup>+</sup> (**Fig.3**). Instead, 3D SH-SY5Y cells showed more linear and compact outlines (**Fig.4**).

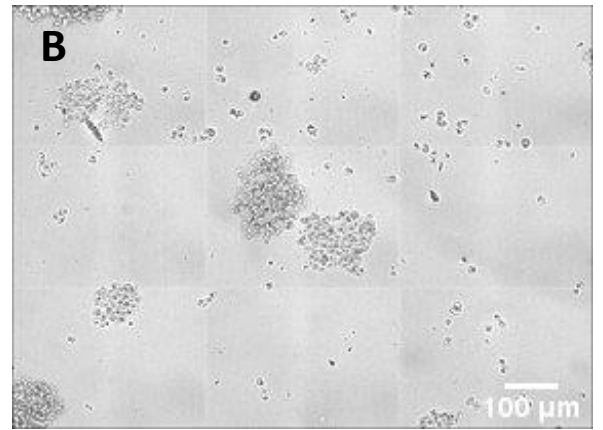
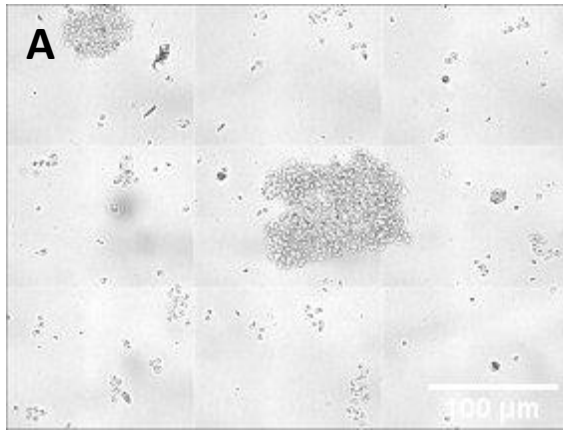


**Fig.3**

3D SH-SY5Y before the treatment of 1,5 mM MPP<sup>+</sup> (time 0, A).

3D SH-SY5Y after the treatment of 1,5 mM MPP<sup>+</sup> (24h, B).

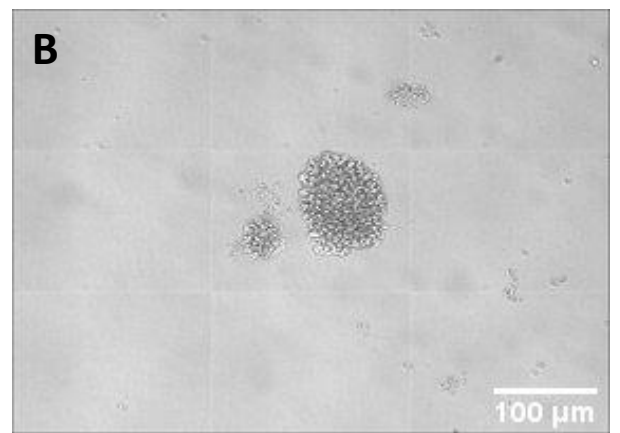
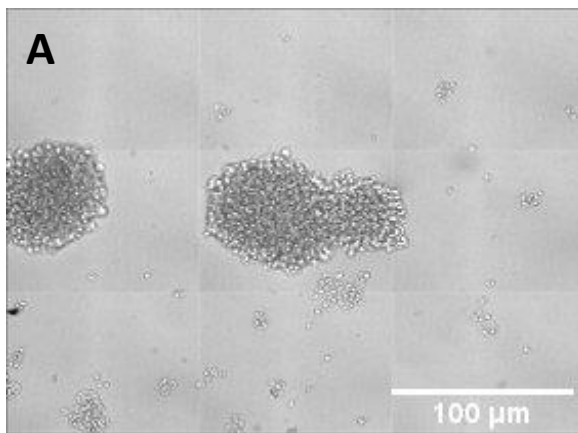


**Fig.4**

3D SH-SY5Y without the treatment of 1,5 mM MPP<sup>+</sup> (time 0, A).

3D SH-SY5Y without the treatment of 1,5 mM MPP<sup>+</sup> (24h, B).

This is probably due to a continuous flow of the MPP<sup>+</sup> contained in the mixing chamber which causes a breakdown of 3D SH-SY5Y. Annexin V-FITC/PI assay shows a majority presence of necrotic 3D SH-SY5Y/MPP<sup>+</sup> (**Fig.5-6**) compared to 3D SH-SY5Y where we can observe more apoptotic cells (**Fig.7-8**). This different behavior is due to MPP<sup>+</sup> action that acts on death of neurons causing cells necrosis.

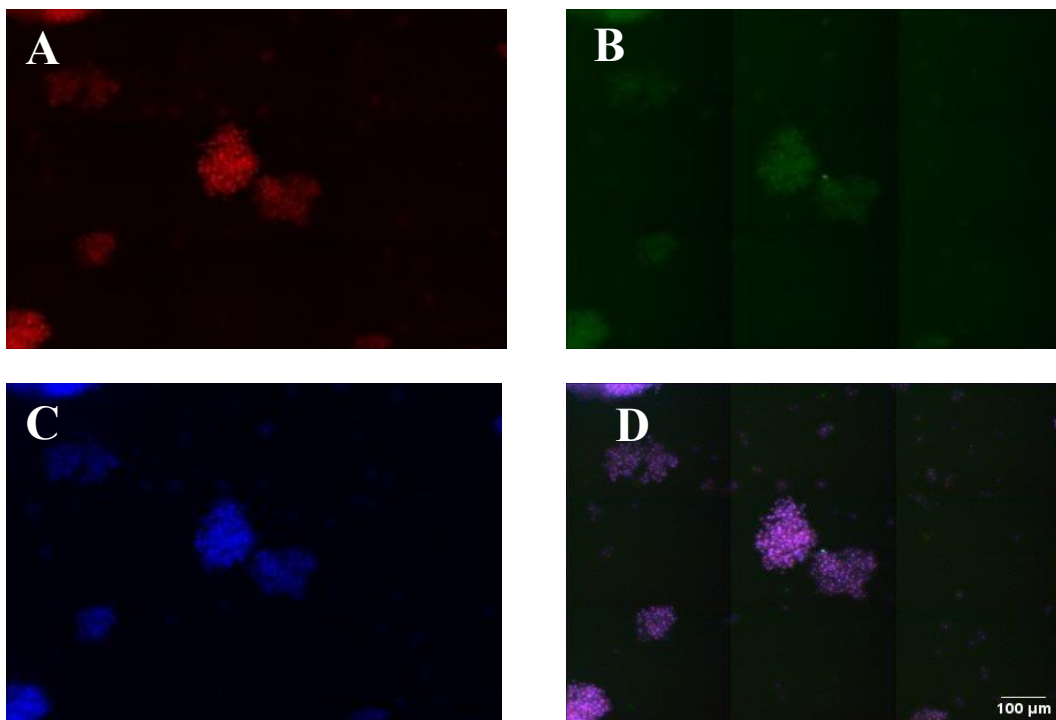


**Fig.5**

Annexin/PI labelling of neural spheroids treated with 1,5mM MPP<sup>+</sup>

A: apoptotic cells

B: necrotic cells

C: DAPI

D: Merge

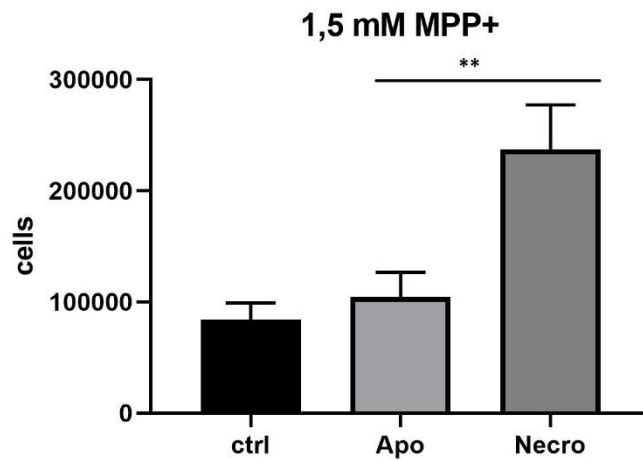


**Fig.6**

Annexin/PI on neural spheroids treated with 1,5mM MPP<sup>+</sup>.

The number of necrotic cells is higher compared to apoptotic cells. The graph shows the means  $\pm$  SEM of three experiments. Statistical analysis was performed through the analysis of variance (ANOVA) and the Dunnet's posttest. The differences were statistically significant between apoptotic and necrotic cells.

\*\* P < 0.01

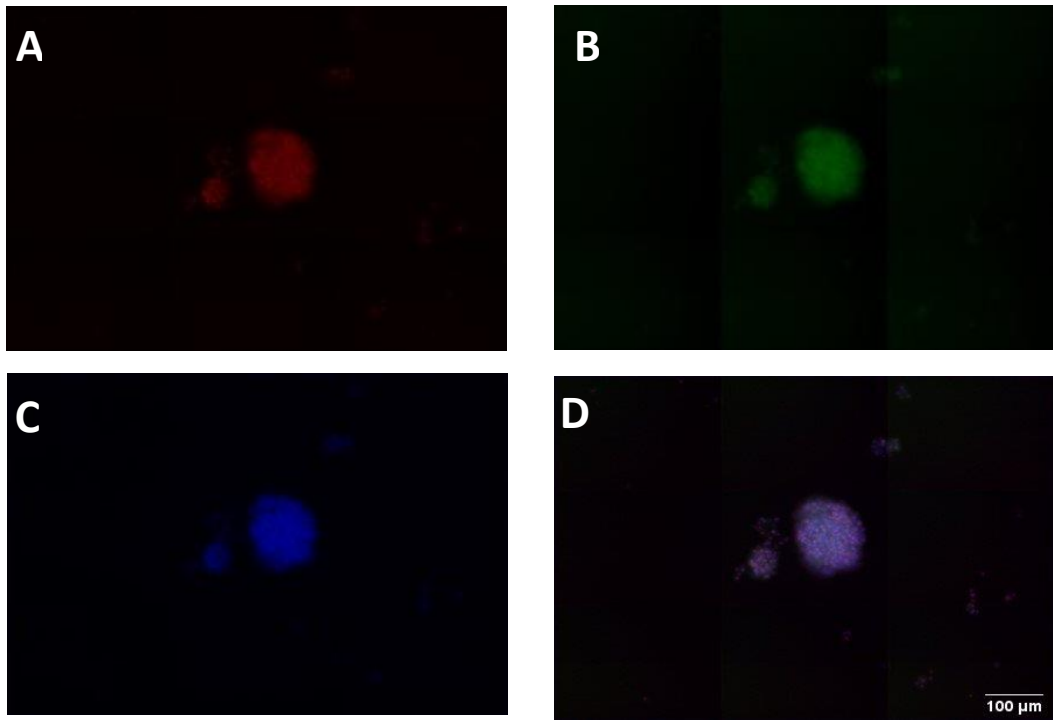


**Fig.7**

Annexin/PI labelling of neural spheroids without 1,5mM MPP<sup>+</sup>

A: apoptotic cells

B: necrotic cells

C: DAPI

D: Merge

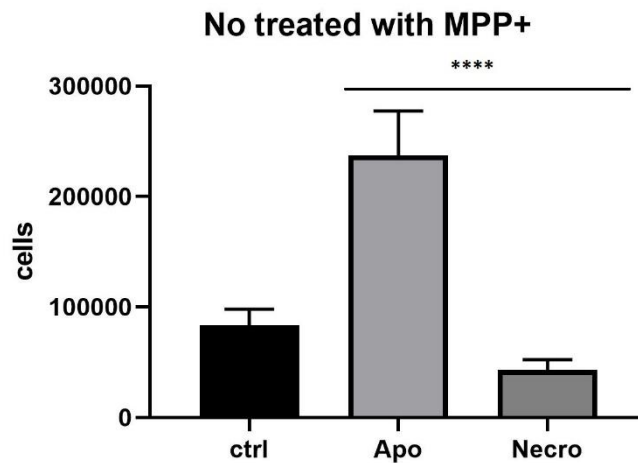


**Fig.8**

Annexin/PI on neural spheroids without 1,5mM MPP<sup>+</sup>

The number of apoptotic cells is higher compared to necrotic cells. The graph shows the means  $\pm$  SEM of three experiments. Statistical analysis was performed through the analysis of variance (ANOVA) and the Dunnet's posttest. The differences were considered significant between apoptotic and necrotic cells.

\*\*\* P <0.01

### **Spectrofluorimetry assay**

Spectrofluorimetry assay was performed to evaluate the capability of gH625-liposome to carry PACAP across endothelial brain cells monolayer in LB2 containing in the lower chamber 3D SH-SY5Y/MPP<sup>+</sup> and 3D SH-SY5Y without MPP<sup>+</sup>. It was conducted only in the two LB2/gH625-lipoPACAP-Rho: one of them containing in the upper chamber bEnd.3 cells seeded and in the upper chamber and 3D SH-SY5Y without MPP<sup>+</sup> seeded in the lower ones (**Fig.8**); in another one LB2 there was in the upper chamber bEnd.3 cells seeded and in the lower chamber 3D SH-SY5Y with MPP<sup>+</sup> 1,5mM (**Fig.9**). In these LB2, the amount of PACAP-Rho is higher in the lower chamber (**Fig.8-Fig.9**) instead in the upper chamber indicating that PACAP crossed endothelial brain cells monolayer in LB2 and reached spheroids in the lower chamber.

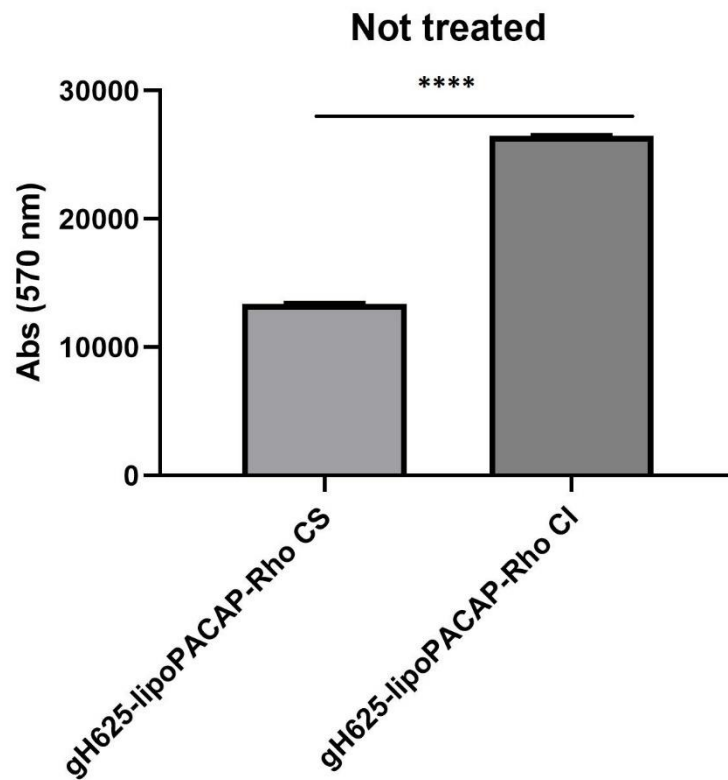


**Fig.8**

Spectrofluorometric analysis of rhodaminated PACAP (PACAP-Rho) delivery across BBB dynamic in vitro model (LB2) with bEnd.3 in the upper chamber and 3D SH-SY5Y in the lower chamber. Functionalized liposome and non-functionalized liposome were loaded with PACAP-Rho and injected in the upper flow. The passage beyond the endothelial cell layer, in the lower chamber where 3D SH-SY5Y/MPP<sup>+</sup> were then evaluated by sampling downstream the upper flow and the lower flow, respectively. The graph shows the means  $\pm$  SEM of three experiments. Statistical analysis was performed through the analysis of Mann-Whitney test. The differences were considered significant between gH625-lipoPACAP-Rho CS and gH625-lipoPACAP-Rho CI.

\*\*\*\* P <0.001

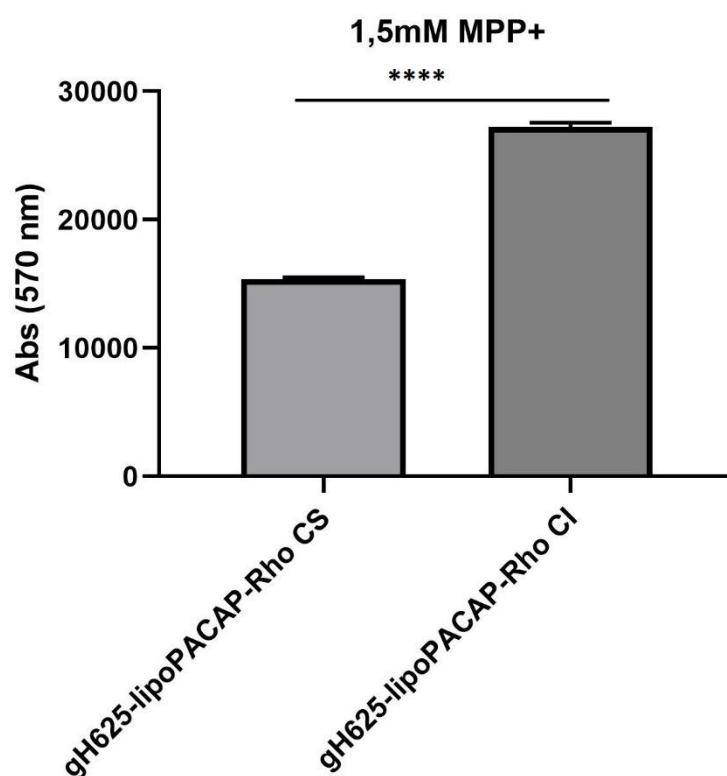


**Fig.9**

Spectrofluorometric analysis of rhodaminated PACAP (PACAP-Rho) delivery across BBB dynamic in vitro model (LB2) with bEnd.3 in the upper chamber and 3D SH-SY5Y/MPP<sup>+</sup> in the lower chamber. Functionalized liposome and non-functionalized liposome were loaded with PACAP-Rho and injected in the upper flow. The passage beyond the endothelial cell layer, in the lower chamber where 3D SH-SY5Y/MPP<sup>+</sup> were then evaluated by sampling downstream the upper flow and the lower flow, respectively. The graph shows the means  $\pm$  SEM of three experiments. Statistical analysis was performed through the analysis of Mann-Whitney test. The differences were considered significant between gH625-lipoPACAP-Rho CS and gH625-lipoPACAP-Rho CI.

\*\*\*\* P <0.001

### 3.4 Prestoblue assay

Prestoblue assay was performed to evaluate cell viability on 3D SH-SY5Y/MPP<sup>+</sup> and 3D SH-SY5Y treated or not with gH625-lipoPACAP-Rho. Results obtained show a higher viability in both LB2 with gH625-lipoPACAP-Rho compared to spheroids treated only with MPP<sup>+</sup>. Moreover, it is of note that viability is higher when cells are both treated with gH625-

lipoPACAP-Rho and MPP<sup>+</sup> compared to only gH625-lipoPACAP-Rho demonstrating a restoration by PACAP on 3D SH-SY5Y when treated with MPP<sup>+</sup> (**Fig.10**).

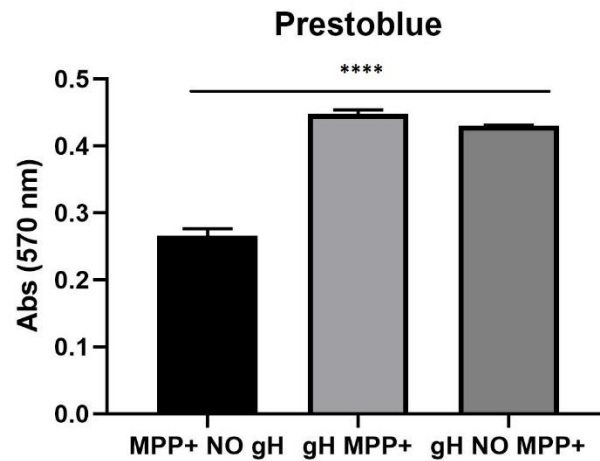


**Fig.10**

Prestoblue assay 3D SH-SY5Y/MPP<sup>+</sup> and 3D SH-SY5Y treated or not with gH625-lipoPACAP-Rho. 3D SH-SY5Y show a higher viability in both LB2 with gH625-lipoPACAP-Rho compared 3D SH-SY5Y/MPP<sup>+</sup>. The graph shows the means  $\pm$  SEM of three experiments. Statistical analysis was performed through the analysis of variance (ANOVA) and the Dunnet's posttest. The differences were considered significant compared gH treatment and Not gH treatment.

\*\*\*\* P <0.01

#### 4. Discussion

PD is one of the most important neurodegenerative disease-causing movement disorders due to death of DAN in the substantia nigra (Samii et al., 2004). Despite the progress in the in this field, to date there is no real cure for these pathologies, except for the use of symptomatic drugs (Fernandez, 2012). Therefore, it is mandatory to develop more therapeutic agents to counter long-term effects. Moreover, the cause of PD is unknown, despite many factors involved in its development, including genetic and environmental factors. Human neuroblastoma cell line: SH-SY5Y have been widely used as *in vitro* model of PD studies. They can acquire neuron-like phenotypes when treated with acid retinoic (RA) (Miloso et al., 2004). RA has a pivotal role to maintain growth and differentiation of cellular differentiation processes from proliferating precursor cells to post mitotic differentiated. MPP<sup>+</sup> is a neurotoxin that can cause the onset of an experimental parkinsonism in SH-SY5Y cells (Amo et al., 2020) involving a reduction of dopamine, noradrenaline and serotonin. PACAP acts with its specific receptors (PAC<sub>1</sub>, VPAC<sub>1</sub>, VPAC<sub>2</sub>) in which share with vasoactive intestinal peptide (Vaudry et al., 2009). PACAP can act as neurotransmitter, neuromodulator or neuroprotective agent against more toxic substances like MPTP or rotenone both *in vivo* and *in vitro* culture (Reglodi et al,2000). PACAP can offer a therapeutic approach in the treatment of PD (Vaudry et al., 2009; Reglodi et al., 2011) but it presents also low bioavailability in the bloodstream. Nanoparticle, like liposome represent good candidate to carry therapeutic molecules in brain parenchyma thanks to their low availability, small size (6-300nm) and low cost. They can also modify on their surface by other penetrating peptides to facilitating drugs uptake in brain (McCarthy et al., 2014). gH625 is a perturbing membrane domain of 19 amino acid residues (625aa to 644aa) derived from the H (gH) glycoprotein of the *Herpes simplex 1* virus. The aim of this work is to study the neuroprotective effects of PACAP loaded with gH625-liposome in an *in vitro* fluid-dynamic model of PD. Our data on cell viability Prestoblue assay conducted on SH-SY5Y cells differentiated with RA and treated with MPP<sup>+</sup> show that PACAP can act as neuroprotective agent both in simultaneous and earlier treatment to MPP<sup>+</sup> (0,5mM, 1mM, 1,5mM). At these MPP<sup>+</sup> concentrations, PACAP acts as neuroprotector in physiological concentrations 10<sup>-8</sup>M (ranging from 10<sup>-8</sup>M to higher concentrations, 10<sup>-6</sup>M). These results confirm data reported by literature as indicated by Vaudry in 2009 (Vaudry et al., 2009.). This result also indicates that our *in vitro* BBB system is suitable and accurate to perform drug effects study on *in vitro* model of PD. It is of note that when PACAP is delivered by gH625-liposomes, has the same

neuroprotective effect on cells treated or not with MPP<sup>+</sup>, suggesting that gH625-liposome does not represent an obstacle but in contrast it guarantees PACAP bioavailability. To better study PACAP neuroprotective action, we have used 3D SH-SY5Y enriched with neural portion. Our cell analysis on 3D SH-SY5Y treated with MPP<sup>+</sup> showed increasing number of necrotic cells in 3D SH-SY5Y/MPP<sup>+</sup>. When 3D SH-SY5Y/MPP<sup>+</sup> were seeded under brain endothelial cells monolayer, results indicate that high amounts of PACAP can be detected in the neuronal compartment, suggesting that the nanodelivery system is efficient to deliver PACAP across the BBB, as already demonstrated in chapter two of this thesis. Moreover, we demonstrate that nanodelivery of PACAP can be useful to protect neuronal 3D SH-SY5Y cells from MPP<sup>+</sup> induced damage, as cell viability increases when cells are treated with gH625-liposomePACAP-Rho and MPP<sup>+</sup>. We are moving forward to conduct further analyses on the total amount of ROS expressed when neuronal cells are treated with MPP<sup>+</sup> with or without PACAP and on the different flow times beyond 24h, to observe the long-term effects of PACAP on MPP<sup>+</sup> treatment.

## 5. Conclusion

In the present study we demonstrated the neuroprotective effects of PACAP, delivered by gH625-liposome using two *in vitro* fluid dynamic model of PD. In the simplest model we have used a millifluidic bioreactor with a single chamber in which 3D SH-SY5Y enriched with neural portion were treated with MPP<sup>+</sup>. MPP<sup>+</sup> acts on 3D SH-SY5Y causing a higher presence of necrotic cells. With the second device, a double chamber bioreactor was used to mimic the BBB; in this configuration PACAP has a consistent neuroprotective action on neuronal compartment, when injected in the blood compartment. This is the first fluid dynamic *in vitro* clue that PACAP can be efficiently delivered in the blood stream within our functionalized nanodelivery system, crossing the BBB and reach the damaged neuronal parenchyma. This result provides support to previous data on the PACAP release in the brain (Iachetta et al., 2019) and broaden them, demonstrating that, in fluid dynamic conditions, PACAP efficiently protects neuronal cell from injuries. Our data after 24h from injection demonstrate that 3D SH-SY5Y are viable compared to cells without injection. Furthermore, we demonstrated that delivered PACAP favours the neuroprotection on MPP<sup>+</sup> treated 3D SH-SY5Y cells. Our data are consistent with reported literatures and demonstrate that our functionalized nanosystem can improve the neuronal bioavailability of this neuroprotective agent when administered systemically.

## References

- Amo, T., Oji, Y., Saiki, S., Hattori, N. (2011). Metabolomic analysis data of MPP<sup>+</sup>-exposed SH-SY5Y cells using CE-TOFMS. *Data Brief*. 2020 Dec 30;34:106707. doi: 10.1016/j.dib.2020.106707. PMID: 33457479; PMCID: PMC7797368
- Botia, B., Jolivel, V., Burel, D. (2011) Neuroprotective effects of PACAP against ethanol-induced toxicity in the developing rat cerebellum. *Neurotox Res* 19:423–434.
- Brown, D., Tamas, A., Reglödi, D., Tizabi, Y. (2013). PACAP protects against salsolinol-induced toxicity in dopaminergic SH-SY5Y cells: implication for Parkinson's disease. *J Mol Neurosci*. 2013 Jul;50(3):600-7. doi: 10.1007/s12031-013-0015-7. Epub 2013 Apr 28. PMID: 23625270; PMCID: PMC3676705.
- Biedler, J.L., Roffler-Tarlov, S., Schachner, M., Freedman, L.S. (1978). Multiple Neurotransmitter Synthesis by Human Neuroblastoma Cell Lines and Clones. *Cancer Res*. 1978;38(11 Part 1):3751–7.
- Dorsey, E.R., Constantinescu, R., Thompson, J.P., Biglan, K.M., Holloway, R.G., Kieburtz, K., (2005). Projected number of people with Parkinson disease in the most populous nations, 2005 through 2030. *Neurology*. 2007;68(5):384–6. 2.
- Chaturvedi, R.K. and Flint Beal, M. (2013). Mitochondrial diseases of the brain. *Free Radic Biol Med*. 37 2013Oct;63:1-29. doi: 10.1016/j.freeradbiomed.2013.03.018. Epub 2013 Apr 6. PMID: 23567191.)
- Chaudhuri, K.R. and Schapira, A.H. (2009). Non-motor symptoms of Parkinson's disease: dopaminergic pathophysiology and treatment. *Lancet Neurol*. 2009;8(5):464–74.
- Delgado, M., Leceta, J., Ganea, D. (2003), "Vasoactive intestinal peptide and pituitary adenylate cyclase-activating polypeptide inhibit the production of inflammatory mediators by activated microglia.", *J Leukoc Biol* 73:155– 164. <https://doi.org/10.1189/jlb.0702372>;
- Dexter, D.T. and Jenner, P. (2013). Parkinson disease: from pathology to molecular disease mechanisms. *Free Radic Biol Med*. 2013;62:132–44.
- Douiri, S., Bahdoudi, S., Hamdi, Y., Cubi, R., Basille, M., Fournier, A., Vaudry, H., Tonon, M.C., Amri, M., Vaudry, D., Masmoudi-Kouki, O. (2016), "Involvement of endogenous

antioxidant systems in the protective activity of pituitary adenylate cyclaseactivating polypeptide against hydrogen peroxideinduced oxidative damages in cultured rat astrocytes.”, *J Neurochem* 137:913–930. <https://doi.org/10.1111/jnc.13614>.

Falanga, A., Vitiello, M.T., Cantisani, M., Tarallo, R., Guarnieri, D., Mignogna, E., Netti, P., Pedone, C., Galdiero, M., Galdiero, S. (2011). A peptide derived from herpes simplex virus type 1 glycoprotein H: membrane translocation and applications to the delivery of quantum dots *Nanomedicine*. 2011; 7:925– 934.

Fernandez, H.H. (2012) Updates in the medical management of Parkinson disease. *Cleve Clin J Med* 79:28–35

Fukuchi, M., Tabuchi, A., Kuwana, Y., Watanabe, S., Inoue, M., Takasaki, I., Izumi, H., Tanaka, A., Inoue, R., Mori, H., Komatsu, H., Takemori, H., Okuno, H., Bito, H., Tsuda, M. (2015), “Neuromodulatory effect of  $G_{\alpha s}$ - or  $G_{\alpha q}$ -coupled G protein- coupled receptor on NMDA receptor selectively activates the NMDA receptor/ $Ca^{2+}$ /calcineurin/cAMP response element-binding protein-regulated transcriptional coactivator 1 pathway to effectively induce brain-derived neurotrophic factor expression in neurons.”, *J Neurosci* 35:56065624.

Galdiero, S., Falanga, A., Vitiello, M., Browne, H., Pedone, C., Galdiero, M. (2005). Fusogenic domains in herpes simplex virus type 1 glycoprotein H. *J. Biol. Chem.*; 280 28632–28643.

Gerlach, M., Riederer, P., Przuntek, H., Youdim, M.B. (1991). MPTP mechanisms of neurotoxicity and their implications for Parkinson's disease. *Eur J Pharmacol*. 1991 Dec 12;208(4):273-86. doi: 10.1016/0922-4106(91)90073- q. PMID: 1815982

Gilany, K., Elzen, R.V., Mous, K., Coen, E., Dongen, W.V., Vandamme, S., Gevaert, K., Timmerman, E., Vandekerckhove, J., Dewilde, S., Ostade, X.V., Moens, L., (2008). The proteome of the human neuroblastoma cell line SH-SY5Y: an enlarged proteome. *Biochim. Biophys. Acta* 1784, 983–985.

Giusti, S. (2015). Bioreattori per la realizzazione di modelli multi-organo in vitro. XXXIV Scuola Annuale “Approcci ingegneristici per lo sviluppo di metodiche alternative alla sperimentazione in vivo”.

Ham, S.L., Joshi, R., Luker, G.D., Tavana, H. (2016). Engineered Breast Cancer Cell Spheroids Reproduce Biologic Properties of Solid Tumors. doi: 10.1002/adhm.201600644. Epub 2016 Sep 7. PMID: 27603912; PMCID: PMC5142748.

Iachetta, G., Falanga, A. Molino, Y., Masse, M., Jabès, F., Mechioukhi, Y., Laforgia, V., Khrestchatsky, M., Galdiero, S., Valiante, S. (2019) gH625-liposomes as tool for pituitary adenylate cyclase-activating polypeptide brain delivery. *Sci Rep.* Jun 24;9(1):9183. doi: 10.1038/s41598-019-45137-8.

Ito, K., Eguchi, Y., Imagawa, Y., Akai, S., Mochizuki, H., Tsujimoto, Y. (2017). MPP+ induces necrostatin-1- and ferrostatin-1-sensitive necrotic death of neuronal SH-SY5Y cells. *Cell Death Discov.* 2017 Feb 27;3:17013. doi: 10.1038/cddiscovery.2017.13. PMID: 28250973; PMCID: PMC5327502

Joshi, S., Guleria, R., Pan, J. (2006). “Retinoic acid receptors and tissue transglutaminase mediate short-term effect of retinoic acid on migration and invasion of neuroblastoma SH-SY5Y cells”. *Oncogene* 25, 240–247 (2006)

Kovalevich, J. and Langford, D. (2013). Considerations for the use of SH-SY5Y neuroblastoma cells in neurobiology. *Methods Mol Biol.* 2013;1078:9-21. doi: 10.1007/978-1-62703-640-5\_2. PMID: 23975817; PMCID: PMC5127451.

Lamine, A., Ngoc Duc, D., Maucotel, J., Couvineau, A., Vaudry, H., Chatenet, D., Vaudry, D., Fournier, A., (2015). “Characterizations of a synthetic pituitary adenylate cyclase-activating polypeptide analog displaying potent neuroprotective activity and reduced in vivo cardiovascular side effects in a Parkinson's disease model”. *Neuropharmacology.* 2016 Sep; 108:440-50. doi: 10.1016/j.neuropharm.2015.05.014. Epub 2015 May 22.

Lemmo, S., Atefi, E., Luker, G.D., Tavana, H. (2014). Optimization of Aqueous Biphasic Tumor Spheroid Microtechnology for Anti-Cancer Drug Testing in 3D Culture”. *Cell Mol Bioeng.* 2014 Sep 1;7(3):344-354. doi: 10.1007/s12195-014-0349-4. PMID: 25221631; PMCID: PMC4159185.

Lesage, S., and Brice, A., (2009). Parkinson's disease: from monogenic forms to genetic susceptibility factors. *Hum. Mol. Genet.* 18,48–50.

Lo Bianco, C., Schneider, B.L., Bauer, M., Sajadi, A., Brice, A., Iwatsubo, T., Aebischer, P., (2004). Lentiviral vector delivery of parkin prevents dopaminergic degeneration in an  $\alpha$ -synuclein rat model of Parkinson's disease. *Proc. Natl Acad. Sci. USA* 101, 17510–17515.

Lopes, F.M., Schröder, R., da Júnior, M.L.C.F., Zanotto-Filho, A., Müller, C.B., Pires, A.S., (2010). Comparison between proliferative and neuron-like SH-SY5Y cells as an in vitro model for Parkinson disease studies. *Brain Res.* 2010;1337:85–94.

López-Carballo, G., Moreno, L., Masiá, S., Pérez, P., Baretino, D., (2002). Activation of the phosphatidylinositol 3-kinase/Akt signaling pathway by retinoic acid is required for neural differentiation of SH-SY5Y human neuroblastoma cells. *J. Biol. Chem.* 277, 25297–25304

Ma, B. Q., Zhang, M., and Ba, L. (2015). Plasma pituitary adenylate cyclase-activating polypeptide concentrations and mortality after acute spontaneous basal ganglia hemorrhage. *Clin. Chim. Acta* 439, 102–106. doi: 10.1016/j.cca.2014.10.010.

Masmoudi-Kouki, O., Douiri, S., Hamdi, Y., Kaddour, H., Bahdoudi, S., Vaudry, D., Basille, M., Leprince, J., Fournier, A., Vaudry, H., Tonon, M.C., Amri, M. (2011), “Pituitary adenylate cyclase activating polypeptide protects astroglial cells against oxidative stress-induced apoptosis.”, *J Neurochem* 117:403–411.

Masuo, Y., Suzuki, N., Matsumoto, H., Tokito, F., Matsumoto, Y., Tsuda, M., Fujino, M. (1993). Regional distribution of pituitary adenylate cyclase activating polypeptide (PACAP) in the rat central nervous system as determined by sandwich-enzyme immunoassay. *Brain Res.* 1993 Jan 29;602(1):57-63. doi: 10.1016/0006-8993(93)90241-e. PMID: 8095427.

McCarthy, H.O., McCaffrey, J., McCrudden, C.M., Zholobenko, A., Ali, A.A., McBride, J.W., Massey, A.S., Pentlavalli, S., Chen, K.H., Cole, G., Loughran, S.P., Dunne, N.J., Donnelly, R.F., Kett, V.L., Robson, T. (2014) Development and characterization of self-assembling nanoparticles using a bio-inspired amphipathic peptide for gene delivery. *J Control Release.* 2014 Sep 10;189:141-9. doi: 10.1016/j.jconrel.2014.06.048. Epub 2014 Jul 1. PMID: 24995949.

- Miloso, M., Villa, D., Crimi, M., Galbiati, S., Donzelli, E., Nicolini, G., Tredici, G. (2004). Retinoic acid-induced neuritogenesis of human neuroblastoma SH-SY5Y cells is ERK independent and PKC dependent. *J Neurosci Res.* 2004 Jan 15;75(2):241-252. doi: 10.1002/jnr.10848. PMID: 14705145.
- Moody, .T.W, Osefo, N., Nuche-Berenguer, B., Ridnour, L., Wink, D., Jensen, R.T. (2012), "Pituitary adenylate cyclase-activating polypeptide causes tyrosine phosphorylation of the epidermal growth factor receptor in lung cancer cells.", *J Pharmacol Exp Ther* 341:873–381.
- Offen, D., Sherki, Y., Melamed, E., Fridkin, M., Brenneman, D.E., Gozes, I. (2000) Vasoactive intestinal peptide (VIP) prevents neurotoxicity in neuronal cultures: relevance to neuroprotection in Parkinson's disease. *Brain Res* 854:257–262.
- Piras, S., Furfaro, A.L., Piccini, A., Passalacqua, M., Borghi, R., Carminati, E., Parodi, A., Colombo, L., Salmona, M., Pronzato, M.A., Marinari, U.M., Tabaton, M., Nitti, M. (2014). "Monomeric A $\beta$ 1-42 and RAGE: key players in neuronal differentiation.". *Neurobiol Aging.* 2014 Jun;35(6):1301-8. doi: 10.1016/j.neurobiolaging.2014.01.002. Epub 2014 Jan 10.
- Rapaport, D. and Shai, Y. (1991). Interaction of fluorescently labeled pardaxin and its analogues with lipid bilayers. *J Biol Chem.* Dec 15;266(35):23769-75. PMID: 1748653.
- Rat, D., Schmitt, U., Tippmann, F. (2011) Neuropeptide pituitary adenylate cyclase-activating polypeptide (PACAP) slows down Alzheimer's disease-like pathology in amyloid precursor proteintransgenic mice. *FASEB J* 25:3208–3218.
- Reglödi, D., Somogyvari-Vigh, A., Vigh, S., Kozicz, T., Arimura, A. (2000) Delayed systemic administration of PACAP38 is neuroprotective in transient middle cerebral artery occlusion in the rat. *Stroke* 31:1411–1417.
- Reglödi, D., Tamas, A., Lubics, A., Szalontay, L., Lengvari, I. (2004) Morphological and functional effects of PACAP in 6-hydroxydopamineinduced lesion of the substantia nigra in rats. *Regul Pept* 123:85–94.
- Reglödi, D., Kiss, P., Lubics, A., Tamas, A. (2011) Review on the protective effect of PACAP in models of neurodegenerative diseases in vitro and in vivo. *Curr Pharm Des* 17:962–972.

Reglodi, D., Atlasz, T., Szabo, E., Jungling, A., Tamas, A., Juhasz, T., Fulop, B.D., Bardosi, A. (2018). PACAP deficiency as a model of aging. *Geroscience*. 2018 Dec;40(5-6):437-452. doi: 10.1007/s11357-018-0045-8. Epub 2018 Oct 22. PMID: 30345481; PMCID: PMC6294727.

Samii, A., Nutt, J.G., Ransom, B.R. (2004) Parkinson's disease. *Lancet* 363:1783–1793

Takahashi, H., Ohama, E., Suzuki, S., Horikawa, Y., Ishikawa, A., Morita, T., Tsuji, S., Ikuta, F. (1994). Familial juvenile parkinsonism: clinical and pathologic study in a family. *Neurology*. 1994 Mar;44(3 Pt 1):437-41. doi: 10.1212/wnl.44.3\_part\_1.437. PMID: 8145912.

Valiante, S., Falanga, A., Cigliano, L., Iachetta, G., Busiello, R.A., La Marca, V., Galdiero, M., Lombardi, A., Galdiero, S. (2015). Peptide gH625 enters into neuron and astrocyte cell lines and crosses the blood–brain barrier in rats” *International Journal of Nanomedicine*; 10(1) 1885—1898.

Vincze, A., Reglodi, D., Zs, H., Hashimoto, H., Shintani, H., Abraham, H. (2011), “Role of pituitary adenylate cyclase activating polypeptide (PACAP) in myelination of the rodent brain: lessons from PACAP-deficient mice.”, *Int J Dev Neurosci* 29:923935;

Wada, Y., Nakamachi, T., Endo, K., Seki, T., Ohtaki, H., Tsuchikawa, D., Hori, M., Tsuchida, M., Yoshikawa, A., Matkovits, A., Kagami, N., Imai, N., Fujisaka, S., Usui, I., Tobe, K., Koide, R., Takahashi, H., Shioda, S. (2013), “PACAP attenuates NMDA-induced retinal damage in association with modulation of the microglia/macrophage status into an acquired deactivation subtype.”, *J Mol Neurosci* 51:493–502;

Wirdefeldt, K., Adami, H.O., Cole, P., Trichopoulos, D., Mandel, J. (2011). Epidemiology and etiology of Parkinson's disease: a review of the evidence. *Eur J Epidemiol*. 2011;26 Suppl 1:1–58. 3.

Xia, R. and Mao, Z.H. (2012). Progression of motor symptoms in Parkinson's disease. *Neurosci Bull*. 2012;28(1):39–48.

Xicoy, H., Wieringa, B., Martens, G.J. (2017). The SH-SY5Y cell line in Parkinson's disease research: a systematic review. *Mol Neurodegener*. 2017 Jan 24;12(1):10. doi: 10.1186/s13024-017-0149-0. PMID: 28118852; PMCID: PMC5259880.

Xie, H., Hu, L., Li, G. (2010). SH-SY5Y human neuroblastoma cell line: in vitro cell model of dopaminerg neurons in Parkinson's disease. *Chin Med J (Engl)*. 2010;123(8):1086–92.

Zhu, J., Wang, S., Liang, Y., Xu, X. (2018). Inhibition of microRNA-505 suppressed MPP<sup>+</sup> - induced cytotoxicity of SHSY5Y cells in an in vitro Parkinson's disease model. *Eur J Pharmacol*. 2018 Sep 15;835:11-18. doi: 10.1016/j.ejphar.2018.07.023. Epub 2018 Jul 17. PMID: 30025813.)

## **Chapter 4:**

### **Comparison between a dynamic millifluidic system and a static system to study 3D brain tumor co-culture**

Adapted from the article in preparation:

Comparison between a dynamic millifluidic system and a static system to study 3D brain tumor co-culture

## Abstract

Advanced *in vitro* techniques are a very important issue to study possible therapeutic agent in toxicology and bioactive research. In the last years many pharmaceutical industries have been focused on advanced *in vitro* model more closely to *in vivo* situation for study predictive approaches to measure molecule toxicity. The use of these powerful tools can permit to study physiological processes in order to go beyond the conventional limits represented by animal traditional *in vitro* tests. The aim of this study is to analyze the main physiological differences of conventional *in vitro* model compared to a novel innovative millifluidic- system studying a 3D brain co-culture represented byof neuroblastoma (SH-SY5Y) cells and glioblastoma cell lines s (SH-SY5Y/U-87MG). We performed different several assays to measure cell viability, cell toxicity and reactive oxygen species for each culture conditions. Compared the different results of these two different culture systems provide us a pivotal reason to use implement advanced *in vitro* models as routinely cell analysis tool, as to obtain solid preliminary investigations that can also overcome to reduce the animal laboratory use.

## 1. Introduction

New advanced techniques have begun to gain fertile ground as the economic vision has recently taken over. In fact, animal tests are considered very expensive, take a long time and can provide unsatisfactory results. Taylor et al., in 2008 collected data from 37 countries, estimated that annual laboratory animal use for 2005 ranging from 28-100 million (Taylor et al.,2008). The current *in vitro* models are simple, fast and reproducible, ethically acceptable and a wide range of cells, including human ones, can be used. The flow is an important factor as it increases the turnover of nutrients, induces a cytoskeletal reorganization, an increase in membrane permeability and a greater elongation of endothelial cells. Microfluidic systems combine microengineering techniques with populations of living cells to mimic the organizational characteristics of the *in vivo* environment (McDonald et al., 2000). Favorable scaling effects such as short diffusion distances, laminar flows and surface tension effects are exploited to replicate biophysical and biochemical signals *in vitro*, allowing for controlled dosing with test compounds, introduction of physiological flows, shear stress, and exposure to well-defined solutes (Beebe et al. 2002; Squires et al. 2005). The disadvantages of these microfluidic systems (small volumes, limited nutrients, physiologically relevant cell density) have allowed to resort to the use of millifluidic systems, which guarantee a high recycling of nutrients, larger volumes, and a physiologically relevant cell density (Giusti, 2015). Among the millifluidic dynamic models used, we recognize the use of bioreactors, tools that allow the autonomous growth of cells. These devices are able to provide an adequate environment for cell growth through the evaluation and modification of chemical-physical parameters, carried out by means of sensors that constantly monitor gas concentrations (such as O<sub>2</sub>, N<sub>2</sub>, CO<sub>2</sub>), temperature, pH and the mixing speed of the bioreactor content (Rouwkema et al., 2012). Cells are maintained with a flow that supports cell proliferation, imposes shear stresses, induces junction formation and establishes polarized tissues. These systems guarantee a high recycling of nutrients, greater volumes, and a physiologically relevant cell density (Giusti, 2015). The large fluid-to-cell volume ratio and static fluid conditions in transwell-based models lead to uncontrollable and unstable biochemical gradients in the cell's environment (Wolff et al., 2015). Pandley et al. have constructed a dynamic *in vitro* BBB (DIV-BBB) based on the culture of endothelial cells inoculated with astrocytes under flow conditions, capable of developing a phenotype like that of cells *in situ* (Pandey et al., 2016). Jeliaskova-Mecheva (2003), instead, with a co-culture model with astrocytes and endothelial cells from pig brains, demonstrated the mechanism of

transport through BBB. This model has also shown promise for the treatment of BBB in neuroinflammatory diseases (Cucullo et al., 2011). Among the millifluidic bioreactor systems we find the LiveBoxes (IVTech, Italy) that accurately recreate the physiological conditions found *in vivo*. They are in polydimethylsiloxane (PDMS), transparent to allow live imaging analysis. There are two models: LiveBox1 (LB1) with single flow, low shear-stress on cell culture, while LiveBox2 (LB2) is double flow, used to recreate physiological barriers *in vitro* as it has a porous membrane that divides in two independent parts. To allow the flow inside them, the LiveBoxes are connected to a peristaltic pump, LiveFlow (IVTech, Italy). These models mimic the anatomical-physiological complexity of organism model *in vivo*, based on ideal criteria, such as reproducibility, easiness of culture, fidelity of the physiological architecture, expression of transporter functions and response to chemical stimuli. This technology is gaining ground in recent times where numerous models have been perfected to reach conditions much closer to physiology (Colombo et al., 2019). The present study aims to investigate physiological differences in biological parameters arising when cells are cultured in static or dynamic conditions. Thus, 3D co-culture, seeded in LB1 single flow bioreactor, of 3D human cell lines SH-SY5Y (neuroblastoma cells) and U-87 MG (glioblastoma cells) were carried out. 3D co-culture spheroids were formed by hanging drop method. This technology that benefits from the spontaneous aggregation of cells in spheroids, allows to control the size starting from the initial number of plated cells (Langhans, 2018), and has been proved useful to produce different tissue specific spheroids (Shri et al., 2017; Chitnis and Weiner, 2017; Polonchuk et al., 2017). We carried out morphological analyses, Annexin V FITC / Propidium Iodure (PI) assay after 24h in static and dynamic co-culture. We monitored pH changes at different time points to evaluate the acidity of the culture medium in both culture conditions. To demonstrate that both cell lines contribute to the co-culture (SH-SY5Y / U-87MG) immunofluorescence using cell specific markers was carried out. To determine the proliferation status of 3D co-cultures, the expression of cell proliferation marker Ki67 was evaluated. The cytotoxic level of spheroids in static and in dynamic culture was determined by LDH assay. Co-culture conditions were monitored to determine difference in viability by Prestoblue assay. Finally, reactive oxygen species (ROS) was evaluated to monitor putative oxidative damage due to co-culturing in static and dynamic environments.

## **2. Materials and methods**

### **2.1 Cell culture**

Human neuroblastoma cells (SH-SY5Y) and primary human glioblastoma cells (U-87MG) were grown individually in Dulbecco's modified Eagle's medium (DMEM) supplemented with 10% fetal bovine serum. (FBS), 2 mM of L-glutamine and antibiotics (100 U/ml penicillin/streptomycin), in incubator at 37 °C, with 5% CO<sub>2</sub> and controlled humidity. Cells grow adherent to the 25 cm<sup>2</sup> flask surface; the culture medium was changed every two days by previously washing with DPBS w / o Ca<sup>++</sup> and Mg<sup>++</sup> (Phosphate Buffer Saline). At 70% confluence, the cells were enzymatically detached with 0.25% trypsin / EDTA.

### **2.2 Spheroids in static and dynamic culture**

Hanging drop method was used for the formation of the three-dimensional structures of SH-SY5Y and U-87MG. Cells are mixed 1: 1.2 (Nzou et al., 2018) and drops are deposited inside a lid of a 60mm dish. A hydration chamber was created using 10ml of PBS on the bottom of the dish. After 48h the aggregates formed were transferred to a 24well-Ultra low attachment (ULA) plate to perform the static experiments and a part in a bioreactor with an only one chamber, Livebox1 (LB1, IVTech, Italy) for perform the experiments dynamically. The mixing chamber of the LB1 is first filled with 10 ml of complete DMEM culture medium and then connected to the peristaltic pump to allow the filling of the tubes and facilitate a liquid-liquid interface between the chambers and the spheroids avoiding air formation. Thereafter, the LB1 was connected to the respective mixing chamber and the flow was then set at 100µl/min for 24h. This flow was chosen after several tests to be suitable not to create shear-stress conditions for the spheroids.

### **2.3 pH medium variations of static and dynamic culture**

Dynamic models allow a higher oxygen supply to cultured cells (Giusti, 2015). In fact, their purpose, thanks to the presence of a continuous flow given by the peristaltic pump, improves the transport of solutes and nutrients. Static models are not nutrient recycling. To corroborate

this thesis, the culture medium was taken from the 24-well-ULA (static) and from the mixing chamber to which it was connected to the LB1 and to the Liveflow circuit. pH was measured in samples taken at different time (0, 2h, 4h, 6h, 8h and 24h). DMEM culture medium is provided with phenol red (pH indicator). Thanks to the products from cell metabolism, the culture medium containing the cells tends to turn yellow. Depending on the cellular origin, the physiological pH is between 6.8 - 7.8.

#### **2.4 Annexin V-FITC / Propidium Iodide assay**

After transferring the spheroids in a static environment (24-well-ULA) and in a dynamic environment (LB1) they were placed at different time points (0, 2h, 8h and 24h) in the JuLi™ Stage RealTime Cell History Recorder microscope to carry out morphological analyses. After 24h, the Annexin V-FITC / Propidium Iodide (PI) assay was carried out for the static spheroids (24-well-ULA) and for the dynamic ones (LB1). This test evaluates the presence of necrotic and apoptotic cells. Annexin V conjugated to green fluorescent dye (FITC) highlights the sites of phosphatidylserine on the surface of the membrane in apoptotic cells. PI, on the other hand, highlights necrotic cells by emitting a red fluorescence. After 24h, the spheroids undergo two washes with cold PBS (Phosphate Buffer Saline) and are subsequently treated for 15 min with both probes (Annexin V-FITC / PI) previously dissolved in 1X binding buffer (Biotool). Images were acquired with the JuLi™ Stage RealTime Cell History Recorder microscope with 10x objective, using three different channels: DAPI, GFP and RFP. For each experimental condition, three morphological analyses and three different assays were performed, and different fields were randomly selected for data analysis. The images were corrected for brightness and contrast using Fiji software.

#### **2.5 Spheroid immunofluorescence**

The indirect immunofluorescence technique was performed to assess the presence of both cell lines (SH-SY5Y and U-87MG) within the spheroids both in static (24-well-ULA) and in dynamic (LB1) environment. After 24h, spheroids were fixed with cold methanol for 15 min and then washed with PBS to eliminate all fixative residues. Nonspecific site blocking was

performed with 3% BSA (bovine serum albumin) in 0.1% Triton-PBS for 30 min. Incubation with primary antibodies was performed for 1:45 min. The antibodies used (1:100 in 1% BSA/PBS) are GFAP (Rabbit anti-GFAP Abcam) to highlight the U-87MG cell line and  $\beta$ -tubulin III (Mouse anti- $\beta$ -tubulin III, Abcam) to highlight SH-SY5Y cell line. Subsequently, after three washes in 0.1% Triton-PBS, cells were incubated with the secondary antibody anti-rabbit AlexaFluor 488 (Invitrogen) and anti-mouse Alexafluor 594 (Invitrogen), for one hour in dark, diluted 1: 500 in 1%. BSA/PBS. After removing the secondary antibody solution, three washes in PBS were carried out to remove the fluorescent antibody that has not bound; cell nuclei were labeled with DAPI (Invitrogen) for 5 min. Images were acquired with the JuLi™ Stage RealTime Cell History Recorder microscope with 10x objective, using three different channels: DAPI, RFP and GFP. For each experimental condition, three immunofluorescences were repeated, and different fields were randomly selected for data analysis. The captured images were corrected for brightness and contrast using Fiji software. The same protocol was performed to evaluate the presence of Ki67 within the spheroids in static (24-well-ULA) and in dynamic (LB1). Ki-67 is a nuclear protein related to cell proliferation, thus representing a marker of cell growth. Antibody (Rabbit Ki67 Abcam) was used 1: 100 in 1% BSA / PBS; Secondary anti-rabbit antibody Alexafluor 488 (Invitrogen) was used 1: 500 in 1% BSA / PBS. Nuclei were labeled with DAPI for 5 min.

## **2.6 LDH assay**

LDH assay was performed to test cytotoxicity of spheroids in static (24-well-ULA) and in dynamic (LB1) culture. Lactate dehydrogenase (LDH), was released by damaged cells and it is employed to catalyze the conversion of lactate to pyruvate reducing  $\text{NAD}^+$  to NADH. Tetrazolium salts are reduced into formazan by NADH which can be measured at 490 nm. Cytotoxicity is indicated with a direct proportionality between the amount of formazan and the amount of LDH into the medium. To perform LDH assay, the static (24-well-ULA) and dynamic (LB1) spheroids are then transferred to a 96-well plate and lysed with 1mM PBS/EDTA solution. Subsequently, the spontaneous and maximum LDH activity is measured. Then 50 $\mu$ l of all the samples are transferred to a new 96-well plate to which 50 $\mu$ l of Reaction Mixture will be added. After dark incubation for 30 min, 50 $\mu$ l of Stop Solution will be added to each well. At the end of incubation, the non-viable cells convert the tetrazolium salts into

formazane. The absorbance, understood as the amount of LDH released by the cells, is expressed in optical density (O.D). It was measured using a spectrophotometric reading at 490 nm (Synergy HTX Multi mode microplate reader). Three assays were performed and for each experimental class the test was performed in triplicate.

## **2.7 Prestoblue essay**

Prestoblue (Invitrogen) assay was performed to evaluate the cell viability of the spheroids in co-culture (SH-SY5Y / U-87MG) in static (24-well-ULA) and in dynamic (LB1) environment. This assay evaluates changes in plasma membrane integrity, DNA synthesis, enzyme activity and the presence of ATP due to resazurin. Resazurin, Prestoblue basic reagent, is a non-toxic, cell-permeable, blue-colored and non-fluorescent compound. Viable cells continuously convert resazurin to resoruphin, resulting in a red, fluorescent color change. The reaction, therefore, can only take place in active cells and give a measure of cell viability. PrestoBlue cell viability reagent is non-toxic and does not require cell lysis. 96-well plates were used for the assay and, in each well, spheroids were transferred. This assay is used to quantize cell viability and does not require many washing or transfer steps (Ham et al., 2016), thus not altering the morphology of the spheroids. It is used for 2D cultures producing viability data like the conventional XTT test (Lall et al., 2013). Based on a statistical analysis, it was validated that 3-4 hours of incubation were optimal for measuring the cell viability of spheroids (Ham et al., 2016). Such prolonged incubation times are likely due to the slower diffusion of resazurin into the spheroids compared to 2D cultures. Incubations longer than 4 hours lead to insignificant changes in the fluorescent signal due to saturation. This test was also used to evaluate increases in fluorescent signal intensity from growing breast tumor spheroids during long-term cultures (Lemmo et al., 2014). After 4h from the adding of the reagent Prestoblue to spheroids in both condition (static, 24-well-ULA, dynamic, LB1), the absorbance, was measured at 570 nm using a plate reader (Synergy HTX Multi mode microplate reader). Three assays were performed and for each experimental class the test was performed in triplicate.

## **2.8 Quantitative measurement of reactive oxygen species (ROS)**

Cells are continuously exposed to reactive oxygen species (ROS) as a product of respiratory metabolism and the amount in ROS production may be due to an increase in mitochondrial activity. Cells, subjected to external stress (thermal shock, high osmolarity), can produce ROS becoming metabolically less efficient. In conditions of excessive stress, the quantity of ROS produced exceeds the antioxidant capacity of the cell, leading to oxidative damage (Canonica et al., 2018). Oxidative stress can be quantified using dichloro dihydrofluoresceine diacetate (DCFH2-DA) (Kalyanaraman et al., 2012; Reiners et al., 2017). It is a fluorescent probe that crosses cell membranes and is trapped by intracellular esterase in the cytoplasm. The presence of oxidizing species oxidizes dichlorofluorescein diacetate to 2,7-dichlorofluorescein (DCF), a highly fluorescent molecule. In this test, spheroids (SH-SY5Y / U-87MG,  $\approx$  50,000 cells) in static (24-well-ULA) and in dynamic (LB1) culture were incubated with 50  $\mu$ M DCFH2-DA (ThermoFisher) for 60 min (37 ° C, 5% CO<sub>2</sub>) (Broekgaarden et al., 2020). Positive control was performed by adding 2mM of H<sub>2</sub>O<sub>2</sub> to the spheroids for 90 min (Engellman et al., 2005). Spheroids were then captured with JuLi™ Stage RealTime Cell History Recorder microscope using a 10x objective in GFP channel. For the different experimental groups similar fields for cell density were chosen. For each experimental condition, three assays were repeated, and different fields were randomly selected for data analysis. Images were corrected for brightness and contrast using Fiji software. To measure fluorescence, spheroids were first lysed with 1 mM PBS/EDTA and then a spectrophotometric reading was performed at the excitation wavelength (Ex) of 485 nm and at the emission wavelength (Em) of 528 nm using a plate reader (Synergy HTX Multi mode microplate reader). Three assays were performed and for each experimental class the test was performed in triplicate.

## **3. Results**

### **3.1 pH medium variations of static and dynamic culture**

Different measurements carried out at different time intervals (0, 2h, 4h, 6h, 8h and 24h) in static culture (24-well-ULA) and in dynamic culture (LB1) showed a different trend. As shown in the figure 1, a slight decrease in pH values (from 7.3 to 7) is observed in static culture. In the dynamic setting pH values tend to be constant throughout the experiments. This difference

highlights what Giusti and colleagues demonstrated in 2015, namely that these millifluidic models allow, thanks to their PDMS structure and the Liveflow flow, a greater supply of oxygen. The static models, on the other hand, have the limitation of the lack of continuous exchange of the culture medium that bring to the cell metabolism waste product accumulation, resulting in medium acidification.

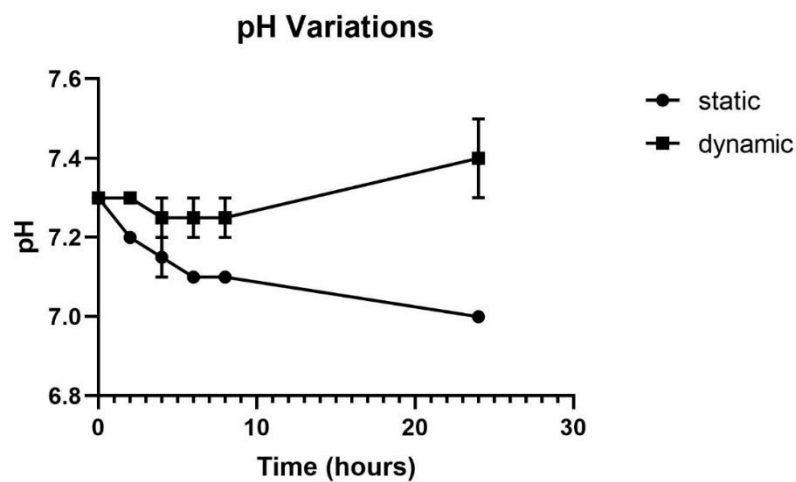


**Fig.1**

pH Variations in static and dynamic culture

Dati  $\pm$  SEM.

### 3.2 Annexin V-FITC / Propidium Iodide assay

Spheroids in the static environment (24-well-ULA) and in the dynamic environment (LB1) placed in the JuLi™ Stage RealTime Cell History Recorder microscope showed a different morphology (Fig.2). **Figure 2** A (time 0), B (2h), C (8h) and D (24h) show that the spheroids in a static environment (24-well-ULA) increase their size from 70  $\mu\text{m}$  (A, time 0) to 200 $\mu\text{m}$  (D, 24h). In a dynamic environment (**Fig.3** A, time 0; B, 2h; C, 8h; D, 24h) (LB1), spheroid size increases from 70 $\mu\text{m}$  to 700 $\mu\text{m}$ .

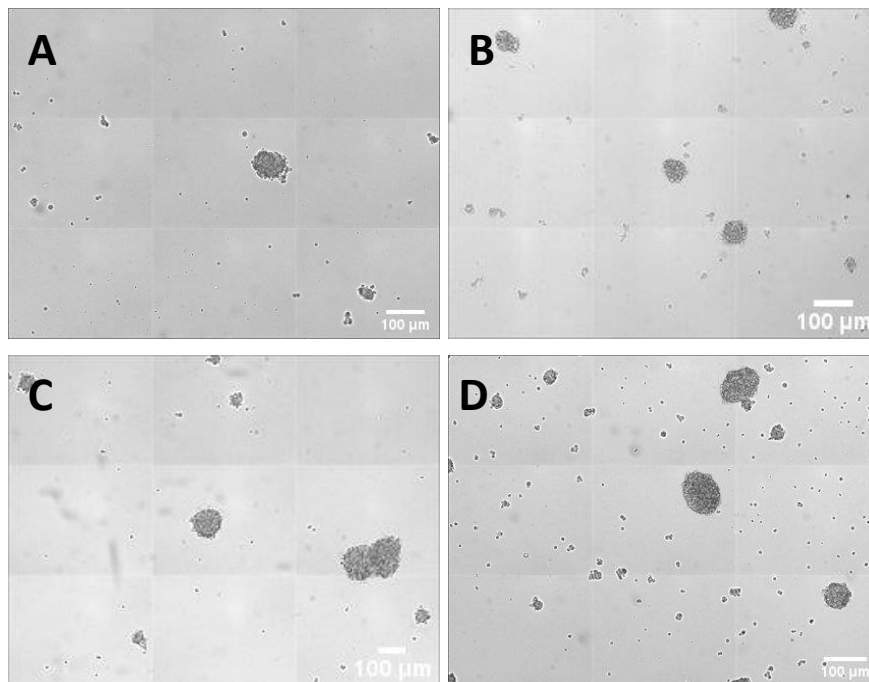


**Fig.2**

Morphological analysis in 3D SH-SY5Y/U-87MG in static environment are carried out in the JuLi™ Stage RealTime Cell History Recorder microscope.

Spheroids increase in size from A (time 0) 70 μm to D 200 μm (24h).

B: 2h

C: 8h

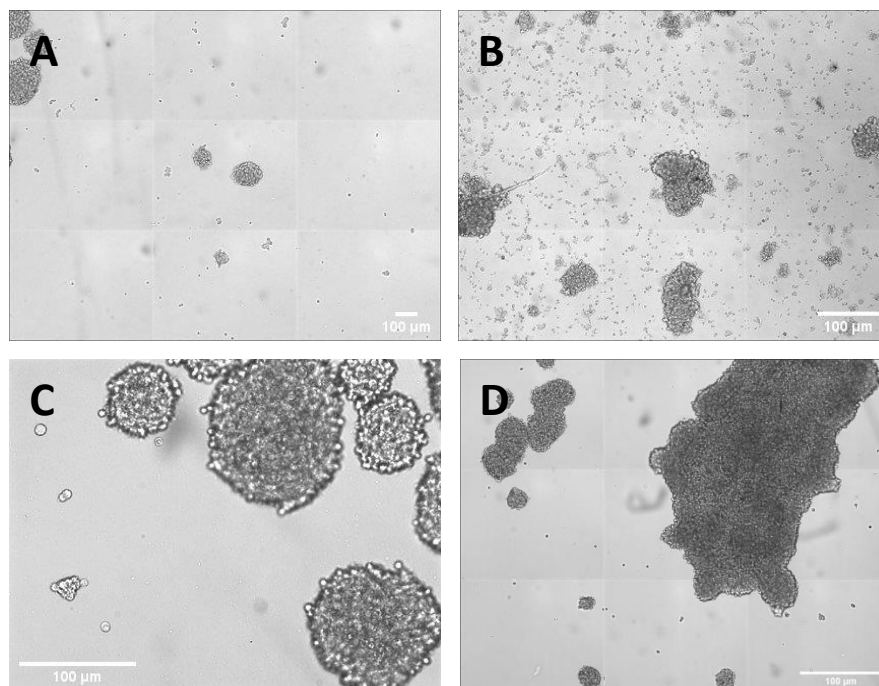


**Fig.3**

Morphological analysis in 3D SH-SY5Y/U-87MG in dynamic environment are carried out in the JuLi™ Stage RealTime Cell History Recorder microscope.

Spheroids increase in size from A (time 0) 70 µm to D 700 µm (24h).

B: 2h

C: 8h

Annexin V-FITC / PI assay on the spheroids in static (24-well-ULA) and in dynamic (LB1) was performed to evaluate the presence of necrotic and apoptotic cells. Results show a consistent presence of necrotic cells compared to apoptotic cells under static conditions. In dynamic conditions, apoptotic cells exceed necrotic cells (**Fig.4a-b-c**). Nuclei were labelled with DAPI.

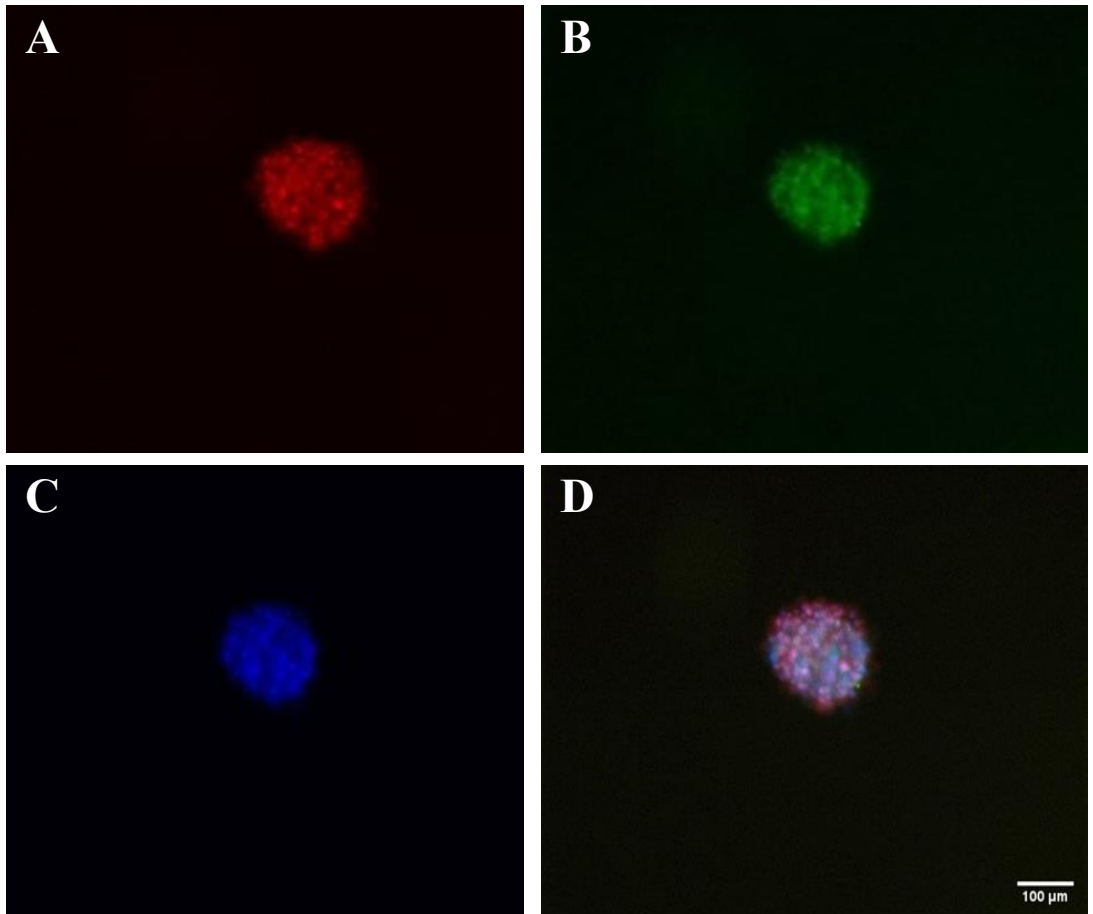


**Fig.4a**

Annexin V-FITC / PI assay on 3D SH-SY5Y/U-87MG in static condition. Necrotic cells (A); Apoptotic cells (B); DAPI (C); Merge channel (D).

Scale bar: 100  $\mu\text{m}$

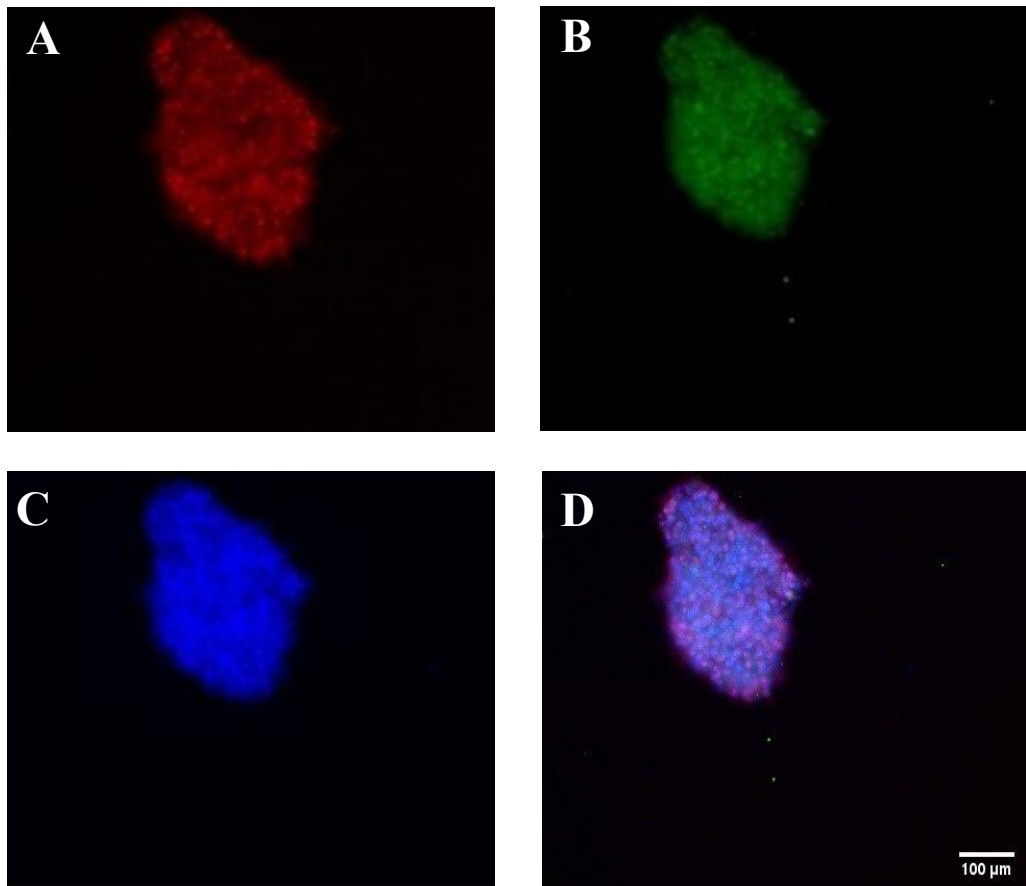


**Fig.4b**

Annexin V-FITC / PI assay on 3D SH-SY5Y/U-87MG in dynamic condition. Necrotic cells (A); Apoptotic cells (B); DAPI (C); Merge channel (D).

Scale bar: 100  $\mu$ m

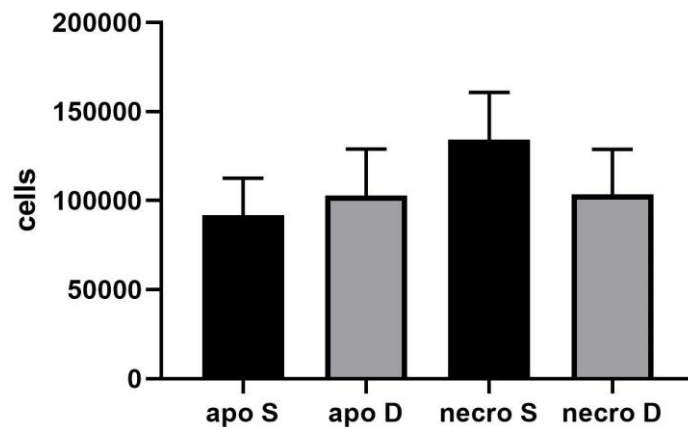


**Fig.4c**

Annexin V-FITC / PI assay on 3D SH-SY5Y/U-87MG shows a consistent presence of necrotic cells that exceeds apoptotic cells under static (S) conditions.

In dynamic (D) conditions, apoptotic cells exceed necrotic cells.

Dati  $\pm$  SEM.

### 3.3 Spheroid immunofluorescence

After 24h in flow conditions, an indirect immunofluorescence with two specific antibodies was performed to verify the presence of both cell lines in the spheroids: anti-GFAP (glial fibrillar acid protein) for U-87MG and  $\beta$ -III tubulin for SH-SY5Y. Figures show the presence of both cell lines in the spheroids: anti-GFAP for U-87MG expressed in GFP and anti- $\beta$ -III tubulin for SH-SY5Y, in RFP. It is of note that GFP fluorescence was distributed in the external portion of the spheroids in dynamic conditions (LB1) (**Fig.5**). This can be explained with a specific topography of the spheroids with SH-SY5Y cells in the internal portion and U-87MG in the external portion of the spheroid, respectively.

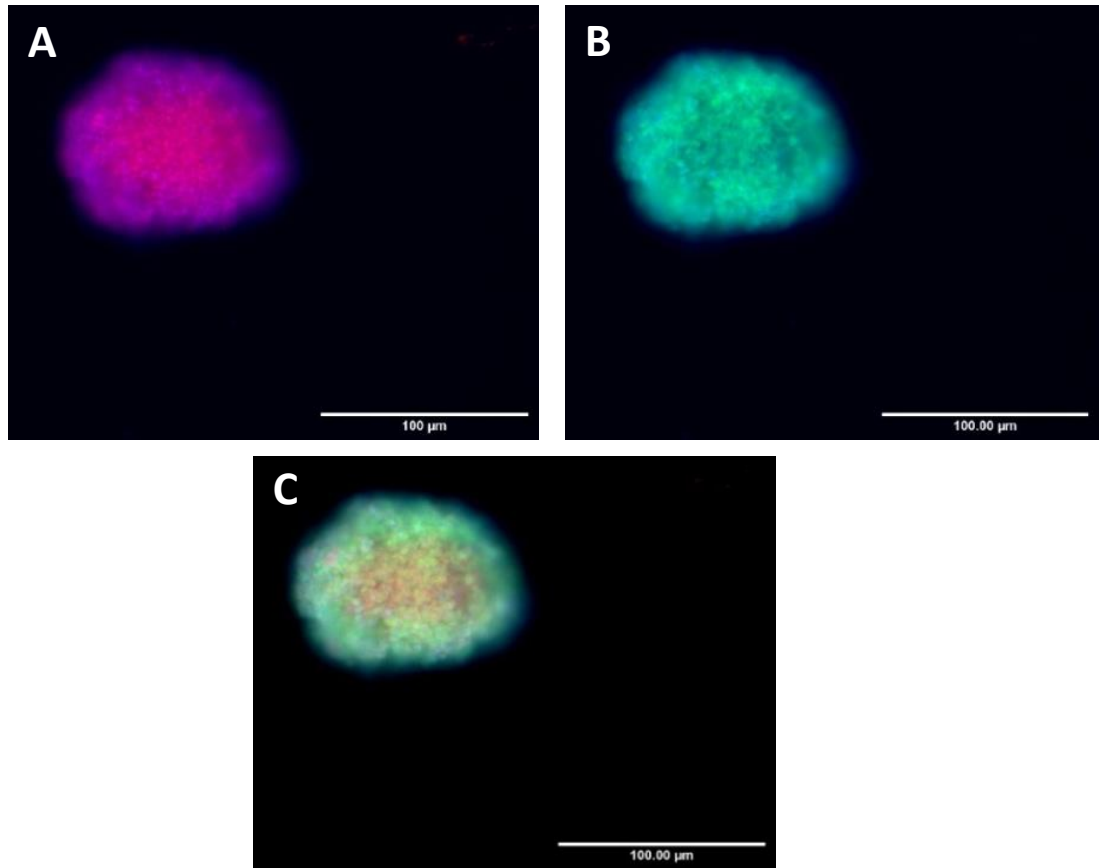


**Fig.5**

3D SH-SY5Y/U-87MG

in dynamic culture labelled with  $\beta$ -III tubulin (A, neural marker), GFAP (B, glial marker). Nuclei in DAPI.

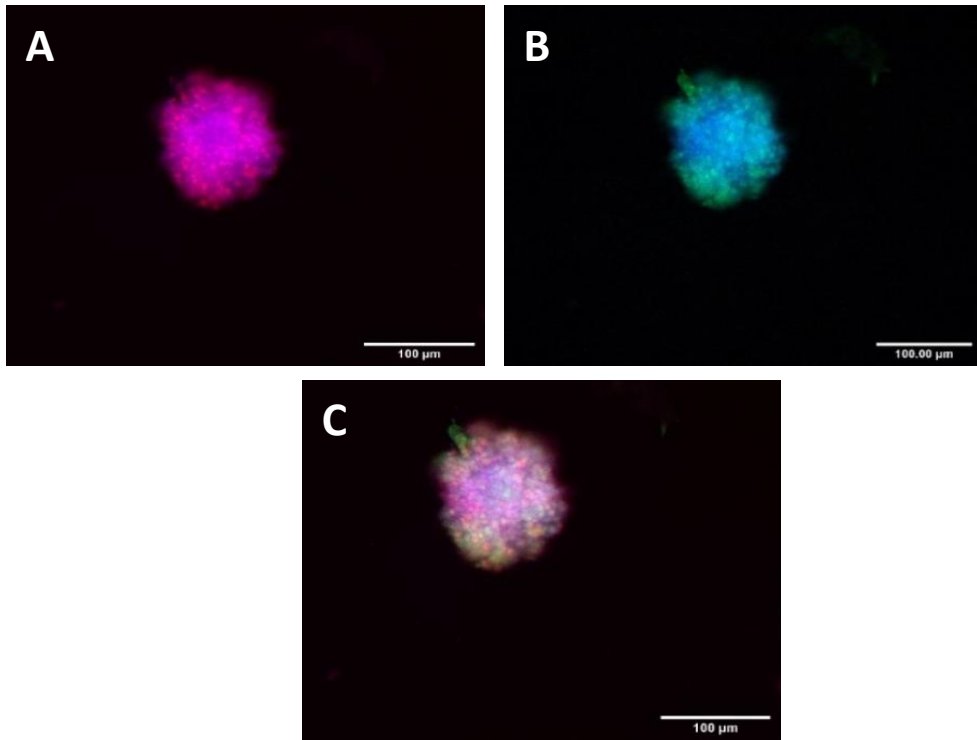


**Fig.6**

3D SH-SY5Y/U-87MG

in static culture labelled with  $\beta$ -III tubulin (A, neural marker), GFAP (B, glial marker). Nuclei in DAPI.

In static conditions however, cells acquire a random distribution (**Fig.6**). Furthermore, spheroids of both conditions, have been reacted by immunofluorescence against Ki67, a marker of cell proliferation. Results (**Fig.7B**) show a preferential distribution of Ki67 in the outer portion of spheroids in dynamic conditions (LB1). Ki67 is, its external marking indicates an increase in this proliferation on the outside of the spheroids, as the recirculation of the nutrients of the flow involves, as has also been made known from the morphological control, an increase in the spheroids starting from the outermost cells. In static (LB1) (**Fig.7A**), however, a lower fluorescence intensity of Ki67 is observed.

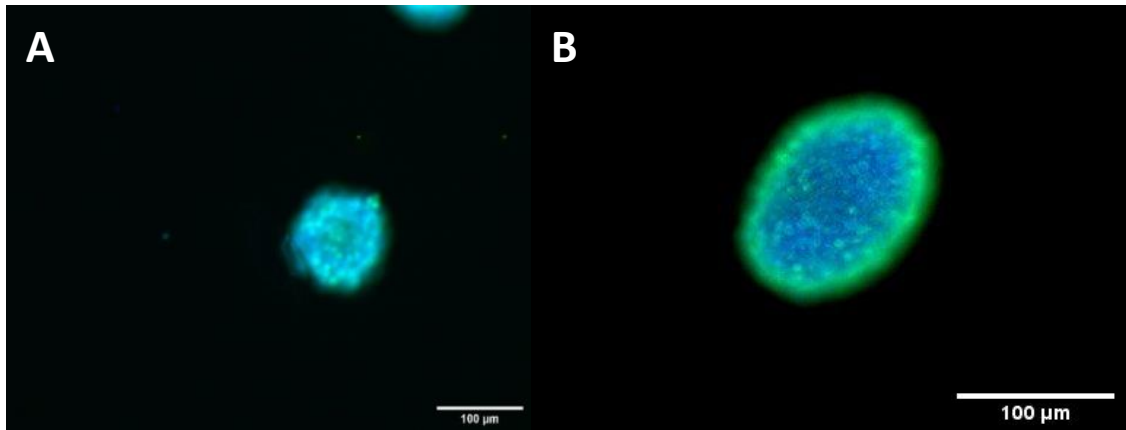


**Fig.7**

3D SH-SY5Y/U-87MG

in static culture (A) and in dynamic culture (B) labelled with GFP (Ki67). Nuclei in DAPI.

### 3.4 LDH assay

To evaluate the cytotoxicity of the spheroids in static culture (24-well-ULA) and in dynamic culture (LB1), LDH assay was used. Graph shows an increase in cytotoxicity in static rather than in dynamic compared to the positive control at 490nm. Furthermore, the percentage of cytotoxicity (**Fig.8**) for both cultures was calculated using this equation:

$$\% \text{Cytotoxicity} = \left( \frac{\text{Spontaneous activity} - \text{Control}}{\text{Maximum activity} - \text{Spontaneous activity}} \right) \times 100$$

From the results it is possible to highlight a higher cytotoxicity in static (52%) compared to dynamic culture (47%).

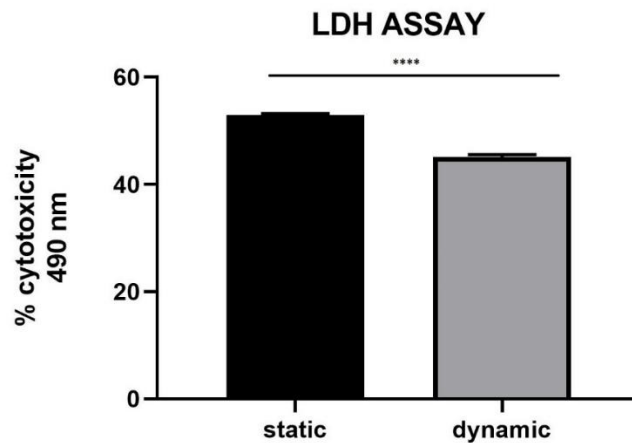


**Fig.8**

LDH assay performed on 3D SH-SY5Y/U-87MG show a major toxicity in static culture compared to dynamic culture. The graph shows the means  $\pm$  SEM of three experiments. Statistical analysis was performed through the analysis of Mann-Whitney test. The differences were considered significant static and dynamic culture.

\*\*\*\* P <0.001

### 3.5 Prestoblue assay

To evaluate the viability of the spheroids (SH-SY5Y / U-87MG) in static culture (24-well-ULA) and in dynamic culture (LB1), the Prestoblue assay was used. The graph shows an increase in cell viability in dynamic rather than static at 570 nm. The increase in absorbance caused by resoruphin, produced by active cells, is directly proportional to cell viability (**Fig.9**).

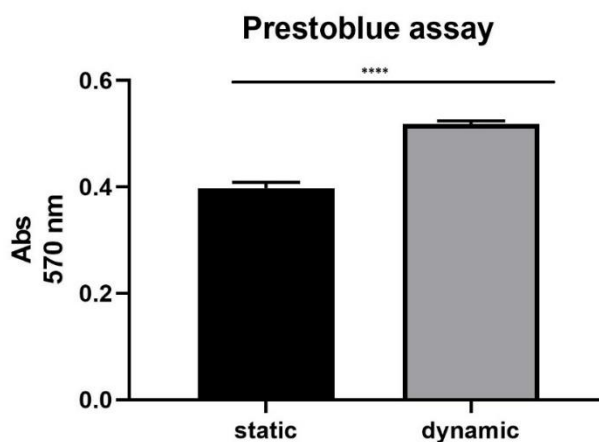


**Fig.9**

Prestoblue assay performed on 3D SH-SY5Y/U-87MG show a major viability in dynamic culture compared to static culture. The graph shows the means  $\pm$  SEM of three experiments. Statistical analysis was performed through the analysis of Mann-Whitney test. The differences were considered significant between static and dynamic culture

\*\*\*\* P <0.001

### 3.6 Quantitative measurement of reactive oxygen species (ROS)

To carry out a quantitative measurement of reactive oxygen species, dichlorodihydrofluorescein diacetate (DCFH2-DA) was used. After incubation with 50  $\mu$ M DCFH2-DA for 60 min, the static (24-well-ULA) and dynamic (LB1) spheroids (SH-SY5Y / U-87MG) were visualized by JuLi <sup>TM</sup> Stage RealTime Cell History Recorder microscope. Compared to the positive control (2mM H<sub>2</sub>O<sub>2</sub>). The spheroids were then lysed by PBS / EDTA to perform the fluorescence measurement. The graph (**Fig.10**) shows a decrease in fluorescence in static (24-well-ULA)

compared to the dynamic (LB1) whose value (in static) is halved compared to the dynamic value.

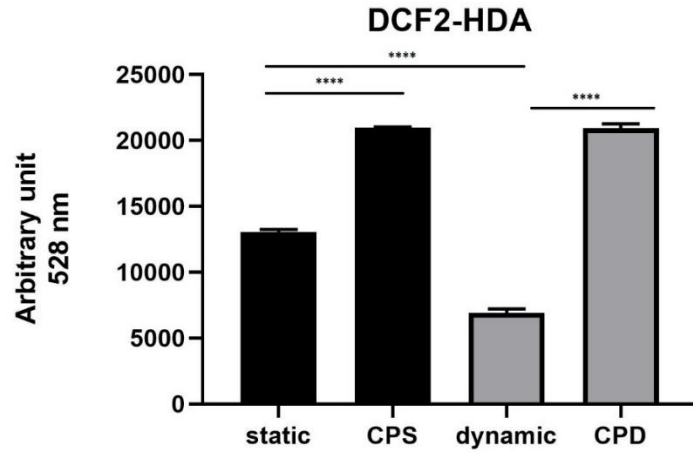


**Fig.10**

DCF2-HDA conducted on 3D SH-SY/U-87MG show a higher fluorescence in static compared to its positive control (CPS) and to dynamic condition. A lesser fluorescence is evident in dynamic condition compared to its positive control (CPD). Positive control:  $H_2O_2$ . The graph shows the means  $\pm$  SEM of three experiments.

Statistical analysis was performed through the analysis of variance (ANOVA) and the Dunnet's posttest. The differences were considered significant between static and dynamic culture, static and its Positive Control (CPS) and dynamic and its Positive Control (CPD).

\*\*\*\* P <0.001.

#### 4. Discussion

Animal tests have a pivotal role in preclinical stage helping to understand the adverse reactions in medical products and to develop promising strategies to prevent them (Meigs et al., 2018). Moreover, animal tests represent a high cost for scientific community, giving most of the time misleading results. It is therefore useful to replace them mainly for the economic consequences and the incorrect results (Bottini and Hartung, 2010; Hartung, 2017). Since the 1950s, *in vitro* models have been used in static conditions, such as Petri dishes or multiwell plates. But the cells, inside the body, live in a dynamic environment, whose behavior is influenced by physical stimuli (Bilodeau and Mantovani, 2006). To be able, therefore, to simulate a real physiological response, a good *in vitro* model should be as close as possible to the *in vivo* situation (Rouwkema et al., 2011). Thus, technical advances have gained more ground as they allow to monitor cells with a highly controlled and reproducible environment, which integrates various functions, such as monitoring of environmental variables, application of measurable chemical-physical stimuli, adequate exchange of nutrients and removal of waste substances of cellular respiration (Giusti, 2015). A valid tool that meets these needs is the bioreactor, capable to recreate the physiological flow to which cells are subjected *in vivo*. The first difference with static models it is clear from the possibility of having an efficient spatial distribution of cells on 3D supports, thus also allowing a better supply of oxygen in the crops (Giusti, 2015). The first bioreactors, in use in the 1970s, were in agitation mechanical and provided by the insertion of gas, the agitation of the cell culture, with the aim of keeping the cells in suspension, allowing them to adhere to structures such as scaffold and improving solute transport. These tools can connect different metabolic compartments This new platform gives the opportunity to connect different compartments, to better reproduce the dynamic circulation of molecules in a continuous flow condition (Colombo et al., 2019; Mazzei et al., 2008). In a typical fabric-on-chip embodiment, microfluidic channels are fabricated using soft lithography techniques by printing an elastomeric material, the polydimethylsiloxane (PDMS), on a photo-defined main mold (Weibel et al., 2007). Microfluidic systems are characterized by small volumes, limited nutrients, and low cells density. For this reason, the use of millifluidic model made it possible to link a high recycling of nutrients with larger volumes, to obtain a physiologically relevant cell density (Giusti, 2015). Considering the abovementioned studies, in this experimental work we have studied 3D brain co-culture (SH-SY5Y/U-87MG) They were grown in co-culture according to the hanging drop method and subsequently transferred in two different conditions:

in static ones represented by 24-well Ultra low attachment (24-well-ULA suitable for the formation of 3D structures) and dynamic ones using a Livebox1 bioreactor. This powerful tool employs the use of a single chamber with an independent flow connected with its mixing chamber containing culture medium to a peristaltic fluid circuit (Liveflow). This study allowed us to analyze these two different approaches in order to learn the differences to get closer to a more like-live condition. Our aim was to investigate physiological differences arising when cells are cultured in static (24-well ULA) or dynamic (LB1) condition, monitoring relevant biological parameters such as pH of the medium, cell toxicity and viability, cell proliferation, apoptosis and necrosis, on spheroids made by SH-SY5Y and U-87MG. It was possible to learn that the culture medium of the spheroids under dynamic conditions showed a variation of pH narrower than in static models (increase in dynamic of the value of about 0.2). It has been reported that in live-cell culture, pH of the medium, as consequence of cell metabolism (mainly the glycolytic lactic acid production) tend to acidification (Michl et al., 2019). Our in vitro model ensures greater pH stability of the medium thus providing healthy environment for cells, which in turn ensures higher result reproducibility. This is probably because in the dynamic models the peristaltic pump guarantees a continuous flow of solutes and nutrients and a consequent greater supply of oxygen. Our data about pH of the dynamic culture medium agree with the reported literature since they showed just about 0.1 points of variation, compared with static culture where 0.3 points of variation is observed. This suggests that dynamic conditions guarantee a more appropriate supply of nutrients and waste elimination. The morphological analysis on SH-SY5Y / U-87MG spheroids in static and in dynamic culture at different times (0, 2h, 8h and 24h), showed a substantial increase in size of the spheroids in dynamic culture compared to static culture (1.50 times dynamic vs static). This result is probably due to a continuous recirculation of the nutrients contained in the mixing chamber which, thanks to the flow of the peristaltic pump, more continuously fed spheroids. Our next goal will be to further test flow conditions to verify the limits of the spheroids growth and consequent eventual break down under dynamic conditions to evaluate the maximum performances of the device. The evaluation of apoptotic and necrotic cells in the spheroids made by SH-SY5Y / U-87MG demonstrated that while static culture conditions favored cell necrosis, dynamic culture conditions slightly favored apoptosis. Although more data are needed, this different behavior can be explained because in static conditions cells go directly into necrosis maybe due to lack of available nutrients or to a worse physiological equilibrium, while in dynamic conditions cells

undergo to a more controlled or well-established physiological equilibrium, based among other factors on the programmed cell death. The indirect immunofluorescence assay allowed to demonstrate the presence of both cell lines (SH-SY5Y and U-87MG) during 3D co-culture experiments. However, it is noteworthy that in static conditions, cells appear to be arranged in an apparently random way to form spheroids, while in dynamic conditions the U-87MG cells arrange themselves mainly on the outside and the SH-SY5Y are arranged inside the spheroids. Regardless of the cause on which we are still investigating on, it is of interest to note, as simple speculation, that this particular topography resembles the structure of the brain parenchyma, where neurons are protected and nourished by astrocytes stand between the neurons and the cerebral endothelium. Our data on cell proliferation marker Ki67 help to support this view. In static conditions, lower Ki67 fluorescence intensity was observed, whose distribution was at random, while in dynamic culture there is a Ki67 higher intensity signal, mainly in the cells that constitute the outermost part of the spheroids; this can be explained with the presence of appropriate nutrients recirculation due to the dynamic flow. This Ki67 immunofluorescence presumably belongs mainly to U-87MG since this cell type occupy the outer part of the spheroids. The LDH dosage indicates the greater cytotoxicity of the static conditions than in dynamic and is consistent with the other cellular health data shown. Finally, the dynamic conditions favor the lowering of ROS levels like the data of the DCFH2-DA probe demonstrate. Hence this also indicates that the cells in these spheroids possess a controlled and physiological cellular respiratory metabolism, becoming metabolically more efficient. We will further conduct an analysis on the total antioxidant capacity at different time points in order to observe when cells express ROS. Although our dynamic system has proved useful to discriminate it with respect to the static culture where the cells are not in physiological conditions, having used only 24h as flow time, could be considered a short time. We aim for a higher time by constantly monitoring parameters such as pH, ROS expression and cell viability. Hence, here we demonstrate that to obtain reliable, viable and health spheroids in cell culture, the fluid dynamic cell culture is of choice favoring better environmental conditions, cell growth, healthier cells and the establishment of more stable cell 3D architecture.

## 5. Conclusions

Animal tests are currently subject of discussion among the entire scientific community in terms of costs compared to unsatisfactory results. Thanks to this reason, many industries like pharmaceutical, (agro-)chemical aim to develop high throughput culture systems in order to obtain predictive clinical studies. *In vitro* cultures whose conditions involve uncontrolled variables result limited in representing the *in vivo* metabolism of cells and their phenotype. In this regard, *in vitro* dynamic cultures provide a much more realistic environment, considering environmental variables, controllable chemical-physical stimuli and nutrient exchange. We have used a bioreactor, able to recreate the physiological flow to which they are subjected cells *in vivo*. This device allowed us to morphologically study a structure 3D brain in co-culture using two different neuronal cell lines. Thanks to cell and molecular analyses we were able to evaluate the differences in morpho-physiological state compared to a conventional static model, whose depletion of the flow results in a worse performance from a morphological and metabolic point of view, making them not suitable for accurate *in vitro* study. Taken together our data demonstrate that dynamic flow 3D cell culture conditions overcome most of the problems associated with traditional static cell culture conditions, outperforming the latter as they provide a well-established and controlled environment, useful for the appropriate onset of physiological relationship between cells. These features can be very useful for the *in vitro* data reproducibility and to provide satisfactory results when compared with *in vivo* data.

## References

- Beebe, D.J., Mensing, G.A., Walker, G.M. (2002). Physics and applications of microfluidics in biology. [PubMed: 12117759].
- Bilodeau, K., and Mantovani, D. (2006). Bioreactors for tissue engineering: focus on mechanical constraints. A comparative review. *Tissue Eng.* 2367-83. doi: 10.1089/ten.2006.12.2367.
- Bottini, A. A. and Hartung, T. (2010). The economics of animal testing. *ALTEX* 27, Spec Issue, 67-77. <http://www.altex.ch/resources/EMS.pdf>.
- Broekgaarden, M., Bulin, A.L., Porret, E., Musnier, B., Chovelon, B., Ravelet, C., Sancey, L., Elleaume, H., Hainaut, P., Coll, J.L., Le Guével, X. (2020). Surface functionalization of gold nanoclusters with arginine: a trade-off between microtumor uptake and radiotherapy enhancement. (2020). doi: 10.1039/d0nr01138j. PMID: 32187249.
- Canonico, B., Luchetti, F., Arcangeletti, M., Valentini, M., Papa, S. (2018). Indagini citofluorimetriche nella vitalità e morte cellulare. II. Studio di altre funzioni cellulari”.
- Chitnis, T., and Weiner, H. L. (2017). CNS inflammation and neurodegeneration. *J. Clin. Invest.* 127, 3577–3587. doi: 10.1172/jci90609.
- Colombo, R., Paolillo M., Papetti, A. (2019). A new millifluidic-based gastrointestinal platform to evaluate the effect of simulated dietary methylglyoxal intakes. DOI: 10.1039/c9fo00332k.
- Cucullo, L., Hossain, M., Puvenna, V., Marchi, N., Janigro, D. (2011) The role of shear stress in Blood-Brain Barrier endothelial physiology. *BMC Neurosci.* 2011 May 11;12:40. doi: 10.1186/1471-2202-12-40. PMID: 21569296; PMCID: PMC3103473.
- Engelmann, J., Volk, J., Leyhausen, G., Geurtsen, W. (2005). ROS formation and glutathione levels in human oral fibroblasts exposed to TEGDMA and camphorquinone”. *J Biomed Mater Res B Appl Biomater.* 2005 Nov;75(2):272-6. doi: 10.1002/jbm.b.30360. PMID: 16080163.
- Giusti S. (2015). Bioreattori per la realizzazione di modelli multi-organo in vitro. XXXIV Scuola Annuale “Approcci ingegneristici per lo sviluppo di metodiche alternative alla sperimentazione in vivo”.

Ham, S.L., Joshi, R., Luker, G.D., Tavana, H. (2016). Engineered Breast Cancer Cell Spheroids Reproduce Biologic Properties of Solid Tumors. doi: 10.1002/adhm.201600644. Epub 2016 Sep 7. PMID: 27603912; PMCID: PMC5142748.

Hartung, T. (2017). Thresholds of toxicological concern – Setting a threshold for testing where there is little concern. ALTEX 34, 331-351. doi:10.14573/altex.1707011.

Jeliazkova-Mecheva, V.V., and Bobilya, D.J. (2003). A porcine astrocyte/endothelial cell co-culture model of the blood-brain barrier. Brain Res Brain Res Protoc. 2003 Oct;12(2):91-8. doi: 10.1016/j.brainresprot.2003.08.004. PMID: 14613810.

Kalyanaraman, B., Darley-Usmar, V., Davies, K.J., Dennerly, P.A., Forman, H.J., Grisham, M.B., Mann, G.E., Moore, K., Roberts, L.J. (2012). 2nd, Ischiropoulos H. Measuring reactive oxygen and nitrogen species with fluorescent probes: challenges and limitations. Free Radic Biol Med. 2012 Jan 1;52(1):1-6. doi: 10.1016/j.freeradbiomed.2011.09.030. Epub 2011 Oct 2. PMID: 22027063; PMCID: PMC3911769.

Lall, N., Henley-Smith, C.J., De Canha, M.N., Oosthuizen, C.B., Berrington, D. (2013). Viability Reagent, PrestoBlue, in Comparison with Other Available Reagents, Utilized in Cytotoxicity and Antimicrobial Assays". Int J Microbiol. 2013;2013:420601. doi: 10.1155/2013/420601. Epub 2013 Apr 4. PMID: 23653650; PMCID: PMC3638707.

Langhans, S.A. (2018). Three-Dimensional in Vitro Cell Culture Models in Drug Discovery and Drug Repositioning. Front Pharmacol. 2018 Jan 23;9:6. doi: 10.3389/fphar.2018.00006. PMID: 29410625; PMCID: PMC5787088.

Lemmo, S., Atefi, E., Luker, G.D., Tavana, H. (2014). Optimization of Aqueous Biphasic Tumor Spheroid Microtechnology for Anti-Cancer Drug Testing in 3D Culture". Cell Mol Bioeng. 2014 Sep 1;7(3):344-354. doi: 10.1007/s12195-014-0349-4. PMID: 25221631; PMCID: PMC4159185.

Mazzei, D., Vozzi, F., Cisternino, A., Vozzi, G., Ahluwalia, A. (2008). A High-Throughput Bioreactor System for Simulating Physiological Environments. IEEE Transactions on Industrial Electronics, vol. 55, no. 9, pp. 3273-3280, Sept. 2008, doi: 10.1109/TIE.2008.928122.

- McDonald, J.C., Duffy, D.C., Anderson, J.R., (2000). Fabrication of microfluidicsystems in poly (dimethylsiloxane). Epub 2000/01/14.
- Meigs, L., Smirnova, L., Rovida, C., Leist, M., Hartung T (2018). Animal testing and its alternatives - the most important omics is economics. *ALTEX*. 2018;35(3):275-305. doi: 10.14573/altex.1807041. PMID: 30008008.
- Michl, J., Park, K.C., Swietach, P. (2019). Evidence-based guidelines for controlling pH in mammalian live-cell culture systems. *Commun Biol* 2, 144 (2019). <https://doi.org/10.1038/s42003-019-0393-7>
- Pandey, P.K., Sharma, A.K. Gupta, U., (2016). Blood brain barrier: An overview on strategies in drug delivery, realistic in vitro modeling and in vivo live tracking” (2016). DOI: 10.1080/21688370.2015.1129476.
- Polonchuk, L., Chabria, M., Badi, L., Hoflack, J.C., Figtree, G., Davies, M.J., Gentile, C. (2017). Cardiac spheroids as promising in vitro models to study the human heart microenvironment. *Sci Rep*. Aug 1;7(1):7005. doi: 10.1038/s41598-017-06385-8. PMID: 28765558; PMCID: PMC5539326.
- Reiniers, M.J., van Golen, R.F., Bonnet, S., Broekgaarden, M., van Gulik, T.M., Egmond, M.R., Heger, M. (2017). Preparation and Practical Applications of 2',7'-Dichlorodihydrofluorescein in Redox Assays” *Anal Chem*. 2017 Apr 4;89(7):3853- 3857. doi: 10.1021/acs.analchem.7b00043. Epub 2017 Mar 15. PMID: 28224799; PMCID: PMC5382573.
- Rouwkema, J., Gibbs, S., Lutolf, M.P., Martin, I., Vunjak-Novakovic, G., Malda J., (2011). In vitro platforms for tissue engineering: implications for basic research and clinical translation. doi: 10.1002/term.414.
- Shri, M., Agrawal, H., Rani, P., Singh, D., Onteru, S.K. (2017). Hanging Drop, A Best Three-Dimensional (3D) Culture Method for Primary Buffalo and Sheep Hepatocytes. *Sci Rep*. Apr 26;7(1):1203. doi: 10.1038/s41598-017-01355-6. PMID: 28446763; PMCID: PMC5430879.
- Squires, T.M., Quake, S.R. (2005). Microfluidics: Fluidphysicsat the nanoliter scale. (2005).*Reviews of ModernPhysics.*; 77:977–1026.

Taylor, K., Gordon, N., Langley, G., Higgins, W. (2008). Estimates for worldwide laboratory animal use in 2005. *Altern Lab Anim.* Jul;36(3):327-42. doi: 10.1177/026119290803600310. PMID: 18662096.

Weibel, D.B., Diluzio, W.R., Whitesides, G.M. (2007). Microfabrication meets microbiology (2007). *NatRevMicrobiol.* 2007; 5:209–18. Epub 2007/02/17. [PubMed: 17304250].

Wolff, A., Antfolk, M., Brodin, B., (2015). In Vitro Blood-Brain Barrier Models-An Overview of Established Models and New Microfluidic Approaches” (2015). *J Pharm Sci.*; 104:2727–46. Epub 2015/01/30. [PubMed: 25630899].

## **Chapter 5:**

### **gH625- lipoPACAP in a 3D dynamic *in vitro* model of blood-brain barrier**

## **Abstract**

The blood-brain barrier (BBB) is the interface that separates the neural tissue from the circulating bloodstream. It is a complex multicellular structure that includes a layer of endothelial cells that cover the blood vessel wall, representing a physical barrier between the blood and the brain parenchyma, the cell-endothelial cell junctions are therefore fundamental to protect brain from external injury exerting a limited passage of potential therapeutic molecules. In this regard, our present study aims to recreate a 3D BBB *in vitro* fluid dynamic model using the three main components of BBB: brain endothelial cells, neuron cells and glial cells connected in the BBB structure seeded in a 3D architecture. To test its utility in drug delivery studies, we carried out the passage through the BBB model of functionalized liposomes loaded with PACAP, a neuroprotective agent.

## 1. Introduction

The blood brain barrier (BBB) is a highly selective structure that does not allow the passage of many drugs, antibodies, and gene carriers (Garbuzova-Davis et al., 2016) from the vascular compartment to the central nervous system (CNS). Due to non-targeted pharmacological approaches, to study many neurodegenerative diseases (Alzheimer's disease, Parkinson's disease, amyotrophic lateral sclerosis) it is important to use non-invasive mechanisms for the delivery of therapeutic molecules through BBB, using innovative *in vitro* models such as preclinical studies. Most of the *in vitro* models studied for BBB are based on cell culture systems using both static and dynamic models. Unlike static models, dynamic models are able to provide cells with a highly controlled and reproducible environment to ensure adequate nutrient exchange, removal of waste substances from cellular metabolism and the application of appropriate physico-chemical stimuli. Furthermore, the dynamic models give the possibility of having an efficient spatial distribution of cells on 3D supports, thus also allowing a better supply of oxygen in crops (Giusti et al., 2014). Among the dynamic models, there are the millifluidic systems like LiveBoxes (IVTech) that we usually use in laboratory. These are modular bioreactors that faithfully recreate the physiological conditions *in vivo*. They have a diameter of 15 mm made of polydimethylsiloxane (PDMS) transparent to allow live imaging analysis (Sbrana and Ahluwalia, 2012). These bioreactors can be inserted into an inverted fluorescence microscope with automated live recorder (JuLi™ Stage Real-Time Cell History Recorder, NanoEntek), which is in turn inserted into the CO<sub>2</sub> incubator. This allows to continuously monitor in real time the microenvironment *in vitro*, following all changes occurring in the flow and/or expression of molecules. During the first year of my PhD, I studied the drug delivery of neuroprotective peptides in the CNS through an *in vitro* dynamic model of BBB. The bioreactor used for my experiments was the “Livebox2” (LB2, IVtech; Italy) used to mimic physiological barriers (Giusti et al., 2014), consisting of two different chambers, upper and lower, each with an independent flow, separated by a porous membrane. The chambers are then connected to a peristaltic pump which allows a continuous exchange of nutrients and allows to evaluate the diffusion of molecules between the two compartments. In the apical compartment, in correspondence of the membrane, murine endothelial brain cells (bEnd.3), commonly used for BBB *in vitro*, (Rodrigues, 2019) were seeded and subsequently liposomes with 20μM of rhodamine-PACAP (gH625-lipoPACAP-Rho) were injected in the upper chamber. Pituitary adenylate cyclase activating peptide (PACAP) can act as a neurotransmitter,

neuromodulator and neuroprotective factor (Vaudry et al., 2009) but has a short half-life in the bloodstream. Therefore, Valiante et al. have developed a transport system that involves the use of a functionalized liposome conjugated to the gH625 peptide. It is a membranotropic peptide, deriving from the H glycoprotein of *Herpes simplex* virus type 1, capable to promote vesicular fusion without ruptures (Falanga et al., 2011). gH625 also crosses the BBB accumulating in nerve cells without toxic effects (Valiante et al., 2015; Iachetta et al., 2019). Results obtained showed in the lower chamber, after 30 minutes, a higher quantity of PACAP-Rho conjugated to the liposome functionalized with gH625, compared to the upper chamber and compared to non-functionalized lipoPACAP-Rho, also maintaining high fluorescence during the 2h of the experiment. bEnd.3 cells observed under the JuLi Stage microscope show an absence of signal for PACAP-Rho, demonstrating the passage of the latter in the lower chamber. To indicate the formation of a stable barrier, immunofluorescence assay was performed for junctions' protein like ZO1 (zonula occludens, tight junction), N-cadherin and  $\beta$  catenin (adherens junctions). During the last year of my PhD, I have recreated a more complex 3D dynamic in vitro BBB by adding a co-culture of 3D SH-SY5Y (neuroblastoma) and U-87MG (astrocytoma) cells in the lower chamber of LB2.

## **2. Materials and Methods**

### **2.1 Cell culture**

Murine endothelial brain cells (bEnd.3), Neuroblastoma cells (SH-SY5Y) and Glioblastoma cells (U-87MG) were individually grown in Dulbecco's Modified Eagle's Medium High glucose, supplemented with fetal bovine serum (10%, Sigma-Aldrich-Saint Louis, USA), penicillin/streptomycin (100 U/ml, Sigma-Aldrich-Saint Louis, USA), L-glutamine (2mM, Sigma-Aldrich-Saint Louis, USA), gentamycin (40 $\mu$ g/ml, Sigma-Aldrich-Saint Louis, MO, USA) at 37°C, 5%CO<sub>2</sub> in a humidified incubator. Cells grow adherent in 25 cm<sup>2</sup> flasks. Medium was changed twice a week. When 70% confluent, cells were enzymatically detached with trypsin-EDTA (Sigma-Aldrich-Saint Louis, USA).

## **2.2 Set up of endothelial cell brain (bEnd.3) monolayer**

To set our 3D BBB fluid dynamic *in vitro* model we used a LB2 bioreactor. As previously reported, this bioreactor is composed of a double chamber with independent flow separated by a porous membrane of 0,45µm. bEnd.3 cells are seeded on this membrane from the inlet tube of the upper chamber in all aseptic condition (Protocol was described in *Chapter 2, 2.4 Lucifer yellow assay*). After 7 days in fluid dynamic condition (Liveflow, 250µl/min), we noted a stable and integer barrier confirmed by the experiments conduct through Lucifer yellow assay (*Chapter 2, 2.4 Lucifer yellow assay*) and Immunofluorescence assay with the formation of junctions' proteins (*Chapter 1, 3.3 Immunofluorescence assay*).

## **2.3 3D co-culture spheroids**

To implement our 3D BBB fluid *in vitro* dynamic system, we were adding a glial cell line (U-87 MG) in co-culture with neuronal spheroids (SH-SY5Y enriched with neural portion). 3D SH-SY5Y/U-87MG were formed by hanging drop method (Protocol described in *Chapter 4, 3.2 Spheroids in static and dynamic culture*). Briefly, SH-SY5Y and U-87MG are mixed 1:1.2 (Nzou et al., 2018) and drops are deposited in a lid of a 60mm dish. After 48h from the aggregates formation, they were transferred in a Livebox1 (LB1) only one chamber bioreactor (LB1, IVTech, Italy) for perform the experiments dynamically. This bioreactor relates to its mixing chamber containing 10 ml of complete DMEM culture medium and then connected to the peristaltic pump fluid circuit (Liveflow, IVTech, Italy). Flow was set to 100µl/min for 24h. The first experiments conducted in LB1 helped us once again to set the suitable flow conditions and we carried out morphological checks at different time points up to 24h, observing how the spheroids in co-culture increase in size (*Chapter 4, Fig.3*). We then performed immunofluorescence experiments (*Chapter 4, Fig.5*) on these spheroids both for cell line markers to ensure the presence of neural cell line and glial cell line.

## **2.4 gH625- lipoPACAP through a 3D fluid-dynamic in vitro BBB**

Once set the suitable flow conditions in LB1 for 3D SH-SY5Y/U-87MG, the experiments were performed in LB2. In the upper chamber we have seeded endothelial brain cells (bEnd.3) for 7

days, then we have transferred our 3D SH-SY5Y/U-87 MG from static condition (Hanging drop culture) to dynamic condition (lower chamber of LB2). LB2 was then connected to its mixing chamber containing 10 ml DMEM complete culture medium and they were connected to Liveflow at 100 $\mu$ l/min for 24h to adapt our 3D fluid-dynamic in vitro BBB to flow conditions. After 24h, gH625-lipoPACAP-Rho was injected in the inlet tube in the upper chamber to perform the passage of PACAP loaded with gH625-liposome (**Fig.1**).

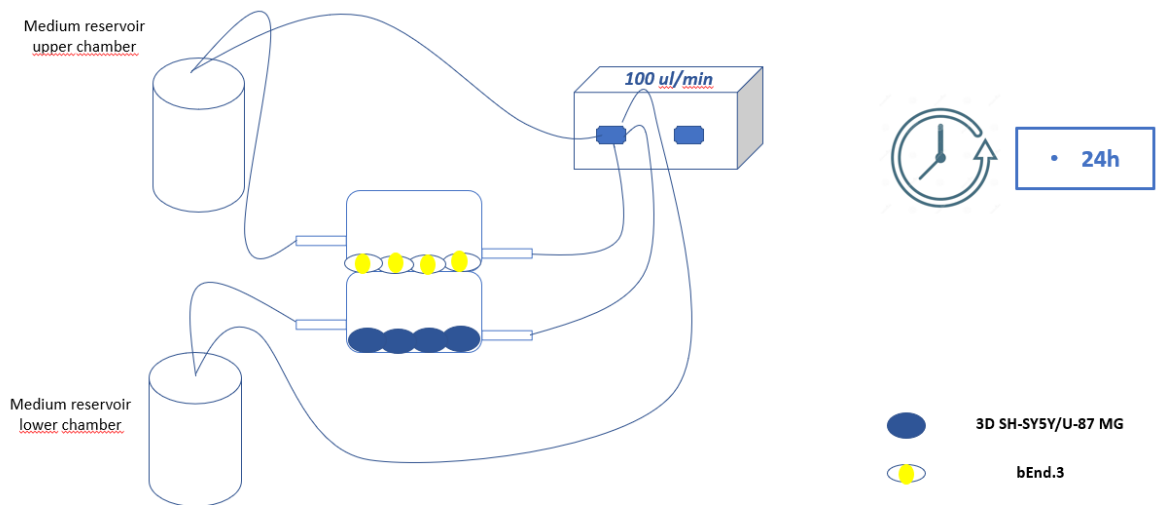


**Fig.1**

Schematic view of a dynamic bioreactor: Live Box 2 (LB2) is composed by an upper chamber connected to a medium reservoir and to a Liveflow pump (100  $\mu$ L/min) and a lower chamber connected to a medium reservoir and to a Liveflow pump (100  $\mu$ L/min). In the upper chamber, bEnd.3 cells are seeded on the porous membrane, in the lower chamber there are co-culture spheroids (3D SH-SY5Y/U-87MG).

### 3.Results

#### **gH625- lipoPACAP through a 3D fluid-dynamic in vitro BBB**

LB2 containing bEnd.3 cells in the upper chamber and 3D SH-SY5Y/U-87 MG in the lower chamber was placed in the JuLi <sup>TM</sup> Stage RealTime Cell History Recorder microscope to acquire spheroids images after the passage of gH625-lipoPACAP-Rho for 24h in dynamic flow conditions in two different channels: bright and RFP. Images show a red fluorescence in 3D SH-SY5Y/U-87MG. Results obtained suggest the passage of PACAP-Rho through endothelial brain cells monolayer and the intake of PACAP-Rho in 3D SH-SY5Y/U-87MG cells (**Fig.2**).

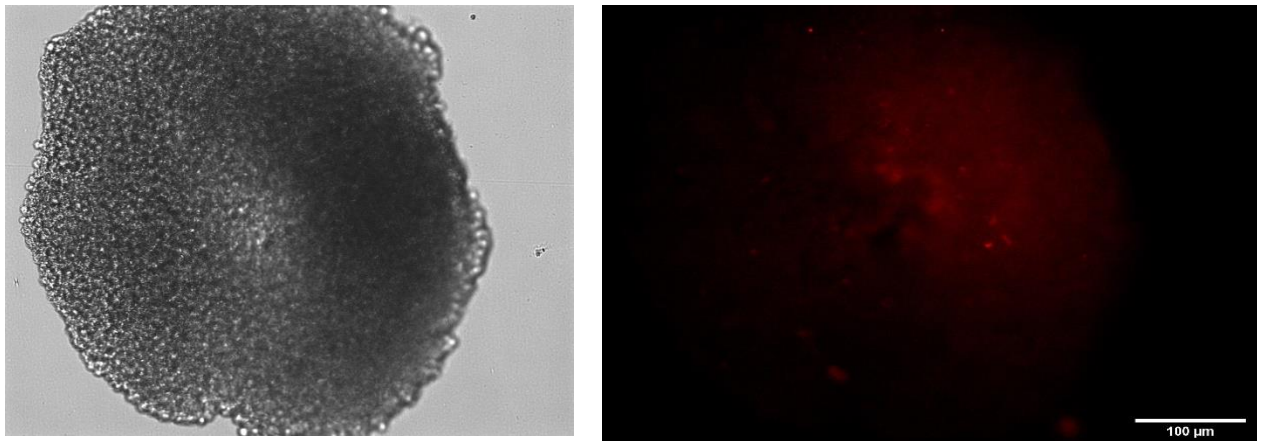


**Fig.2**

Representative image of spheroids obtained by co-culturing human neuroblastoma cell line enriched by neural portion SH-SY5Y and glioblastoma cell line U-87MG cells in the lower chamber of LB2/bEnd.3 cells. After the passage of gH625-liposome PACAPrho, spheroids were labelled with PACAP-Rho. Image were acquired as Z stack with the JuLI Stage fluorescence recorder and maximum intensity projection was showed.

#### **4. Discussion**

The BBB is the interface that separates the neural tissue from the circulating blood stream. It is a complex structure that includes a layer of endothelial cells that cover the blood vessel wall, representing a physical barrier between the blood and the brain parenchyma, the cell-endothelial cell junctions are therefore fundamental (Abbot et al., 2010). BBB allows the CNS to be a protected compartment in which the composition of extracellular fluids must be regulated as precisely as possible in terms of solute concentration (Zlokovic and Apuzzo, 1998). Most of *in vitro* models that try to mimic BBB include static models that do not represent what happens *in vivo* due to a lack of stimuli due to the static culture. Instead, dynamic models can guarantee a continuous nutrient recycle applying physico-chemical stimuli. Based on this background, we evaluated the efficacy of gH625-functionalized liposomes to deliver a well-established neuroprotective molecule such as PACAP in an *in vitro* 3D model of BBB previously described (*Chapter 4*). We used a bioreactor, connected to a peristaltic pump, which allows two different flows: tangential flow and perfusion flow. In our setup we have chosen a tangential flow. This configuration is suitable for our system as it can reliably mimic both the apical membrane domain and the basolateral membrane domain of the BBB. The treatment of 3D neuronal coculture with the functionalized liposome loaded with PACAP in our *in vitro* 3D BBB model resulted in the uptake of PACAP by 3D spheroid. Hence, our results showed that the functionalized nanodelivery system settled can be useful to perform pharmacokinetics, pharmacodynamics for drug delivery *in vitro* tests, in particular when applied to a suitable 3D dynamic *in vitro* model of the BBB. These experiments also confirmed the ability of our nanodelivery system to efficiently release molecules across the BBB *in vitro*. This feature is mandatory to support and ameliorate studies on brain diseases.

#### **5. Conclusion**

In the present study we demonstrated the passage of PACAP loaded with gH625-liposome in a 3D fluid dynamic *in vitro* model of BBB. The fluid dynamic model was LB2 bioreactor with double chamber and independent flow condition. In the upper chamber brain endothelial cells (bEnd.3) were seeded on the porous membrane dividing the lower chamber in which 3D SH-SY5Y/U-87MG were seeded. We recreated a 3D BBB model using three different cell lines

which normally contribute to the *in vivo* BBB formation: endothelial brain cells, neuron like cells, glial like cells. Hence, we realized a drug delivery *in vitro* test system useful to assess the effects of pharmacological substances and their relationship during the reaching and passing across the BBB. This highly innovative drug delivery *in vitro* system can be useful in the preclinical studies of many brain and neurodegenerative diseases.

## References

- Abbott, N.J., Patabendige, A.A., Dolman, D.E., Yusof, S.R., Begley, D.J. (2010). Structure and function of the blood-brain barrier. *Neurobiol Dis* 2010; 37(1):13-25; PMID:19664713; <http://dx.doi.org/10.1016/j.nbd.2009.07.030>.
- Falanga A, Vitiello MT, Cantisani M, Tarallo R, Guarnieri D, Mignogna E, Netti P, Pedone C, Galdiero M, Galdiero S (2011). A peptide derived from herpes simplex virus type 1 glycoprotein H: membrane translocation and applications to the delivery of quantum dots. *Nanomedicine*. Dec;7(6):925-34.
- Garbuzova-Davis, S., Thomson, A., Kurien, C., Shytle, RD., Sanberg, PR. (2016). Potential new complication in drug therapy development for amyotrophic lateral sclerosis. *Expert Rev. Neurother.* 16, 1397–1405 (2016).
- Giusti S, Sbrana T, La Marca M, Di Patria V, Martinucci V, Tirella A, Domenici C, Ahluwalia A (2014). A novel dual-flow bioreactor simulates increased fluorescein permeability in epithelial tissue barriers. *Biotechnol J*. 2014 Sep;9(9):1175-84. doi: 10.1002/biot.201400004. Epub 2014 Jun 3.
- Iachetta G, Falanga A Molino Y, Masse M, Jabès F, Mechioukhi Y, Laforgia V, Khrestchatisky M, Galdiero S, Valiante S (2019). gH625-liposomes as tool for pituitary adenylate cyclase-activating polypeptide brain delivery. *Sci Rep*. 2019 Jun 24;9(1):9183. doi: 10.1038/s41598-019-45137-8.
- Nzou, G., Wicks, R.T., Wicks, E.E. et al. Human Cortex Spheroid with a Functional Blood Brain Barrier for High-Throughput Neurotoxicity Screening and Disease Modeling. *Sci Rep*8, 7413 (2018). <https://doi.org/10.1038/s41598-018-25603-5>.
- Rodrigues B, Lakkadwala S, Kanekiyo T, Singh J. Development and screening of braintargeted lipid-based nanoparticles with enhanced cell penetration and gene delivery properties (2019). *Int J Nanomedicine*. 2019 Aug 14;14:6497-6517. doi: 10.2147/IJN.S215941. eCollection 2019.
- Sbrana, T., Ahluwalia, A. (2012). Engineering Quasi-vivo in vitro organ models. *Adv. Exp. Med. Biol.* 745,138–153. doi: 10.1007/978-1-4614-3055-1\_9.

Valiante S, Falanga A, Cigliano L, Iachetta G, Busiello RA, La Marca V, Galdiero M, Lombardi A, Galdiero S (2015). Peptide gH625 enters into neuron and astrocyte cell lines and crosses the blood-brain barrier in rats. *Int J Nanomedicine*. 2015 Mar 10;10:1885-98. doi: 10.2147/IJN.S77734. eCollection 2015. 13.

Vaudry D, Falluel-Morel A, Bourgault S, Basille M, Burel D, Wurtz O, Fournier A, Chow BK, Hashimoto H, Galas L, Vaudry H. Pituitary adenylate cyclase-activating polypeptide and its receptors: 20 years after the discovery. *Pharmacol Rev*. 2009 Sep;61(3):283-357. doi: 10.1124/pr.109.001370. Review.

Zhu J, Wang S2, Liang Y3, Xu X3 (2018). Inhibition of microRNA-505 suppressed MPP<sup>+</sup>-induced cytotoxicity of SHSY5Y cells in an in vitro Parkinson's disease model. *Eur J Pharmacol*. 2018 Sep 15;835:11-18. doi: 10.1016/j.ejphar.2018.07.023. Epub 2018 Jul 17.

Zlokovic., B.V and Apuzzo, M.L. (1998). Strategies to circumvent vascular barriers of the central nervous system. *Neurosurgery* 43 (4): 877–878.

## **Chapter 6:**

### **Delivery test of gH625-liposome in minibrains**

## **Introduction**

In the last months of PhD, we have established a scientific collaboration with Professor Adrien Roux from Tissue Engineering Laboratory, Haute école du paysage, d'ingénierie et d'architecture de Geneva, Switzerland, to study the delivery and intake of our functionalized liposome gH625-liposome on neurosphere, called “minibrain” (Govindan et al., 2021). Minibrain is a 3D brain *in vitro* spheroid model, composed by neurons and glial cells, from human iPSC derived neural stem cells. Neurosphere possess a fundamental link to study both drug and molecular screening. Usually, 3D brain *in vitro* models have too large size for wide scale screening studies they undergo rapidly in necrosis. In the study conduct by Govindan et al., they have optimized protocol to generate neurospheres where the size is adapted for large-scale screening. After 12 weeks of differentiation, minibrain present synchronized neural networks (Sandström et al., 2017). Moreover, they express genes related to neurons, oligodendrocytes and astrocytes. Transcriptomic analysis of minibrain vs NSChiPS show activation of biological process like synaptic signaling, neuron morphology projection, neuron differentiation and neurotransmitter release. Other genes expressed are related to cortical regions such as striatum, sub pallium, layer 6 of motor cortex, piriform, anterior cingulate and occipital cortex. The novel methodologies proposed by Govindan et al., is useful in using Minibrains for large scale screening and to study neuronal disorders, drug testing and chemical screening. In this regard, we focused our attention on the delivery and intake of our liposome functionalized with gH625 peptide in to minibrains.

## **2. Material and Methods**

### **2.1 Delivery of gH625-liposome in minibrains.**

After 12 weeks from neurosphere maturation (Govindan et al., 2021) gH625-liposome were incubate in minibrains for 24h under orbital agitation in the incubator at 37°C, 5% CO<sub>2</sub> and controlled humidity. gH625-liposome were prepared as described in *2.1 Peptide synthesis and 2.2 Liposome preparation, Chapter 1*. Liposomes have initial concentration at 1mM, delivery peptide gH625 at 60 µM, Rhodamine fluorophore, (RHO –PE) at a concentration of 10 µM. Rhodamine labelled phosphatidylserine residues of liposome. Control was obtained labelling minibrains with only liposome RHO-PE, without gH625. After 24, minibrains were harvested

and fixed with a solution containing 4% of paraformaldehyde (PFA) in phosphate buffered saline (PBS). Minibrains were then stored at 4°C until shipment in Italy. Nuclei were labelled with DAPI for 15 min. Images were acquired with the JuLi™ Stage RealTime Cell History Recorder microscope with 10x objective, using two different channels: DAPI and RFP. Images are corrected using Fiji software in maximum intensity projections.

## 1. Results

gH625-lipoRHO-PE was incubated for 24h in minibrains under orbital agitation. After 24h, images below showed a higher Rho fluorescence starting from the contours up to the inside of the neurosphere (**Fig.1**). On the other hand, minibrains incubated with lipoRHO-PE without gH625 peptide show a higher external fluorescence (**Fig.2**).

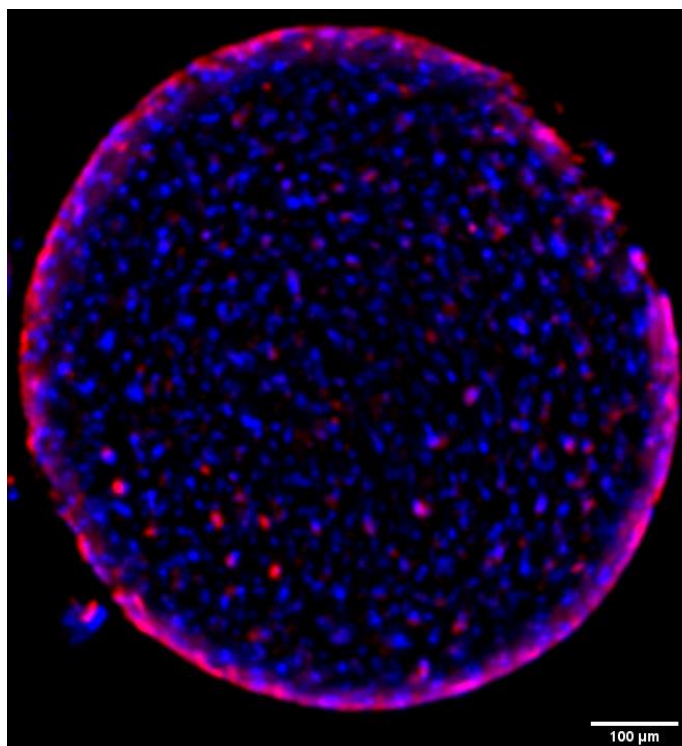


**Fig.1**

Representative image of minibrains labelled with gH625-lipoRHO-PE.

Image were acquired as Z stack with the JuLI Stage fluorescence recorder and maximum intensity projection was showed.

Nuclei in DAPI.

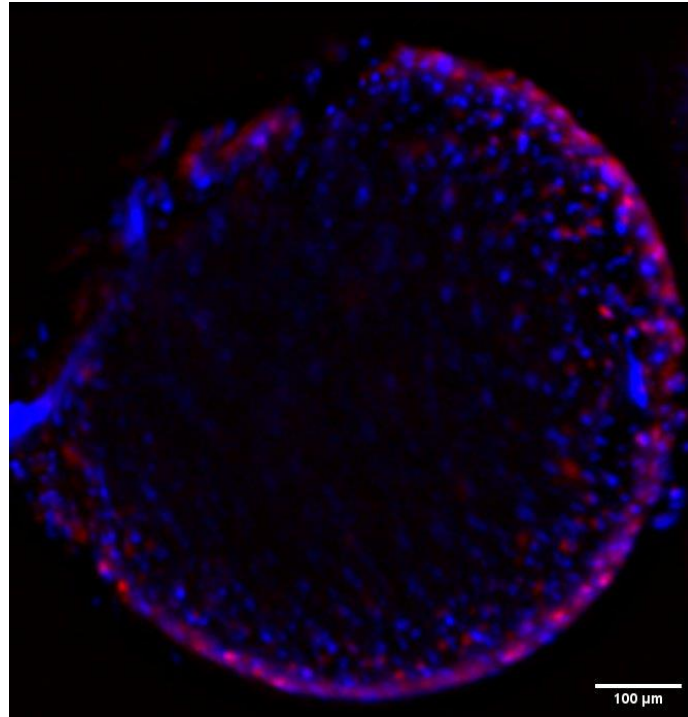


**Fig.2**

Representative image of minibrains labelled with liporHO-PE.

Image were acquired as Z stack with the JuLI Stage fluorescence recorder and maximum intensity projection was showed.

## **Discussion**

Thanks to the collaboration with the Tissue Engineering Laboratory in Geneve , we evaluated the inclusion of our nanodelivery system in minibrains. These are derived from human iPSC neural stem cells (Govindan et al., 2021). Minibrains express genes related to neurons, oligodendrocytes and astrocytes and other brain regions. The differential distribution of fluorescence within samples treated or not with functionalized nanosystem, with main central fluorescence inside minibrains treated with functionalized nanosystem and peripheral fluorescence in non-functionalized nanosystem indicate that our gH625 functionalized nanodelivery system can easily penetrate minibrain structures. These results also, confirm our previously investigations about the ability of gH625 as highly effective drug delivery system. In our future studies, we aim to obtain minibrains and seeded them in our 3D blood-brain barrier fluid system.

## References

Govindan, S., Batti, L., Osterop, S.F., Stoppini, L., Roux, A. (2021). Mass Generation, Neuron Labeling, and 3D Imaging of Minibrains. *Front Bioeng Biotechnol.* 2021 Jan 7;8:582650. doi: 10.3389/fbioe.2020.582650. PMID: 33598450; PMCID: PMC7883898.

Sandström, J., Eggermann, E., Charvet, I., Roux, A., Toni, N., Greggio, C., et al. (2017). Development and characterization of a human embryonic stem cell-derived 3D neural tissue model for neurotoxicity testing. *Toxicol. In Vitro* 38, 124–135. doi: 10.1016/j.tiv.2016.10.001

## **Chapter 7:**

### **Conclusion**

## Conclusion

We have successfully obtained a preliminary reliable 3D dynamic *in vitro* model of blood-brain barrier (BBB) to test drug delivery of neuropeptides, like PACAP. This 3D *in vitro* model includes brain endothelial cells, neuron cells and glial cells. Our liposome system carried out by gH625 peptide can cross this *in vitro* model of BBB, efficiently delivering neuroprotective agent with beneficial effects in cells treated with MPP<sup>+</sup> neurotoxins. Thanks to Swiss collaboration, we have obtained the delivery of our liposome system in neurosphere derived from iPSC-derived neural stem cells. Next goals aim to improve our 3D fluid dynamic *in vitro* model of BBB by adding human pericyte cell line in the upper chamber of millifluidic bioreactor, along with human endothelial cells, neurosphere expressing gene related to neurons, oligodendrocytes and astrocytes, in the lower chamber. In conclusion, we projected and realized an *in vitro* test system useful for drug delivery evaluation that can easily be used to assess the effects of pharmacological substances during the reaching and passing across the BBB. This highly innovative drug delivery *in vitro* system can be useful in the preclinical studies of many brain and neurodegenerative diseases.

## **Publications**

## **Publications**

Rosati, L., Agnese, M., Di Lorenzo, M., **Barra, T.**, Valiante, S., Prisco, M. (2020). Spermatogenesis and regulatory factors in the wall lizard *Podarcis sicula*. *Gen Comp Endocrinol.* 2020 Aug 7; 298:113579. doi: 10.1016/j.ygcen.2020.113579.

Di Lorenzo, M.<sup>1</sup>, **Barra, T.**<sup>1</sup>, Rosati, L., Valiante, S., Capaldo, A., De Falco, M., Laforgia, V. (2020). Adrenal gland response to endocrine disrupting chemicals in fishes, amphibians and reptiles: a comparative overview. *Gen Comp Endocrinol.* 2020;113550. doi: 10.1016/j.ygcen.2020.113550.

Di Lorenzo, M., Sciarrillo, R., Rosati, L., Sellitti, A., **Barra, T.**, De Luca, A., Laforgia, V., De Falco, M. (2020). Effects of alkylphenols mixture on the adrenal gland of the lizard *Podarcis sicula*. *Chemosphere.* 2020;258: 127239.doi: 10.1016/j.chemosphere.2020.127239.

